The Institute of Paper Chemistry

Appleton, Wisconsin

Doctor's Dissertation

An Investigation of the Time-Dependent Structural and Mechanical Behavior of Individual Pulp Fibers When Subjected to an Applied Stress

Richard L. Hill

January, 1967

AN INVESTIGATION OF THE TIME-DEPENDENT STRUCTURAL AND MECHANICAL BEHAVIOR OF INDIVIDUAL PULP FIBERS WHEN SUBJECTED TO AN APPLIED STRESS

A thesis submitted by

Richard L. Hill

B.S. (Ch.E.) 1961, The University of Texas
M.S. 1963, Lawrence College

in partial fulfillment of the requirements
of The Institute of Paper Chemistry
for the degree of Doctor of Philosophy
from Lawrence University
Appleton, Wisconsin

January, 1967

TABLE OF CONTENTS

SUMMARY

Several theories recently have been proposed which relate the mechanical properties of paper to the mechanical properties of the component fibers. In the literature there are numerous studies of paper properties, but little is known about the properties of individual fibers. This is particularly true of the viscoelastic or creep behavior of wood fibers. The purpose of this investigation was to study the time-dependent structural and related mechanical behavior of individual fibers subjected to applied stress. Fiber behavior was determined by axial tensile creep and creep recovery tests, x-ray diffraction analysis, and load-elongation studies.

Previous workers have determined that drying wood pulp fibers under an axial tensile load increases the modulus of elasticity, the tensile strength, the work-to-rupture, and the crystallite orientation and decreases the ultimate elongation. Recent work has also shown that the removal of hemicelluloses from the fiber structure decreases these mechanical properties and that the effect probably results from inhibition of internal stress redistribution.

The present study was concerned with summerwood fibers of a longleaf pine holocellulose pulp. It was shown that at least two types of structural modifications occur in these fibers when an external stress is applied. These modifications are separated in time during creep tests but there is a continuous change from one to the other. The first type of modification leads to a redistribution of internal stress and occurs at early times and low initial stresses. This behavior results in rapid creep deformation and is thought to be controlled by secondary bonding and molecular configurational changes in the amorphous regions of the fiber. The internal stress redistribution occurs through minute adjustments in the fibrillar structure which allow a more equal sharing of the external load among these fibrillar elements. The second type

of modification produces no further stress redistribution and continues until the fiber ruptures. This type of fiber deformation leads to permanent structural changes and is linearly related to the logarithm of time under stress.

It was further shown that, as creep deformation increases, the mechanical properties of modulus of elasticity, tensile strength, and work-to-rupture increase and approach a limiting value as the fiber deformation becomes linear with the logarithm of time. The ultimate elongation of these fibers continued to decrease throughout creep.

Comparison of these changes in mechanical properties produced by sustained stress in dry fibers with the reported effects of drying fibers under tensile load shows that very similar limiting properties are attained by both processes. This indicates that the structural response of these fibers leads to the same or very similar final states by these dissimilar processes.

Data obtained after creep recovery showed that the initial creep deformation is largely recoverable and that the observed changes in fiber mechanical properties are also largely recoverable. As creep deformation increases, structural response mechanisms lead to permanent fiber deformation and to permanent changes in mechanical properties.

Investigation of the crystalline portion of the fiber by x-ray diffraction methods confirmed the improved arrangement of the cellulose crystallites or fibrils and indicated that the amount of crystalline material did not change as a result of sustained tensile stress.

INTRODUCTION AND OBJECTIVE

All of the many and varied uses of paper require the finished product to have a certain level of "strength." In the past, the manufacture of paper with specific strength properties was made possible largely through the experience and artistic ability of the papermaker. In more recent times, the work of many investigators has developed the technology so that now it is more nearly possible to engineer a sheet with desired strength characteristics.

Before the mechanical properties of paper can be adequately controlled in a manufacturing process, a thorough understanding of the mechanisms by which paper responds to stress is required. The use of rupture tests to evaluate the stress/strain properties has been successful in that the general importance of both sheet structure and fiber properties has been recognized. The results of many other studies concerned with prerupture stress behavior have demonstrated the viscoelastic nature of paper and the importance of both interfiber and intrafiber deformation mechanisms. These studies have led to the development of several theories of paper structure which relate sheet properties to fiber properties and to fiber arrangement in the sheet.

The relative importance of interfiber and intrafiber mechanisms of sheet viscoelastic behavior has not been resolved due to the difficulty of independently controlling either of these factors in a sheet of paper. Therefore, the study of individual fibers is a logical approach to elucidating the intrafiber viscoelastic behavior of paper. The results of such studies should, when combined with theories of paper structure, aid in understanding the viscoelastic nature of paper and in selecting proper fibers for specific paper properties. For these reasons it was felt that an investigation of individual fiber viscoelastic behavior was justified.

The objective of this thesis was to show that both the structure and the mechanical properties of individual wood pulp fibers exhibit time-dependence on applied stress and, further, to evaluate such dependence for certain experimental conditions. A longer range objective of the study was, of course, to gain a better understanding of the properties of wood pulp fibers and information which would further our knowledge of the viscoelastic nature of paper.

HISTORICAL REVIEW

Studies of the mechanical properties and chemical composition of fibers are very broad and plentiful in the literature. With the development of the field of polymer chemistry, the relationships between the molecular structure and mechanical properties have received careful investigation and, in some cases, explanation. Most of these fiber studies have been concerned with textile fibers. Only recently has much work been done with papermaking fibers. There are, however, similarities between the structure and physical properties of the natural cellulosic fibers used both in textiles and papermaking.

The purpose of the following literature review is (1) to present to the reader the structure and composition of wood pulp fibers, (2) to relate the fiber structure to its mechanical properties, and (3) to discuss the factors affecting and the experimental methods of evaluating fiber properties pertinent to this study. The work in this area has been summarized by several authors, and this review will be taken in large part from the books by Morton and Hearle (1), Ott and Spurlin (2), and Meredith (3).

STRUCTURE OF CELLULOSE FIBERS

Wood fibers are composed of three major polymer systems: cellulose, hemicellulose, and lignin. A fourth group of miscellaneous materials is also present which includes pectinaceous materials, inorganic compounds, etc. Of these, the lignin system is almost completely removed in pulping as are the miscellaneous materials. Cellulose is the main constituent of wood pulp fibers, and the mechanical properties of these fibers are largely determined by the structures formed by cellulose molecules. The hemicelluloses, due to their association with cellulose in the overall fiber structure, also influence fiber properties. The

pulp fiber is, in general, formed from cellulose molecules uniting to make elementary fibrils which in turn unite to form macrofibrils. The fibrils thus formed are of indeterminate length and are found as springlike elements forming successive layers which make up the plant cell wall.

MOLECULAR STRUCTURE

Wood pulp fibers, and other natural cellulosic fibers, are polycrystalline materials. Formation of crystalline regions in the cellulose system of fibers is due to the regularity of the molecular structure, especially the regular spacing of polar groups along the molecule. Cellulose is a linear polymer composed of anhydroglucose units linked by beta-1, 4 glycosidic bonds. The hemicellulose system is composed of several different sugar polymers, forms a less-ordered structure than does cellulose, and does not tend to crystallize.

All naturally occurring cellulosic fibers have a crystal lattice which is termed cellulose I. Meyer and Misch (4), on the basis of x-ray diffraction data, postulated the generally accepted monoclinic unit cell for the cellulose I lattice structure as shown in Fig. 1. The planes of the anhydroglucose units lie in the ab plane, and the axes of the cellobiose units are parallel to the b axis.

It is interesting to note the three kinds of forces which hold the lattice together. Along the cellulose chain, or the b axis, the glucose units are joined by the beta-1, 4 glycosidic primary valence bonds. Along the a axis, the adjacent chains are joined by hydrogen bonds where the oxygen atom separation is within the required 2.5 A. It has been suggested that along the c axis the lattice is held together by Van der Waals forces, since the nearest atomic centers are separated by 3.1 A. The approximate dissociation energies of these bonds are 80, 5, and 3 kcal./mole, respectively (5). Due to the polycrystalline

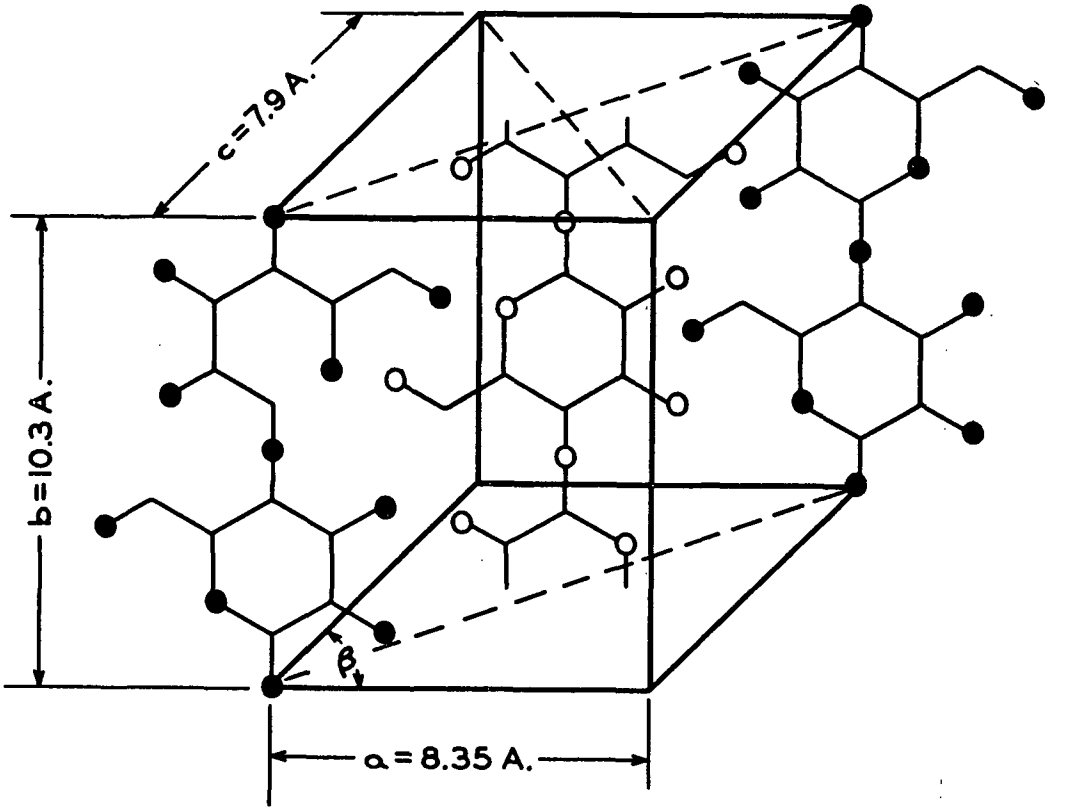

Figure 1. Unit Cell Cellulose I According to Meyer and Misch (4)

nature of cellulose, the size, shape, and arrangement of the crystalline and noncrystalline regions are important to its mechanical properties. It is generally agreed, on the basis of chemical and physical tests, that distinct crystalline and amorphous regions (two-phase system) do not exist. It is now felt that there are gradual transitions from crystalline to amorphous regions, or that there are varying degrees of lateral order.

Two principal theories of cellulose crystallinity have been proposed which meet the general requirements of a gradual transition in the degree of lateral order. In the older theory, the fringed micelle theory, the micelles (or crystallites) are considered as statistically distributed regions of lattice order in a mass of less-

ordered, but approximately parallel, cellulose chains (5). The crystalline regions alternate with the less-ordered amorphous regions; and, in general, an indefinite number of distributions may exist for the size, shape, and degree of perfection of the crystalline regions. There is no apparent correlation between the length of the crystalline regions and the molecular chain length.

A more recent theory, the fringed fibril theory of cellulose crystallinity, has been proposed by Hearle (6,7). This theory combines the microscopically (both optical and electron) evident features of fibrillar structure with the major features of the fringed micelle theory. This is accomplished by abandoning the assumption that there are discrete crystallites present in the structure. Instead, the crystalline regions are regarded as continuous "fringed fibrils" made up of molecules diverging from an essentially crystalline core at various points along the length of the fibril. Hearle assumed that branching of the fibrils is possible and that some distortion of the crystal lattice may occur. Such distortions would allow a slight curvature of the fibrils. Jentzen, investigating the load-elongation behavior of individual wood pulp fibers (8,9), felt that his data best supported the fringed fibril theory.

The latter theory would explain both the presence of microscopic fibrils and the division between crystalline and noncrystalline regions. The main difference between the two theories is that in the fringed fibril theory, the amorphous regions lie along the periphery of the fibril; but in the fringed micelle theory, the amorphous and crystalline regions alternate along the fibrillar axis. This difference could be of major importance when interpreting fiber response to axial stress in terms of fiber structure.

A third possible theory of fiber structure with new supporting evidence has recently been suggested. This theory is based on the folding of the cellulose

molecule upon itself in the crystalline regions. The possibility of chain folding in cellulose molecules has been discussed by Tønnesen and Ellefsen (10). These authors can account for many properties of cellulose with this model; however, they do not account for the strength of the cellulose fibril. Manley (11) obtained data supporting the chain folding hypothesis. In his model, the basic structural element of the plant cell wall is a filament 25-A. wide which consists of a ribbon wound as a tight helix. The molecules assume a folded configuration, and the microfibrils exist in ordered arrangement in the cell wall. Manley's work was with single crystals of a cellulose derivative. Dolmetsch (12) noted that when cellulose is formed "freely" in the substrate, it can follow its "own laws of crystallization," but when formed in cellular tissues, its freedom is spatially limited. Thus, the internal structures that may occur in a single crystal may not occur in a cellulosic fiber.

It can be recognized from the preceding discussion that the terms "crystalline," "crystallinity," and "amorphous" and terms concerning the relative amounts of these materials are rather poorly defined. These terms, however, frequently appear in the literature and are defined by the method used to measure them. Chemical methods, which measure what is termed the accessibility, generally utilize the rate or extent of reaction of various compounds with cellulose and, more recently, the rate of isotope exchange of deuterium or tritium for the hydroxyl hydrogens in the amorphous regions. Physical methods, in general, measure what is termed crystallinity or percentage crystallinity. X-ray diffraction is the principal physical method. Some of the other methods depend on measuring the density of cellulose, the dielectric constant, or the amount of moisture absorbed by cellulose.

It should be pointed out that none of these methods actually measures the lateral order distribution of the sample, but they do rank various cellulosic materials in the same order and are useful methods for comparative purposes.

MICROSCOPIC STRUCTURE

The length and diameter of wood fibers vary greatly with species and to a lesser extent within species, even within the individual tree. The average length of coniferous fibers is in the 3.0 to 5.0 millimeter range, and the average diameter lies between 30 and 45 microns (13).

The fiber cross section is roughly elliptical and has a hollow center which forms the fiber lumen.

Morphologically, wood pulp fibers have a structure which is commonly divided into four layers. These layers are referred to as: (1) P layer, or primary wall; (2) S_1 layer, or the outer layer of the secondary wall; (3) S_2 layer, or the central layer of the secondary wall; and (4) S_3 layer, or the inner layer of the secondary wall (sometimes referred to as the tertiary wall). A diagrammatic representation of the layered structure of a fiber wall as presented by Wardrop (14) is shown in Fig. 2.

The various layers of a fiber wall are concentric about the fiber axis and may be further subdivided into lamellae about 0.1 micron (15), roughly five microfibrils thick (16). The separation of single microfibrils from a lamella sheet is difficult (17). This indicates that the cohesion of the fibrils is relatively strong. These lamellae are complex structural units composed of a series of elements ranging down in size to the cellulose molecule. Frey-Wyssling (18) classifies the elements based on their cross-sectional dimensions as macrofibrils, microfibrils, and elementary fibrils. Their sizes, respectively, are 4000 by 4000 A., 250 by 250 A., and 30 by 100 A. These dimensions were determined for the elements in ramie and would be expected to vary somewhat in other fibers.

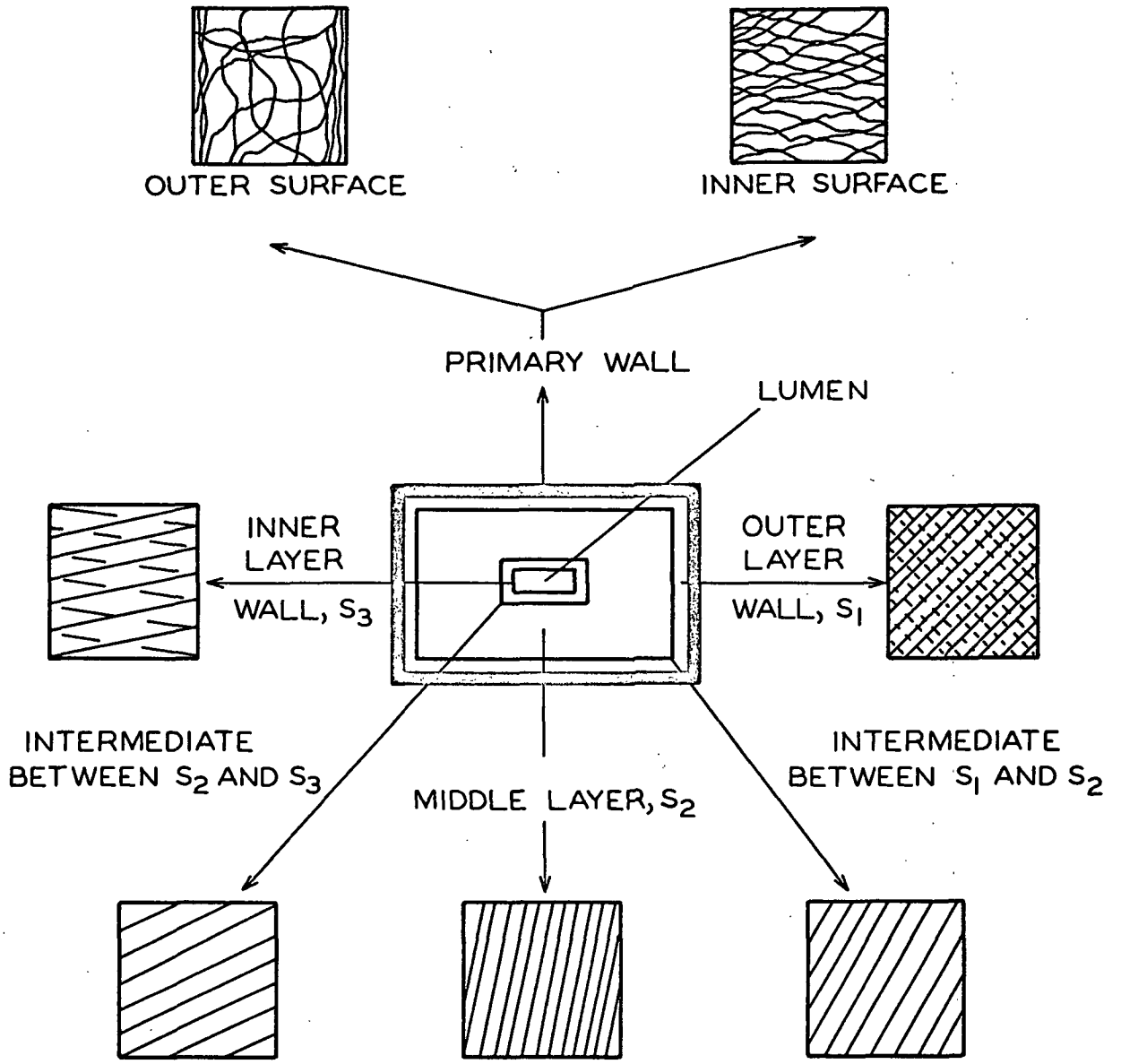

Figure 2. A Diagrammatic Representation of the Layers and Their Organization in a Typical Wood Fiber (14)

The fibrils of all layers except the primary wall are wound helically around the fiber axis. The fibrils in the primary wall are randomly oriented in a loosely woven texture except at the corners where they are longitudinal (14). The S_1 layer has at least two counterrotating symmetrical helixes arranged at an angle of 55 to 75° to the fiber axis in softwood tracheids (19). The fibrils of the S_2 layer are closely parallel, run in a steep helix, and form an angle of 10 to 20° to the fiber axis (14). This layer forms the bulk of the fiber cross section, particularly in summerwood fibers. The tertiary, or S_3 layer, exhibits a tendency toward a crossed helix structure (20) as does the S_1 layer; however, the helix angles do not appear to change abruptly, but tend to exhibit a progressive radial variation across the various layers and from layer to layer.

Both springwood and summerwood tracheids have similar structures, but they differ in cell wall thickness, cell diameter, and size of the lumen (13). The difference in cell wall thickness is largely accounted for in the amount of the S_2 layer. Jayme (21) gives the following volume results for the relative amounts of material in the various layers for a spruce springwood tracheid: the P layer – 10%, S_1 layer – 8%, S_2 layer – 78%, and S_3 layer – 4%. These percentages are approximate values but serve to emphasize the importance of the S_2 layer.

Important morphological characteristics of wood fibers are the discontinuities in the structure. The various types of pits are the most readily recognized discontinuity, and the fibrils of the layers are circumferentially oriented around these pits. Bucher (20) points out that dislocations and slip planes in the fibers are transverse discontinuities, and that the lamellae between and within the layers are also discontinuities. The various discontinuities in the fiber structure should have an important effect on fiber mechanical behavior since they introduce areas of localized stress-concentration.

HEMICELLULOSE DISTRIBUTION IN THE CELLULOSE STRUCTURE

The work of Spiegelberg (22), investigating the effects of hemicelluloses on the mechanical properties of pulp fibers, showed that these materials, in particular the highly branched xylans and galactoglucomannans, aid the redistribution of internal stresses in the fiber and contribute significantly to its mechanical properties. This is in agreement with the work of Leopold and McIntosh (23) and others. The chemical compositions of the layers of a wood pulp fiber are significantly different, but there is little difference between springwood and summerwood tracheids (24). Meier (25) found that 30 to 35% of the carbohydrate material in the cell wall was composed of various hemicelluloses, the remainder of 65 to 70% being cellulose. The location and physical state of this material most likely has an important bearing on the fiber properties.

There has been no investigation which directly locates the hemicelluloses in the microstructure of the wood pulp fiber. The work of Meier indirectly located the hemicelluloses in the cell wall layers. The data indicated that the primary cell wall is 60 to 65% hemicellulose, the S_1 layer is 40 to 50% hemicellulose, and the S_2 layer is 35 to 40% hemicellulose. The cellulose was in reverse order.

Meier (25) felt that the hemicelluloses may lie between the cellulosic fibrils either as amorphous material or as a crystalline granular material, or they may form their own microfibrils which may or may not contain crystalline regions. Most workers, however, feel that the hemicelluloses are located around the outside of the microfibrils (26, 27) although there are data to indicate that some may be located within the cellulosic microfibrils (27, 28). It is generally accepted that the hemicelluloses are located within the microstructure of the fibers, but exact placement of the various polysaccharides is at present indeterminate.

PRERUPTURE STRESS BEHAVIOR

In studying the structural and mechanical behavior of a polymer to an external stress, it is theoretically possible to relate the behavior of the material to molecular mechanisms within the specimen. In the case of materials of porous, heterogeneous, microscopic structure, such as wood pulp fibers, it is not possible to relate the overall deformation of the specimen to its molecular structure; but the more probable of several possible molecular mechanisms may be inferred from the time, stress, and strain relationship of the system. These inferences may be drawn by understanding the various molecular processes of simpler systems and how they produce the observed viscoelastic properties.

When a material is subjected to an external load, it will deform in a manner governed by the nature of the material. In general, there are three major types of deformations which account for the total deformation of the specimen. These are the immediate elastic deformation, the delayed elastic deformation, and nonrecoverable deformation. The following discussion has been taken largely from Alfrey (29) and Ferry (30).

IMMEDIATE ELASTIC DEFORMATION

The immediate elastic deformation of a material is the perfectly elastic or instantaneous deformation which occurs upon the application of a load. This deformation is considered to be recovered instantly upon removal of the load and is not time dependent. Such deformation follows Hooke's law which defines the modulus of elasticity as the ratio of applied stress to the resulting strain. For viscoelastic materials, such as cellulosic fibers, it is frequently very difficult to measure accurately their elastic modulus due to the presence of extremely short-time delayed deformation.

Elastic deformations result from the stretching of bonds and the straightening of molecular chains. The three types of bonds present in cellulose fibers, which were discussed earlier in the review, have different stretching and bending energies. Primary valence bonds form intramolecular bonds, and Van der Waals forces and hydrogen bonds form both intermolecular and interfibrillar bonds. When stress is applied, all of these bonds will be deformed to some extent. It has been estimated that secondary bonds of the Van der Waals and hydrogen types will extend 10 to 20% before bond rupture. Stretching or extension of these bonds implies relative movement of the fibrils and molecules.

Meyer and Lotmar (31) have calculated the value of Young's modulus for the cellulose molecule to be 120 x 10^{10} dynes/cm.^{2}. This value is based on primary valence bond deformations, and it is interesting to compare it with measured values of various cellulosic fibers. Meredith (3) found a dynamic Young's modulus of 90 x 10^{10} dynes/cm.^{2} for ramie fibers dried under tension. This suggests that for these highly oriented, highly crystalline fibers the primary structural deformation was due to mechanisms involving the primary bonds of the cellulose molecules. Jentzen (9), studying holocellulose fibers from longleaf pine, found a Young's modulus for summerwood fibers of about 64 x 10^{10} dynes/cm.^{2} when the fibers were dried under a 3-gram load. By basing the modulus on the cross-sectional area of cellulosic material, the value for Young's modulus was found to be 103 x 10^{10} dynes/cm.^{2}. Spiegelberg (22), studying fibers similar to those used by Jentzen, found the Young's modulus based on cellulose area to be about 97 x 10^{10} dynes/cm.^{2} for fibers dried under tension. The data of both Jentzen and Spiegelberg indicate that the theoretical value of Young's modulus can be closely approached in the case of these holocellulose fibers dried under tension.

Spiegelberg found that the removal of hemicelluloses changed the Young's modulus of fibers dried under no load from 24 x 10^{10} dynes/cm.^{2} unextracted to 6.7 x 10^{10} dynes/cm.^{2} for heavily extracted fibers. He attributed this pronounced decrease in modulus to stress-concentration effects being more pronounced in the extracted fibers. Minimizing the stress-concentration effects by drying the fibers under tension, Spiegelberg observed a common Young's modulus for both the unextracted and extracted fibers of about 45 x 10^{10} dynes/cm.^{2}. These data indicate that the secondary bonds which unite the hemicelluloses to the cellulose fibrillar structure play an important roll in the immediate elastic deformation of these fibers when dried under no load conditions.

A lower elastic modulus may, in general, be related to higher percentages of amorphous material and to greater heterogeneities in the structure of polymers. For a broad range of polymeric materials, there appears to be a general inverse relationship between the elastic modulus and the delayed deformation of the polymer, but the relationship is too vague to be of use in relating creep properties to structure (29).

DELAYED DEFORMATION

Time-dependent deformation, or creep, can be divided into two components: primary creep, which is recoverable; and secondary creep, which is nonrecoverable. Primary creep is commonly referred to as the delayed elastic deformation, and secondary creep and nonrecoverable deformation are corresponding terms. For a thorough treatment of the creep behavior of textile fibers, the reader is referred to Leaderman (32). No studies of the creep behavior of wood pulp fibers have been reported, but there are several studies of paper viscoelasticity (33-36).

Primary Creep

Primary creep is the time-dependent recoverable portion of the delayed deformation. This response of viscoelastic materials is thought to be due principally to configurational changes in molecular structure produced by the applied stress. Alfrey (29) discusses the mechanisms of such molecular movement. The packing of molecules in the amorphous regions of high polymers is less than optimum; hence, the solid may be considered to contain void spaces through these regions. When the amorphous regions are subjected to stress, the molecules tend to align themselves in the direction of the stress by moving into new positions. Such movement may occur when there is a void space available to be occupied and when sufficient strain energy is supplied to overcome the forces which previously defined the molecular vibrational paths. These movements in fibers may require the breaking of secondary bonds which may be reformed in new positions. Upon removal of the external stress, the stored energy is released; and the molecules tend to return to their normal, more random, positions. Theoretical treatment of configurational response is vastly complicated by the presence of crystalline regions and strong secondary bonding, but this mechanism should be active in the stressed amorphous material of pulp fibers.

Leaderman (32) has suggested that the configurational changes may extend to the point where crystal growth occurs. He postulated this phenomenon for nylon filaments and further suggested that it was completely reversible. Effects of the same type have been observed by Press (37) for viscose rayon and by Mark and Press (38) for acetate rayon. The evidence for crystallization was indirect and was based on the departure from the characteristic creep and recovery behavior noted at lower loads. Negishi (39, 40) found by x-ray studies that increased crystallinity, or at least better molecular packing, occurred in

cotton and ramie yarns dried under tension. However, Jentzen (9), employing similar methods, did not observe such behavior in his holocellulose fibers.

Secondary Creep

Secondary creep is that portion of the total sample deformation which is nonrecoverable at the test conditions after removal of the load. A portion of the configurational elastic response may not be recoverable at the test conditions, but may be recovered if the polymer is swollen by raising its moisture content or if the temperature of the polymer is increased. Truly permanent deformations are caused by viscous flow, irreversible crystallization, and molecular chain rupture (30).

Configurational deformations are susceptible to being "frozen in" or to attaining metastable equilibrium states in those polymers in which secondary bonding per unit length of the molecule is high (such as cellulose and hemicelluloses). It is necessary to rupture these relatively weak secondary bonds to allow configurational changes in the amorphous material of the fiber. Once broken, these bonds may form new bonds with previously unbonded atoms; they may unite with other broken bonds; or they may remain broken. The formation of new bonds can lead to secondary creep when the load is released if there is not enough energy stored in the system to break the new bonds and return the bonding group to its original position. The breaking and reforming of bonds and molecular configuration changes are equilibrium processes. All such processes require a finite time to attain equilibrium. The time required to reach new equilibrium states is one of the factors which produce creep. If metastable equilibrium states are reached, permanent deformations will result. The rate and amount of creep recovery will depend on the stability of the new bonds and on the stored energy of the system.

The term viscous flow, to describe the stress behavior of polymeric materials, is rather indiscriminately used. Viscous flow is normally applied only to truly permanent deformations involving the transfer of entire molecules in amorphous polymers. It is generally agreed that flow of entire molecules is not possible in polycrystalline materials such as cellulose, and it is doubtful that such flow would occur even in the amorphous hemicelluloses.

Crystal growth might occur as configurational changes bring the molecules into very close proximity and alignment, but as discussed earlier, the evidence for this phenomenon is indirect and inconclusive. Such growth would necessitate the formation of a very high secondary bond density in the crystal structure and should be resistant to reversal.

A final important response mechanism of pulp fibers when subjected to an external stress is the rupture of primary valence bonds. Rupture of a primary valence bond produces free radicals at the newly formed chain ends which react almost instantaneously. The reformation of these bonds is not likely since the stress on the molecule would serve to separate the new chain ends and prevent the coupling reaction. The free radicals will most likely react with a water molecule. The occurrence of a region of stress-concentration sufficient to rupture valence bonds may possibly initiate failure of the entire fiber.

FACTORS AFFECTING THE AXIAL MECHANICAL PROPERTIES OF CELLULOSE FIBERS

The prerupture behavior of the cellulose fibers is determined by its molecular and fibrillar structure; several factors affect this structure and thus the mechanical properties of the fiber. The following is a review of some of the more important factors affecting the mechanical properties of cellulose fibers.

The behavior of cellulose fibers, both natural and regenerated, is strongly dependent on the mechanical history of the specimen. Meredith (3) has stated that secondary creep increases with both time and applied load. Characteristic of this behavior is the hysteresis exhibited in the stress-strain curves for repeated loading and unloading cycles.

Several studies have been made concerning the effects of drying fibers under an axial tensile stress. For a brief review and a detailed study of this work for holocellulose pulp fibers, see Jentzen (8, 9). The principal effect is to increase the orientation with the accompanying mechanical effects as discussed above. Spiegelberg's study of holocellulose pulp fibers (51) concurs with this result.

Several workers (22, 23, 52, 53) have observed that summerwood fibers have a higher tensile strength and Young's modulus but a lower ultimate elongation than do springwood fibers. Leopold and McIntosh (23) have attributed the difference to the increased percentage of the S_2 layer in the summerwood fiber. Jentzen (8, 9) found that summerwood fibers were better oriented (helix angle of 7.9°) than were the springwood fibers (helix angle of 14°). This difference in orientation accounts for much of the difference in mechanical properties of these fibers.

Orientation effects have been studied by many workers. Sisson (47) was the first to investigate quantitatively the increase in strength with increasing orientation. It has been shown that, as the orientation increases, the strength and Young's modulus increase and the ultimate elongation decreases (9, 48, 49). Wardrop (50) showed that the orientation of wood increases from the pith outward as a function of the growth ring and becomes constant after the fifteenth growth ring.

In a study of paper behavior, Brezinski (34) has shown that increasing the relative humidity of the test acts to decrease the stress required to reach a specified level of deformation in a given period of time. He showed also that appreciable amounts of secondary creep could be recovered by increasing the relative humidity during recovery measurements. Hartler, Kull, and Stockman (41) have found that the ultimate strength of pulp fibers increases as the relative humidity increases. This effect has also been noted for cotton (3).

Temperature effects are, in general, exhibited by changes in the rate of deformation; the rate of creep or recovery increases as the temperature increases. Larger temperature-dependent effects are noticed in those polymers which undergo a glass transition or phase change, but for the normal range of temperature (15-30°C.) such changes would not be expected for cellulose (30).

Pierce (42) and many other workers have shown that the tensile strength of cotton increases as the test span decreases. This has been attributed to weak spots in the fiber. Hartler, Kull, and Stockman (41) observed a similar effect for wood pulp fibers.

The effect of the degree of polymerization (D.P.) on the tensile strength of fibers has been discussed by Wakeham (43). In most work with natural fibers, the D.P. has been changed by chemical degradation, and the tensile strength has remained constant until the D.P. fell below 800. In investigating the effects of D.P., it has so far been impossible to change the D.P. and keep all other variables constant.

The effect of crystallinity on fiber properties has not been studied thoroughly since it is difficult to separate the effect of crystallinity from the effect of orientation. The studies of amine decrystallization treatments

conducted by Segal, et al. (44), Orr, et al. (45) and Ward (46) show that the ultimate elongation increases, but the strength may increase or decrease slightly due to decrystallization.

MECHANICAL TESTS

It is most desirable from a theoretical standpoint to specify the mechanical properties of fibers in terms of the molecular nature and structure of the material. The various methods of specifying the prerupture mechanical properties of viscoelastic materials have been reviewed by Ferry (30). All describe the time-dependency of stress or strain. Experimentally, the mechanical properties frequently are described by mapping out the overall behavior in a particular kind of test. In highly crystalline materials such as wood pulp fibers, this technique is normally used.

The three types of tests commonly used in studying viscoelastic materials may be classified according to the type of loading applied to the specimen. These are (1) transient loading, (2) oscillatory loading, and (3) constant rate of loading and its counterpart, constant rate of straining. Constant rate tests do not allow separation of time effects. Transient loading of viscoelastic materials involves creep and stress relaxation experiments. These experiments are limited at the low-time end by inertial effects and the finite time required to apply the stress or strain. In investigations of long-time effects, the precision of the experimental method, the stability of the material, and the time schedule of the investigator are the limiting factors.

THE CREEP TEST

Creep tests of individual wood pulp fibers most closely approximate the service conditions to which the fibers will be subjected in their utilization

as paper. An excellent survey of the creep test and the creep properties of some textile polymers was presented by Leaderman (32) in which he emphasized reversible creep behavior. The following discussion is presented to familiarize the reader with the nomenclature and fundamental principles of creep testing and was taken largely from the discussion of Brezinski (34).

Creep data are recorded as the deformation observed at various times after application of a constant load to the specimen. The load is applied rapidly compared to the first reading of deformation in order to minimize effects caused by the manner in which the load is applied. The data are obtained within a limited time interval. In other words, the test is terminated before its logical conclusion which is the cessation of creep deformation or rupture of the specimen. The data are presented as a creep curve which is normally a semi-logarithmic plot of deformation as a function of log-time. Time is measured from the instant of load application.

The various stages of deformation are illustrated in Fig. 3 where the creep curve is presented in rectangular coordinates. Total creep deformation is the sum of the immediate elastic deformation and the delayed deformations. In order to calculate the delayed deformation, the elastic modulus must be known so that the immediate elastic deformation may be removed from the total deformation. The elastic modulus is frequently determined by using the initial slope exhibited by the material in a load-deformation or normal tensile test. At low loads and short times the creep effects are small, and the initial slope of the test is a good measure of the elastic modulus.

The delayed deformation may be separated into primary and secondary creep by determining the creep recovery of the material upon removal of the load. The recoverable deformation is termed primary creep, and the nonrecoverable

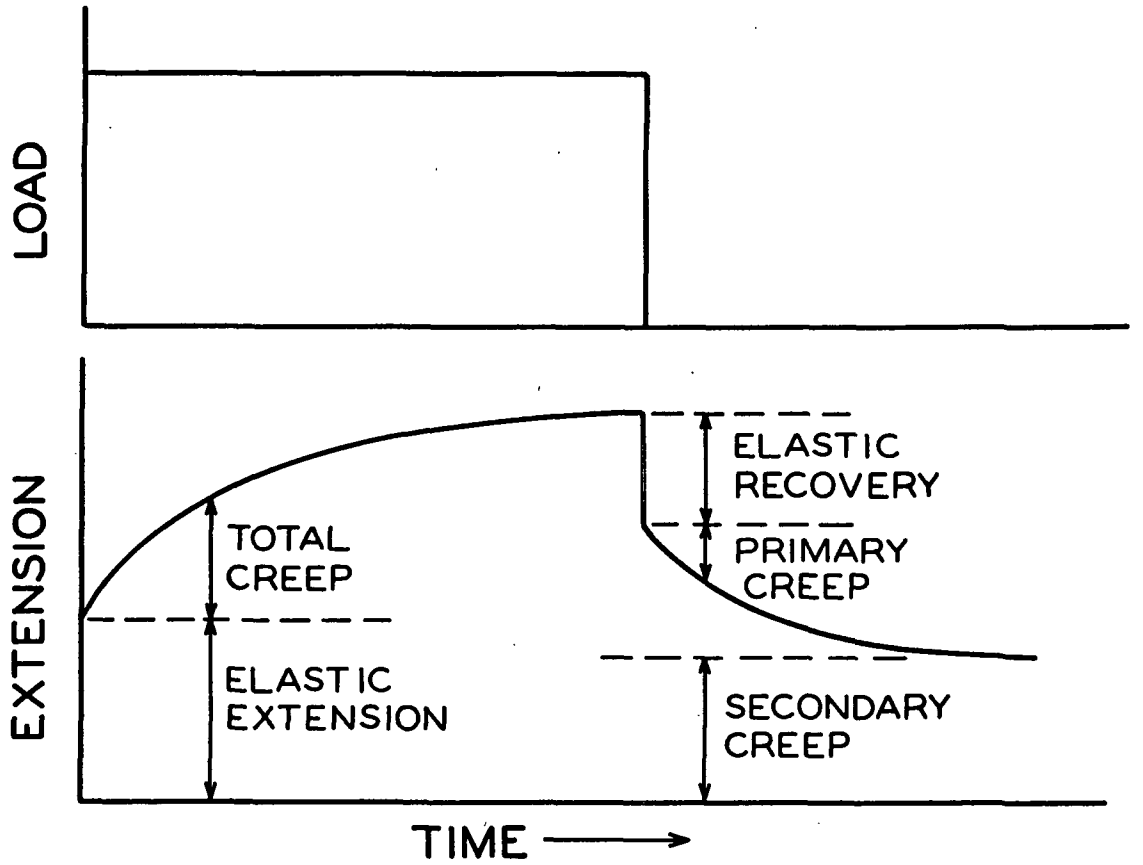

Figure 3. Load-time and Deformation-time Diagrams (32)

deformation is termed secondary creep. Once again the immediate elastic behavior must be known in order to determine the two delayed deformations. The deformations which occur during creep may change the elastic modulus of the material in such a way that a new modulus must be determined, or the recovery data must be extrapolated to zero recovery time in order to determine the immediate elastic contraction.

ANALYSIS OF CREEP DATA

The experimental problem in any study of viscoelastic behavior is to determine the relationships among stress, strain, and time for a particular loading pattern and a particular type of deformation. It is desirable to use a limited amount of data to predict the relationships for loading patterns and types of deformation other

than those used originally in obtaining the data. Various mathematical relationships and mechanical analogies have been proposed for polymers which not only describe the overall behavior of the material but also are theoretically significant. For polymers exhibiting linear viscoelastic behavior, these relationships may be interpreted in terms of molecular processes occurring in the specimen. For highly crystalline, anisotropic, heterogeneous materials such as wood pulp fibers, however, the various mathematical and mechanical analogies are reduced to empirical descriptions and are of little or no theoretical significance. Empirical descriptions of viscoelastic behavior such as Boltzmann's superposition principle and the master creep curve concept are also useful in the analysis of creep data. The following discussion was taken from Ferry (30) and Leaderman (32), and the reader is referred to these works for a more detailed discussion.

Mathematical Equations and the Creep Function

Creep data are frequently expressed in terms of a time-dependent compliance $D(t)$ for extension deformation. The quantity used for stress relaxation is the modulus $E(t)$, or Young's modulus, for extension deformation. In general $D(t) \neq 1/E(t)$, and comparison of data from creep and stress relaxation experiments is difficult. The relationship between the creep compliance, $D(t)$, and the variables: stress, strain, and time, is called the creep function and may theoretically be determined for a very wide time span (10 to 15 logarithmic decades). The creep function is of theoretical significance for those materials which exhibit only primary creep and is very complex and difficult to determine. For materials such as cellulose fibers which exhibit both primary and secondary creep, one or more simplified mathematical relationships may be developed to describe limited portions of the creep function. Since the creep function has

little theoretical importance for cellulosic fibers, various mathematical relationships are normally used only to describe various portions of the creep curve. Analysis in terms of a time-dependent compliance is of little value.

Mechanical Analogies

Early investigators utilized mechanical analogies to describe the creep behavior of high polymers. These analogies were composed of various series and parallel arrangements of springs and dashpots which represented the mechanical behavior of a viscoelastic material. It should be remembered that an infinite number of such mechanical models could be used to represent the viscoelastic behavior of a material. Except for the most simple systems, the elements of the mechanical models are not theoretically related to the molecular phenomenon occurring in the material, and such analogies are of little value in describing the complex behavior of crystalline polymers.

Boltzmann's Superposition Principle

The superposition principle was originally proposed by Boltzmann (54) in 1876 to describe the mechanical behavior of polymeric materials in the absence of secondary creep or nonrecoverable deformations. Leaderman (32) extended the principle to include nonlinear primary creep behavior. The superposition principle is an empirical description of mechanical behavior in which configurational elastic mechanisms of response are predominant. In effect, the principle states that a substance will respond to a complex loading history as if each load were applied independently for an indefinite period of time. The observed deformation at any time during the test is the simple summation of the deformations caused by all the loads in the sequence up to that instant. The removal of a load is considered as the application of a negative load, and

the creep function for a negative load is the same as that for a positive load. By accounting for the stress-dependency of the creep function, Leaderman showed that the principle may be applied to materials exhibiting secondary creep. Once the creep function is known for a material, the superposition may be utilized to predict the mechanical behavior for any desired loading history. The reader is referred to Leaderman (32) and Ferry (30) for discussions of the implications of this theory.

Generalized Creep Curve

The generalized creep curve is an empirical concept which relates a material's creep behavior to the applied stress. O'Shaughnessy (55), investigating the creep behavior of viscose rayon, found that when the specimen elongation was divided by the applied stress, and plotted versus the logarithm of time, the creep curves varied in a regular manner. He also observed that for all applied loads at both long and short times the reduced creep behavior appeared to approach a limiting value asymptotically. The creep curves could be regarded as lying between two horizontal asymptotes and crossing from one to the other following a sigmoidal curve.

Further work by Catsiff, Alfrey, and O'Shaughnessy (56) concerned with the creep of nylon led to a more generalized form for creep curves. This was termed the master creep curve. Creep data from tests at various loads were fitted to the master curve by vertical and lateral shifts after multiplication of the elongation scale by an appropriate factor. There was no speculation by the authors as to the significance of the master creep curve except that it might be related to an effective speeding up of response with increasing stress. If this is valid, then the formation of a master creep curve and the correlation of the temperature dependency of a linear viscoelastic polymer by the method of reduced variables would appear to be analogous.

The master creep curve concept has been shown to apply to paper by Brezinski (34), Schulz (36) and Sanborn (57). Since the behavior of paper is at least in part governed by intrafiber mechanisms, and since regenerated cellulosic fibers have been shown to follow this generalized treatment, it is logical to expect that the concept will also apply to individual pulp fibers.

APPROACH TO THE PROBLEM

It was hypothesized that the prerupture stress behavior of individual wood pulp fibers should be associated with changes in the fine structure of the fiber. The problem was to evaluate the prerupture stress behavior of fibers in terms of their structure and their mechanical properties.

Since time is an important factor in the prerupture behavior of pulp fibers, it was decided to use axial tensile creep experiments to separate the variables of time, stress, and strain. Axial tensile loading was selected since wood pulp fibers are most readily stressed along the fiber axis, and methods were available to apply loads of this type. The creep variables chosen for study were limited to load, time-under-load, and time of creep recovery. Investigation of other variables such as temperature, humidity, and hemicellulose content would provide useful information but would involve a prohibitive amount of experimental work.

As is true with all viscoelastic materials, the stress/strain behavior of pulp fibers is dependent on the past mechanical history of the specimen. In order to maintain a uniform population, all fibers were subjected to the same conditions before actual creep testing. Particular attention was given to drying conditions in order to eliminate the pronounced drying effects reported by Jentzen (9).

The mechanical properties chosen to be studied were creep response and the load-elongation characteristics of the fibers. The load-elongation characteristics to be evaluated as a function of creep conditions were the tensile strength, modulus of elasticity, ultimate elongation, and the work-to-rupture.

Creep recovery data yielded the permanent deformation of the entire fiber and indicated internal changes which must accompany such permanent deformation. Other indirect indications of internal structural changes came from the mechanical properties of the fibers. To test directly the hypothesized structural changes, x-ray diffraction methods were used. Analysis of Laue diffractograms was used to evaluate changes in crystallinity and crystallite orientation. The internal stress distribution of a fiber was not amenable to available or conceivable experimental methods, and such effects were inferred from the other data.

A holocellulose, longleaf pine pulp was selected as the source of fibers for this study. Only summerwood fibers from a single growth ring were studied, and each fiber used was microscopically examined to eliminate those with obvious defects. The selection of this pulp was based on obtaining as uniform a fiber population as possible so that significant results could be obtained from testing a reasonable number of fibers. Also, this pulp was used by Jentzen and Spiegelberg, and comparisons of the data from the three studies should result in additional information.

EXPERIMENTAL APPARATUS AND PROCEDURES

PULP PREPARATION

Longleaf pine (Pinus palustris) was selected as the wood species to be used in this thesis for several reasons: (1) It has long fibers which simplifies handling procedures. (2) It has relatively large growth rings which makes it possible to obtain all the required fibers from the same section of a single ring. (3) This species was used by both Jentzen (9) and Spiegelberg (22); and their data, when combined with that of this study, should provide additional useful information.

The actual pulp used was supplied by Spiegelberg and was from the same material used in his study. The holocellulose fibers were obtained in chip form, and a single chip supplied the needed fibers. This chip was from the summerwood portion of either the 27th or 28th growth ring of a 49-year old tree and measured about 1/8 x 1/4 x 3 inches.

The pulping procedure used in converting the wood into holocellulose pulp was a modification of that of Wise, et al. (58) and is described in detail by Spiegelberg (51). The delignified chip was relatively rigid, and fiber separation was facilitated by splitting the chip into fine slivers. The slivers were defibered by placing them in a one-liter plastic bottle filled with distilled water and containing ten rubber balls and then rotating the bottle at a rate of 10 r.p.m. The rubber balls were about 16 mm. in diameter and weighed approximately 5 grams each. After two hours of rotation, the resulting fiber slurry was decanted from the remaining slivers; fresh water was added, and the cycle was repeated until a sufficient supply of single fibers was obtained. The supply of never-dried single fibers and the remaining slivers

were stored at 5°C. in distilled water with 0.01% phenylmercuric acetate added to prevent biological growth.

FIBER DRYING

In order to control the conditions to which the fibers were subjected during drying, the apparatus developed by Jentzen (8, 9) and modified by Spiegelberg (22, 51) was used. The reader is referred to the work of Spiegelberg for a detailed description of the device and the operating procedures.

The apparatus basically consists of two clamps (one fixed and the other free-swinging), a spring assembly for applying a drying load (0 to 10 grams), and an optical lever system for determining the axial deformation of the specimen. The entire assembly is contained in a tank so that it may be covered with water or drained. A small fan supplies a low velocity stream of air from the room which is maintained at 73°F. and 50% R.H.

The fiber was mounted in the clamps and aligned with a jig designed for this purpose. It was never allowed to dry before removing the water from the drying apparatus. The spring assembly was attached to the movable clamp to stabilize it, and then the fixed clamp was closed. The resulting drying load was very small (estimated to be about 0.1 gram). Both Jentzen and Spiegelberg found that due to room vibrations a 1.0-gram drying load was necessary to stabilize the apparatus when the optical lever system was used. However, the optical lever system was not used in the present study, and the system was quite stable as used. Examination of the movable clamp at 60 diameters magnification revealed that vibration at right angles to the fiber axis was just noticeable (estimated to be $\pm$ 10 microns), and no axial vibration was apparent. Each fiber was dried in the apparatus for 15 minutes. The fiber was removed from the apparatus, stored individually in a marked test tube,

and given a two-number code indicating the month dried and identifying the individual fiber. This code was used to identify the fiber in all future testing.

Drying under these conditions served two purposes. First, the mechanical history of the fibers was reproducible in respect to drying tension. The second purpose was to prevent twisting of the fibers by drying them under rotational restraint. A fiber dried under no restraint will twist along its axis. The extent of this twisting varies from fiber to fiber. In preliminary creep testing, it was observed that the amount and type of twisting introduced significant variation in the fiber deformation at low times (less than 10 minutes). All fibers dried as described above were free from localized twist along the fiber, but did exhibit an end-to-end rotation of about 90° when they were removed from the drying clamps. It was felt that when dried under rotational restraint, internal stresses were set up in the fiber, and these were at least in part relieved by the observed end-to-end rotation.

CREEP-RECOVERY TESTING

APPARATUS

In order to follow the creep and creep-recovery behavior of individual wood pulp fibers, a special piece of equipment had to be designed and built. The requirements of this apparatus were: (1) a set of clamps which would hold the fiber securely but not damage the fiber; (2) a device to measure the time-dependent elongation after the load was applied and to measure the time-dependent contraction when the load was removed; and (3) a device to apply a constant load which would not change appreciably as the fiber elongated and contracted. The apparatus which was used and which meets these requirements is shown in Fig. 4. A schematic diagram is shown in Fig. 5.

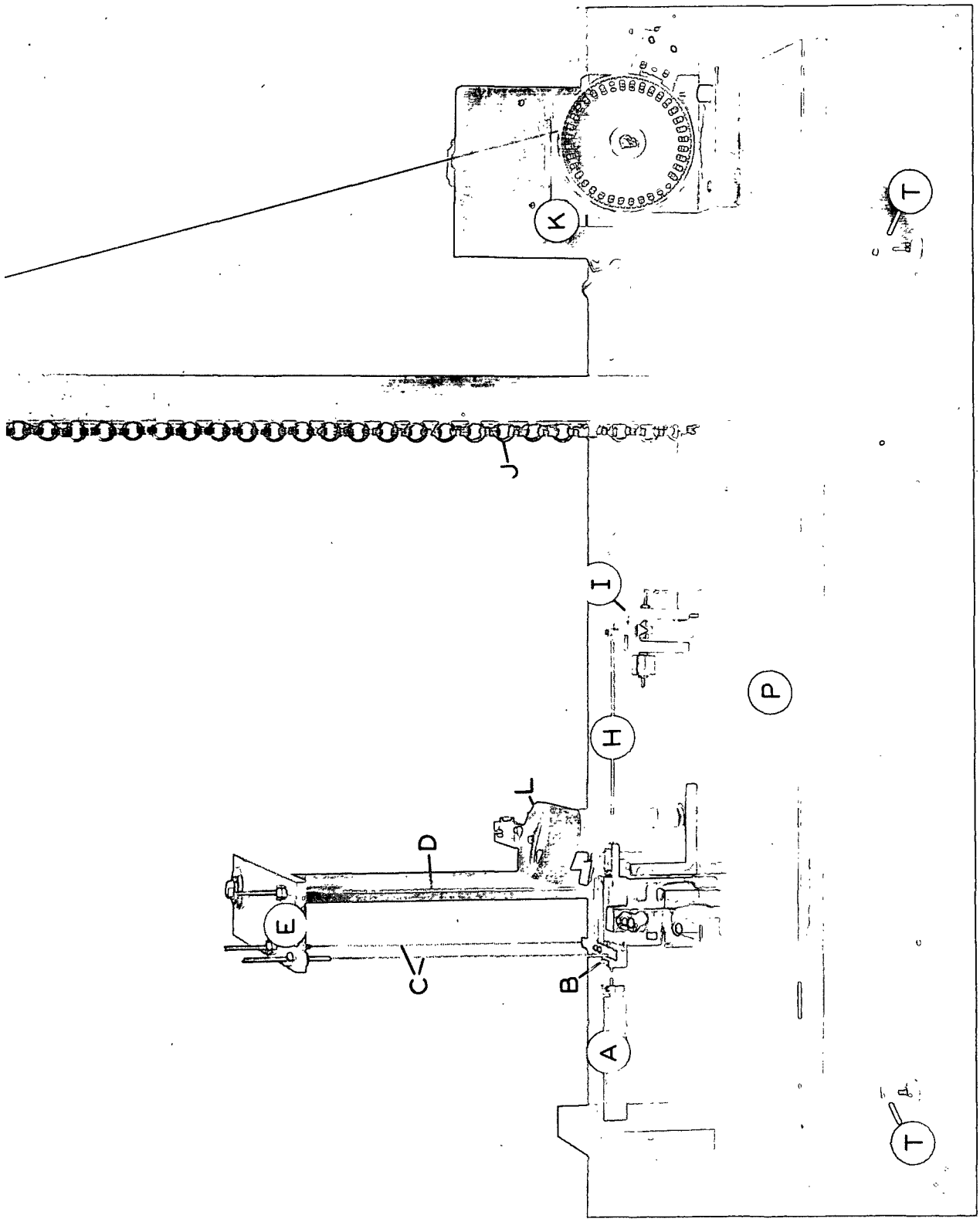

Figure 4. Photograph of Fiber Creep-Recovery Recorder

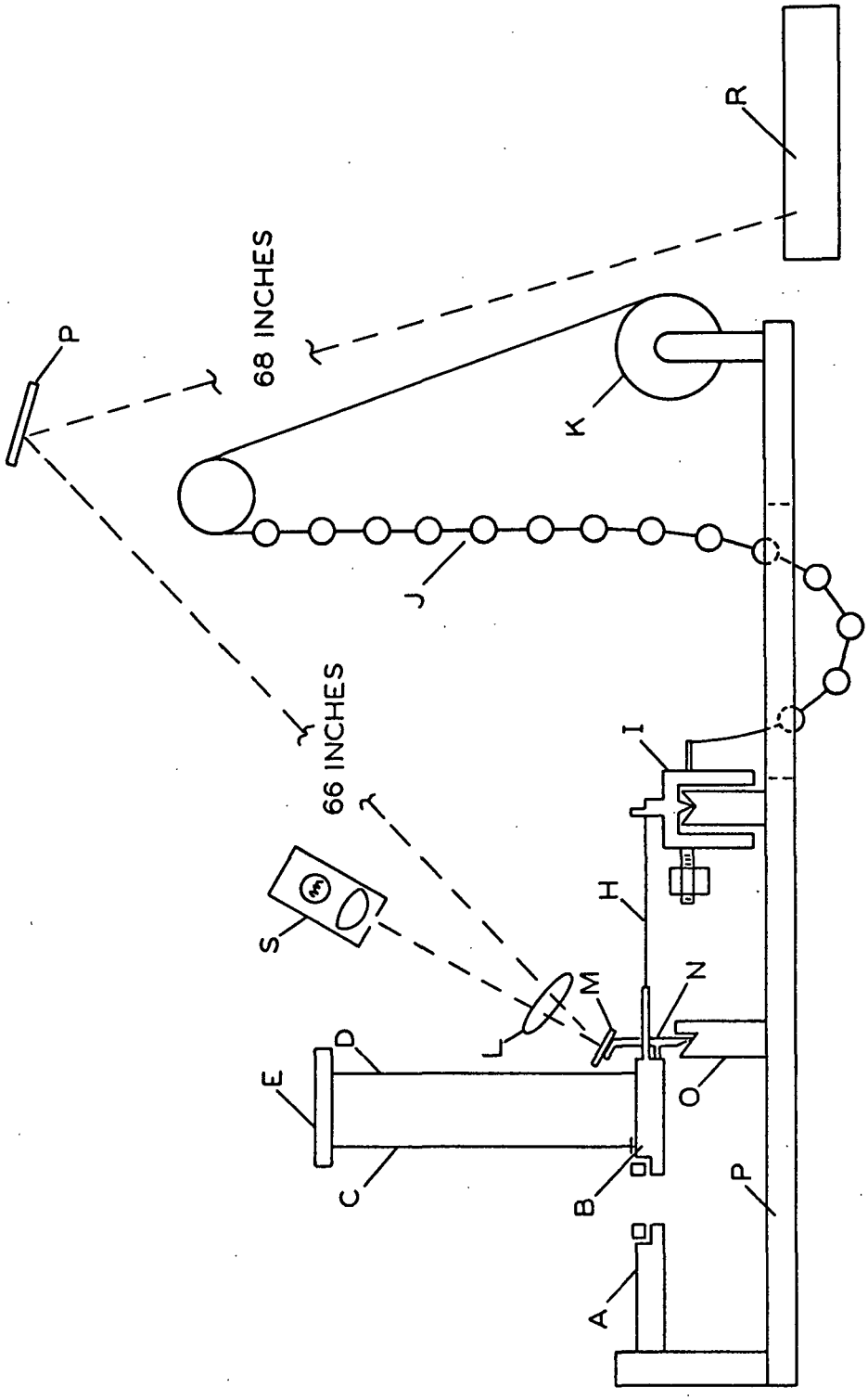

Figure 5. Schematic Diagram of Fiber Creep-Recovery Recorder

Design

It was decided that individual fibers would be mounted and held in the same manner used for the I.P.C. Fiber Load-Elongation Recorder (FLER) (59) in order to facilitate later load-elongation testing. This method first glues a fiber between two 1/32-inch diameter stainless steel pins. Therefore, the problem of designing clamps so as to prevent fiber damage was eliminated. Instead, clamps were needed to hold the pins. The pins were gripped in a fixed clamp (A) and a movable clamp (B). The clamps were made from 1/2-inch square aluminum stock, center-drilled to receive the pins. Clamping was achieved by removing a 1/8-inch segment of the stock down to the pin hole center line and affixing a 1/8-inch square aluminum bar over the exposed pinhole by means of two hex head screws. The jaw thus formed was opened by loosening the screws; the pin inserted; and the screws tightened so that the pin was securely held in the clamp.

As shown in Fig. 4, the fixed clamp (A) was fastened securely to a rigid brass support mounted on the apparatus base plate (P), and the movable clamp (B) was suspended by three fine jeweler's chains (C,D). The two chains (C) closest to the fixed clamp were attached to a cross arm fixed to the clamp and were 1-3/4 inches apart. The chain (D) was attached directly to the clamp 1-3/8 inches back of the chains (C) and on the center line of the clamp. Adjustment of the movable clamp in all directions was provided by the chain holder (E). The movable clamp was designed to be held in this manner so that its center line could be aligned with that of the fixed clamp.

A locking mechanism (F,G) was added so that the movable clamp could be locked in place to prevent fiber damage when the clamp jaws were tightened on the pins. Locking was accomplished by having a plate (F) fixed to the apparatus

base and a pivot arm (G) to apply a force to hold the clamp against this plate. The plate (F) was fixed parallel to the movable clamp and separated from it by less than 10 microns. The two surfaces which touch in the locked position were carefully machined and polished to allow close alignment and were very lightly dusted with Molykote* (molybdenum disulfide) to prevent sticking.

The load was applied to the fiber by means of the system composed of parts labeled H, I, J, and K. The load was applied to the movable clamp (B) through a jeweler's chain (H) connected to a pivot arm (I) supported on an agate plate and a steel knife-edge. This pivot translated the weight of the chain (J) into the desired horizontal force. The load was varied by raising or lowering the chain (J) utilizing the reversible, motor-driven winch assembly (K). The motor drive for this part is equipped with a "positive clutch and instantaneous brake" which made it possible to stop the drive within four-tenths of a degree. The winch is equipped with a vernier scale reading 0-360° to the nearest 10' of arc. The rate of loading the fiber was about 1 gram per second. As the fiber extended, the load changed slightly due to rotation of the pivot arm; but for the very small angular rotation (estimated 0°-30') which this arm experiences, the load variation was negligible.

To measure the fiber elongation and contraction, an optical lever was used in conjunction with a slit camera (R). This system is shown in Fig. 6. A mirror (M) was glued to a T-shaped support (N). The bottom of the support was ground to a sharp knife-edge, and this rested in the V-groove of the mirror support (O). A steel pin about 0.140 inch long was attached to the mirror support about 0.170 inch above the knife-edge, and this rested against the back

*Manufactured by The Alpha Corporation, Greenwich, Conn.

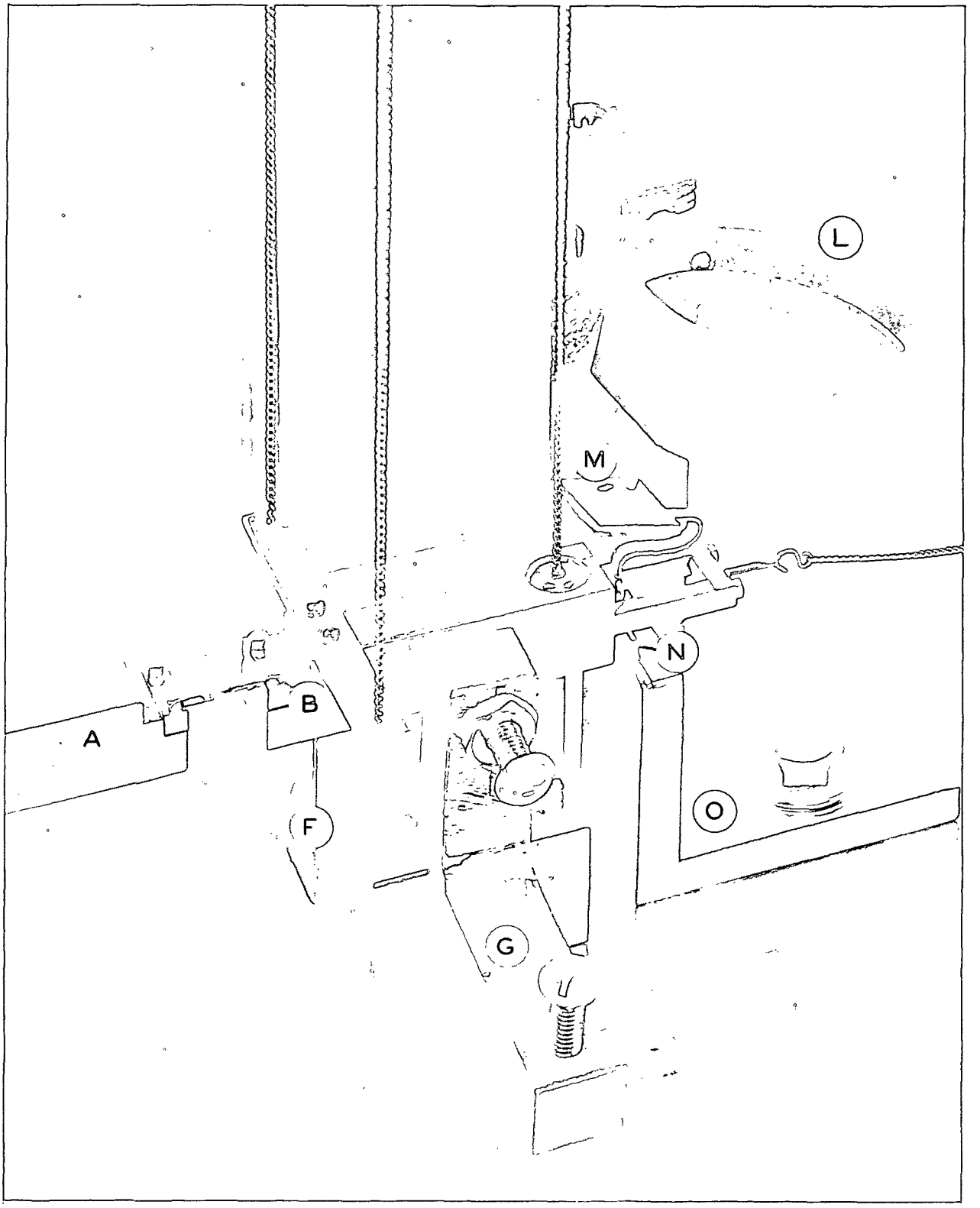

Figure 6. Detail Photograph of Fiber Creep-Recovery Recorder

of the movable clamp. The image of a slit (from Part S) was focused on a distant recorder (R) by means of the acromatic lens (L). When the fiber changed length, the clamp (B) moved a corresponding amount. This produced a rotation of the mirror support about its knife-edge. Thus, the position of the illuminated slit changed on the recorder.

The recorder (R), a slit camera, turned at the rate of one revolution in twelve hours. The image of the light source slit (from Part S) was at a right angle to the slit running along the recorder axis; thus, a dot of light reached the photographic paper. Movement of this dot along the recorder axis recorded the fiber deformation, and the clock mechanism revolving the photographic paper past the camera slit provided the time measure.

Five photographic recording papers were evaluated for use in the recorder. These were: Kodak Linagraph papers Numbers 480, 697, and 622 and Ansco Linatrace N-1 and N-3 photo recording papers. It was necessary to have an emulsion with a wide exposure latitude and high speed. Both Kodak Linograph 622 paper and Ansco Linatrace N-3 photo recording paper were satisfactory, but the Ansco product had the fastest emulsion and proved the most desirable.

A total of six of these Fiber Creep-Recovery Recorders (FCRR) were constructed. Each unit was equipped with four leveling legs (T) attached at the corners of the base plate (P). A cathetometer equipped for determining vertical angles as well as level was used to aid in careful leveling and alignment of each unit. The units were placed on cement tables weighing approximately 1500 pounds which in turn were supported on four 1-inch thick Unisorp pads. The result of this was that room vibrations were not noticeably transferred to the apparatus. The room in which the units were placed was maintained at 50% R.H. and 73°F.

Calibration – Optical Lever

In order to calibrate the optical lever, the fixed clamp (A) was removed, and the micrometer head built by Jentzen (8) was inserted in its place. This head provided a positive incremental method to displace the movable clamp (B). A 3-micron glass fiber was attached to the movable clamp to serve as a reference mark, and its displacement was measured using a microscope with a calibrated eyepiece scale. The eyepiece scale was calibrated by means of a stage micrometer, and each eyepiece scale division represented 5 microns. The microscope was focused so that the fiber appeared as two dark lines separated by a bright center about 1 micron wide. The image of the scale and the glass fiber were projected onto a strip of Kodak Linograph 480 paper at an enlargement which gave a one centimeter separation of the scale divisions, and both the scale and fiber positions were recorded. On the resulting photographs, interpolation to 1/2 micron was possible by determining the center of the bright area of the fiber at successive displacements in reference to the fixed scale. The corresponding displacement of the optical lever was recorded using the same photographic paper in the recorder (R). The paper in the recorder was printed in a contact printer with a rectangular grid of twenty lines per inch; after development, the displacement record in the recorder was read to the nearest one-half grid division or 1/40 inch. This procedure prevented errors in the record from being introduced by localized distortions of the photographic paper which might occur during development and print drying. Figure 7 is a calibration curve for FCRR – Unit I and is typical of all six units. Three complete passes were made across the recorder, and the data were taken corresponding to a fiber extension, a contraction, and another extension. It should be noted that the scales used to show both the actual displacement (microns) and the chart readings (inches) are greatly compressed in this figure.

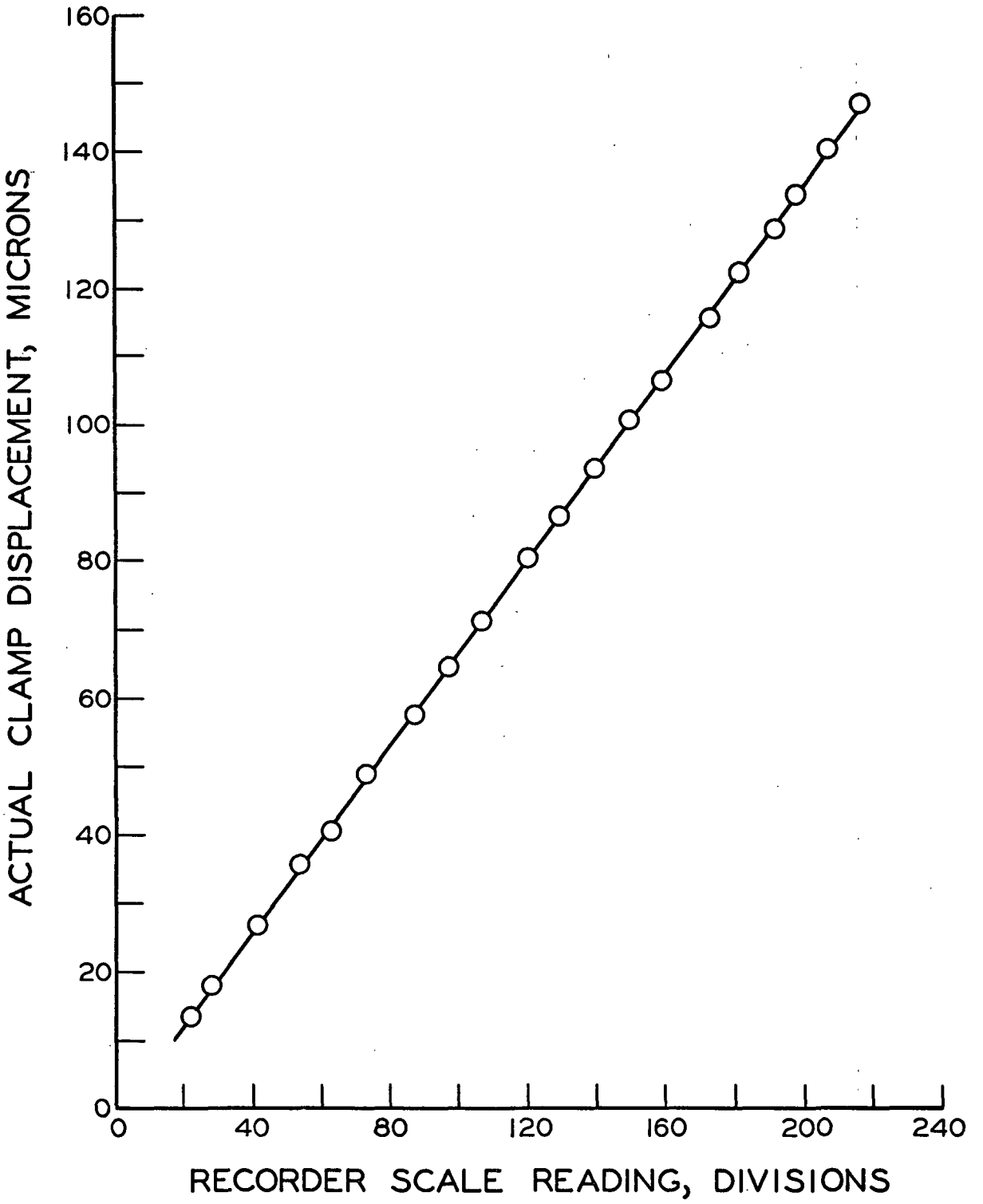

Figure 7. Optical Lever Calibration, FCRR – Unit I

Although the theoretical relationship based on the dimensions of the optical lever system is nonlinear, examination of the data shows that for practical purposes a linear relationship fits the data very well. Linear regression analysis of these data gives the straight line $\underline{x} = 0.6757\ (\underline{R})$; where $\underline{x}$ is the actual displacement in microns, and $\underline{R}$ is the recorder reading in scale division. The regression has a correlation coefficient of 0.9998 and a variance about the line of 2.86. The magnification of this system was 1880X.

Calibration – Load

Calibration of the loading system was made against a dead weight load. The initial position of the movable clamp was located by setting the initial space between the clamps with a gage block (as is done in creep testing) and using the optical lever system as a balance indication. The initial position was located by drawing a reference line on a piece of white paper placed over the recorder opening.

The dead weight load was applied by removing the fixed clamp (A), running a glass core, radio dial cord from the movable clamp over a needle-bearing pulley, and attaching known weights to a pan on the end of the cord. The weight of the cord and pan was accounted for in the calibration. During calibration, the known load was balanced by using the winch assembly (F). Balance was indicated when the optical lever returned the slit image to less than 1/2-inch of the reference mark. The sensitivity of the optical lever system was much greater than the instrument capability of stopping the winch at the exact balance point. Known load increments of 0.05 gram could be balanced. Figure 8 shows the calibration curve for Unit I and is typical of all units. The scale of the instrument reading (degrees winch rotation) and

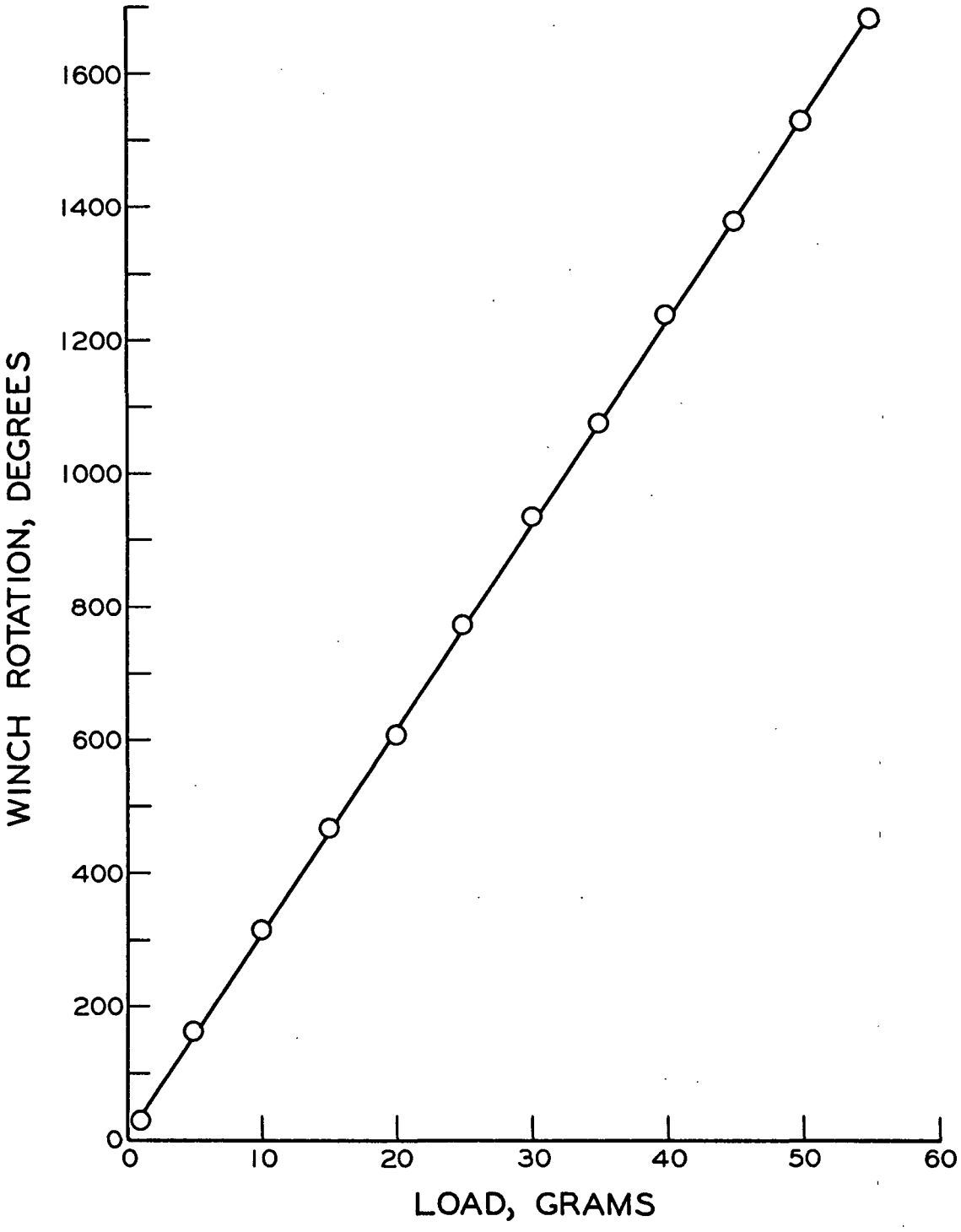

Figure 8. Load Calibration, FCRR – Unit I

the load (grams) is greatly compressed in this figure. Linear regression analysis of the data gives a slope of 0.0323 g./deg. for the load calibration line with a correlation coefficient of 0.9999. Since the scale may be read to the nearest 10' of arc and the winch stopped to within plus or minus 1/3°, any desired load may be applied with an error of approximately 0.01 gram or 0.1% of the minimum load used (10 grams) in fiber testing.

PROCEDURE

Before creep testing, the fibers which had been dried as discussed above were glued between the ground ends of two pins. The pins were first placed in a numbered spring-loaded holder and gapped with a thickness gage. Nominal span was set at 1.00 mm. A fiber was placed on the pins, and a small amount of Epon 907* was used to glue the fiber. This glue was prepared by weighing 10 parts of Component A and 6 parts of Component B and then mixing thoroughly. The glue was used no longer than 15 minutes after mixing, and it was possible to mount about 20 fibers in this 15-minute period. The epoxy was allowed to cure for 48 hours before fiber testing. The actual span between glue lines was determined using a calibrated microscope eyepiece scale and recorded. A discussion of the glue behavior when supporting a fiber under load is presented in Appendix I. There was no apparent creep in the glue when mixed as above.

The fiber thus mounted was inserted in the FCRR. To insert the fiber, the pin holder was first gripped in a spring-loaded clamp to insure no slippage. Then the movable clamp was swung back, and one of the pins was placed in the jaws of the fixed clamp. Next, the movable clamp was carefully swung into position and the second pin was placed in its jaws. The movable clamp was located relative to the fixed clamp with a gage block, locked in position, and

*Manufactured by Shell Chemical Company.

the jaws tightened. After the jaws were tightened, the pin holder was removed and the pivot mirror positioned. Next, the chain for applying the load was attached, and a load of 0.1 gram was applied to insure that no accidental compressive force buckled the fiber. The recorder clock drive was started, and the light source turned on. The movable clamp was released, and at least 15 minutes passed before application of the creep load in order to establish the zero line on the recorder. After this period, the time was recorded at the start of loading; the load was then applied and the scale reading recorded. At the end of the test, the time was again recorded at the start of unloading. Creep runs were made at 10, 15, 20, and 25-gram loads and for 12, 24, and 48 hours.

If it was desired to follow the creep recovery of the fiber, the recorder continued to operate for a period equal to the time of creep; and a residual load of 0.1 gram was left on the fiber to stabilize the system.

At the end of testing either creep or creep recovery, the movable clamp was again locked into position, and the fiber was removed by following the reverse of the procedure described above for insertion.

The mechanical properties of the fibers thus removed were determined within a maximum of 15 minutes, usually within 5 minutes, on the I.P.C. Fiber Load-Elongation Recorder (FLER). For those fibers on which load-elongation data were obtained before creep recovery, the procedure for removing them from the FCRR was to lock the movable clamp as soon as the load was reduced to 0.1 gram, grasp the pins in the holder and spring-loaded clamp, and then immediately remove them from the clamp jaws. Of necessity a period of about 5 minutes of stress relaxation was experienced by the fibers before testing in the load-elongation recorder.

LOAD-ELONGATION MEASUREMENTS

All load-elongation measurements on the individual fibers were made on the FLER (59). The fibers as mounted for the creep apparatus were used. The nominal span length for all fibers was 1.00 mm. as previously mentioned; and just before loading the specimen, the span between glue lines was again determined with a calibrated eyepiece in a bifocal microscope mounted on the FLER.

A 9.17-g./cm. chain and a 10-r.p.m. motor were used in the FLER for all testing. This resulted in a loading rate of 2.0 g./sec. Room conditions were maintained at 73°F. and 50% R.H.

CROSS-SECTIONAL AREA MEASUREMENTS

The fiber cross-sectional area was determined with the I.P.C. Compacted Fiber Dimension Apparatus (60). In this apparatus, the fiber is compressed between two optical sapphire plates. The compressive force collapses the pores and lumen of the fiber, and the area measured approximates that of the solid fiber. The thickness was measured by a linear-variable transducer, which measured the plate separation by the difference between two null point readings. The collapsed width was determined by a Cooke-A.E.I. image-splitting eyepiece* inserted in a microscope with a 10-power objective (total magnification was 100X).

The area was calculated by a formula which accounts for the rounded edges of the compressed fiber:

$$\underline{A} = 0.001369\ T\ W - 0.0000654\ \underline{T}^2$$

where $\underline{T}$ = the thickness in transducer values, $\underline{W}$ = the difference in the image-splitting eyepiece micrometer readings, and $\underline{A}$ = the cross-sectional area in square microns.

*Vickers Instrument Ltd., York and Croydon, England.

CRYSTALLINITY AND CRYSTALLITE ORIENTATION MEASUREMENTS

To obtain measurements of both crystallinity and crystallite orientation, Laue x-ray diffraction patterns were taken of the fibers. The microdensitometer built and described by Jentzen (9) was used for quantitative analysis of the photographic film negative on which the diffraction patterns were obtained. The reader is referred to the above work for a detailed discussion of this apparatus and its use.

X-RAY CAMERA

In order to take the Laue patterns of fibers under load, the camera built and described by Jentzen (8) was modified. The x-ray camera as modified is shown, in section, in Fig. 9. One modification of the camera consisted of removing the section of pipe used to space the front and back plates and, instead, using 3/8-inch I.D. pipe over each of the bolts originally holding the plates together. This necessitated enclosing the photographic film in a light-tight envelope since the interior of the camera itself was no longer light-tight. A rubber O-ring was forced over the beam catcher to seal the hole in the film and envelope through which the beam catcher passes. The back side of this opening required no light seal.

The major modification of this camera consisted of adding a device which provided a means for applying a load to a bundle of 25 fibers and allowing them to creep. Figure 10 is a photograph of the straining device and the front plate of the camera. This device was one used by Lathrop and Hardacker (61) to strain fibers. It was attached to the front plate of the camera in such a way that the fiber bundle was in line with the collimator. This device has been described by the above authors; in essence, it is composed of a balanced beam free to move

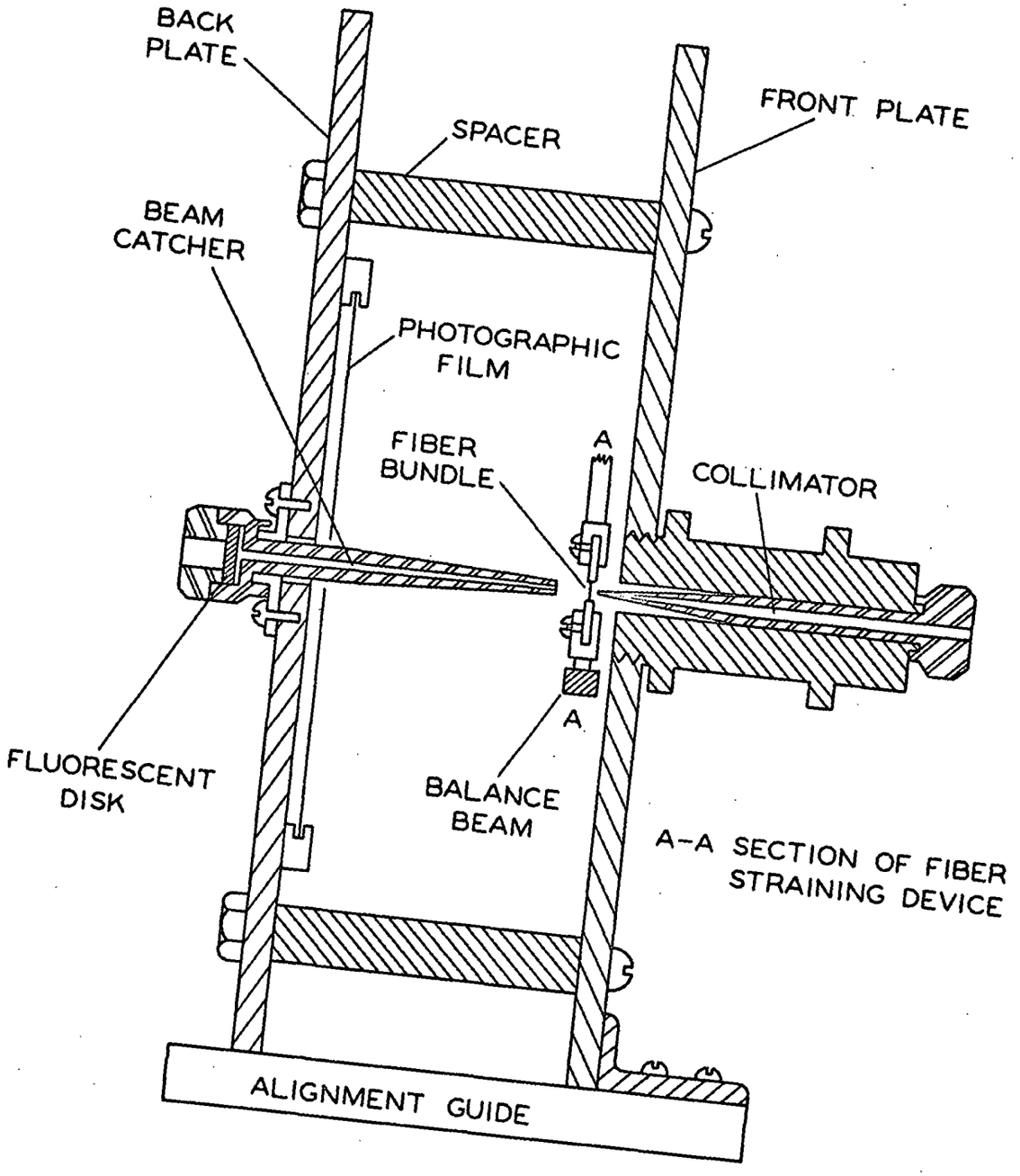

Figure 9. Schematic of Laue X-ray Camera

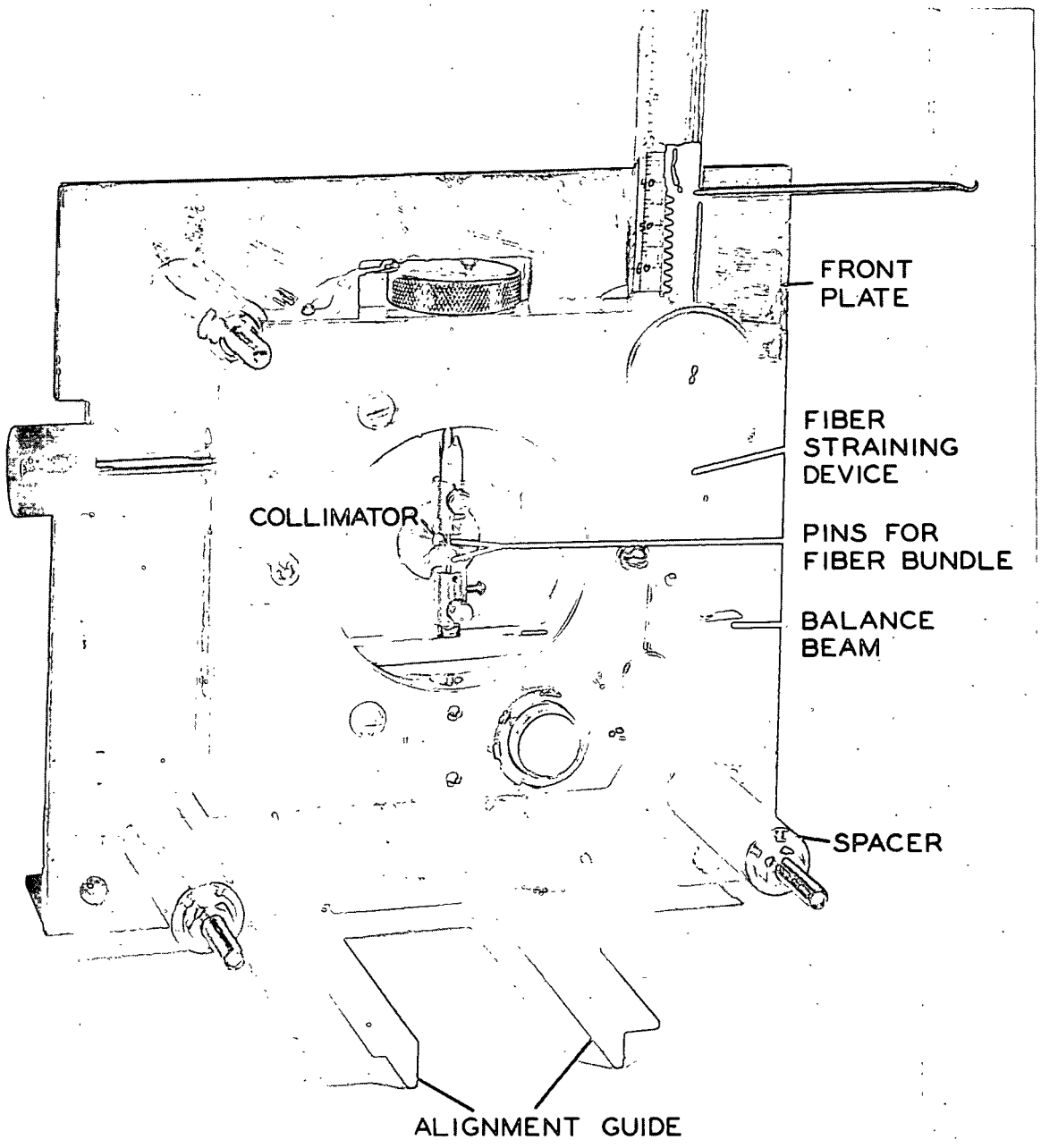

Figure 10. Photograph of Laue X-ray Camera

with a jaw for gripping the pins mounted on it, a beam-arresting device, a device for gently applying a load to the beam, and a fixed jaw in line with the jaw on the beam.

X-RAY DIFFRACTION PROCEDURE

Jentzen found that an exposure time of about 30 hours was required to obtain a satisfactory diffraction pattern of one fiber, and this would be much too long to check the response of these structural parameters under a loaded condition. Thus, it was decided to test a bundle of 25 fibers mounted in a parallel array five fibers wide and five fibers deep. An exposure time of 120 minutes was used for this bundle.

The fibers for use in the x-ray camera were dried using the apparatus previously mentioned. In this case, instead of drying one fiber at a time, sheets of five fibers each were carefully separated from the stored slivers of the original pulp chip. One end of this sheet was inserted and gripped in the movable clamp of the drying apparatus. Then, with a knife ground from the flattened point of a dissecting needle, the fibers were separated down to the clamp jaws. The separated ends of the fibers were then gripped and dried as before. The sheets thus dried remained joined at one end, and mounting on the pins was greatly facilitated.

All x-ray diffraction patterns were taken with a Norelco x-ray unit using $CuK\alpha$ radiation obtained with the tube operating at 50 kilovolts and 20 milliamperes. Kodak Type KK X-ray Film was used to record the diffraction patterns. The pins holding a bundle of twenty-five fibers were carefully placed in the jaws of the stressing device, the loading beam was locked, and the bundle was checked to make certain the fibers were centered on the collimator opening. The front and back plates of the camera were then assembled.

The assembled camera and fibers were taken to the x-ray unit and aligned with the beam by observing the fluorescent disk in the end of the beam catcher at low x-ray intensity (in a darkened room). A 120-minute exposure was taken. The room in which the x-ray unit was located was uncontrolled and subject to atmospheric temperature and humidity fluctuations. After the initial exposure under no load conditions, the camera was returned to a conditioned room at 50% R.H. and 73°F. The beam was released, and a load of either 250 or 500 grams was applied to the fiber bundle (10 or 20 g./fiber). These loads were selected since the study of individual fibers indicated that the amount of permanent deformation was significantly different between these loads. After a period of twelve hours under load, the load was removed and the beam locked; the camera was then returned to the x-ray unit. The load was reapplied and an exposure made. To determine the changes which occurred after creep recovery, the camera was once again placed in a conditioned room for at least twelve hours with no load on the fibers; and the third diffraction pattern was recorded.

Scheduling time on the x-ray unit caused the recovery period to extend to a maximum of 5 days; but since no significant recovery occurs after about 10 hours, this should not affect the data.

FILM DEVELOPING PROCEDURE

All the films used in the x-ray work were developed by the following procedure. The developing, stop, and fixing solutions were placed in a constant temperature bath held at 20° $\pm$ 0.2°C. The film was placed in Kodak Rapid X-ray Developer for eight minutes, in a 1% by volume glacial acetic stop bath for 30 seconds, in Kodak X-ray Fixer for 15 minutes, and finally, washed in running water for 30 minutes. In all cases the film was agitated to insure fresh solution on the emulsion. This procedure was selected to give uniform reproducible development and maximum density.

CRYSTALLINITY ANALYSIS

A typical Laue x-ray diffraction pattern of a fiber bundle is shown in Fig. 11. This pattern is indistinguishable from that of a single fiber taken by Jentzen. The two spots farthest from the center of the film were produced by the 002 lattice diffraction, which is the most intense lattice diffraction for cellulose I. The other two spots along the same axis are produced by diffractions from both the 101 and $10\bar{1}$ lattice planes. These diffractions are not resolved. The four less intense spots at a 45° angle relative to the axis of the 002 arcs are caused by the 021 lattice diffraction.

In general, the crystallinity is related to the intensity of the arcs compared to the amorphous background. The lighter strips at the top and bottom of the pattern are unexposed, and the amorphous background is easily distinguishable. Jentzen (8) has thoroughly reviewed the procedure and methods for determining the crystallinity from a Laue pattern, and the reader is referred to his work for this discussion.

Two measures of fiber crystallinity were determined. The crystallinity index as proposed by Segal, Creely, Martin and Conrad (62) is defined as

$$CrI = (I_{002} - I_{am}) \cdot 100/I_{002}$$

where CrI is the crystallinity index; I_{002} is the maximum intensity of the 002 arc; and I_{am} is the minimum intensity between the 002 and 101 arcs. The measure of crystallinity based on the integral half width of the 002 lattice diffraction proposed by Gjonnes, Norman, and Viervol (63) was also evaluated.

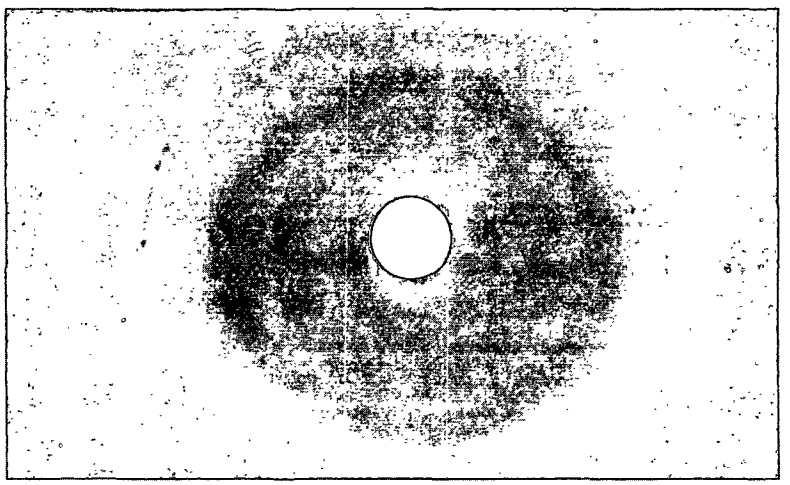

Figure 11. Laue X-ray Diffraction Pattern of a 25-Fiber Bundle

CRYSTALLITE ORIENTATION ANALYSIS

The reader is referred to Jentzen (8) for a discussion of the various methods of determining the crystallite orientation of a fiber. The method used in this study was the one he found most useful for work with single holocellulose fibers. This method consisted of fitting the entire circumferential scan of the 002 arcs to a normal distribution. The standard deviation of the normal curve is a measure of the width of the curve and, thus, the orientation.

The method requires first that the accumulative area under the circumferential scan from -90° to +90° be calculated. This area was then normalized to change it to accumulative probability. The accumulative probability $P(u)$ is

$$P(u) = (1/\sqrt{2\pi}) \int_{-\infty}^{U} \exp(-u^2/2)\, du$$

The variable $\underline{u}$ is defined as $\underline{u} = (\underline{x} - \mu)/\delta$, where $\underline{x}$ is the value of an observation, μ is the universe mean of the observations, and δ is the universe standard deviation. By a trial and error solution, the value of μ may be determined for each value of the accumulative probability. A linear regression of $\underline{x}$ on $\underline{u}$ results in the slope of the line which is the desired standard deviation of the normal curve.

EXPERIMENTAL DATA AND DISCUSSION OF RESULTS

INTRODUCTION

This study was based on the hypothesis that the time-dependent response of individual wood pulp fibers to an applied stress should be associated with changes in the fine structure of the fiber. In particular, the rate of fiber deformation should be controlled primarily by molecular configurational changes within the fiber leading to changes in the nature and arrangement of the load-bearing fibrils. Such changes may possibly result in an increase in the crystallinity of the cellulosic elements and would result in better alignment of the fibrils (increase in crystallite orientation). Removal of the external stress would allow at least partial recovery of these changes. Further, as the result of these structural changes, the modulus of elasticity and tensile strength should increase.

In order to test this hypothesis, the following studies were made: axial tensile creep and creep recovery, x-ray diffraction, and load-elongation recording. The following is a discussion of the results of these tests and an interpretation of how they support the hypothesis.

AXIAL TENSILE CREEP AND RECOVERY

A single creep curve describes the relationship between the delayed deformation and time, within the limited test interval, at a single initial stress. A number of creep curves at different initial stresses are necessary to investigate the effects of stress on creep response. The tests should embrace the widest range of initial stress and time. The practical ratio of the highest to lowest initial stress is limited by specimen rupture at the higher stresses and by the small delayed deformation at the lower stresses.

TREATMENT OF DATA

In this study of individual fibers, it was not possible to determine the creep response at various predetermined initial stresses because the cross-sectional area may be determined only by destructive testing. Preliminary determinations revealed a range of 414 $(\mu m.)^2$ to 645 $(\mu m.)^2$ for fiber areas. Since this was the case, creep tests were made at constant load. The loads used were 10, 15, 20, and 25 grams, and the tests were run for 12 and 24-hour periods on about 50 fibers at each condition. Very limited data (about 10 fibers) were obtained for creep of 48-hour duration. The range of loads was about 20 to 60% of the average breaking load of these fibers.

The typical variation in the creep response of the fibers is shown in Fig. 12. The three creep curves (for three individual fibers) plotted in this figure were selected to represent the range of response of 98 fibers tested at a load of 20 grams. The total fiber deformation as percentage of the initial span is plotted versus the logarithm of the time in seconds. These tests were terminated after 12 hours (43,200 seconds). The initial stress for these fibers is also indicated in the figure.

There are two principal sources of variation which combine to produce the spread in the data shown in this figure. First, there is the variation in response due to inherent structural differences between fibers leading to different creep behavior. The second source of variation is due to the stress dependency of creep or viscoelastic response. Even if the inherent nature of the fibers produced a population varying only in cross-sectional area, this unknown difference in area would result in variations in creep response at constant load similar to that observed. However, it is probable that other, independent sources of variation also exist. Due to wide variances and a large

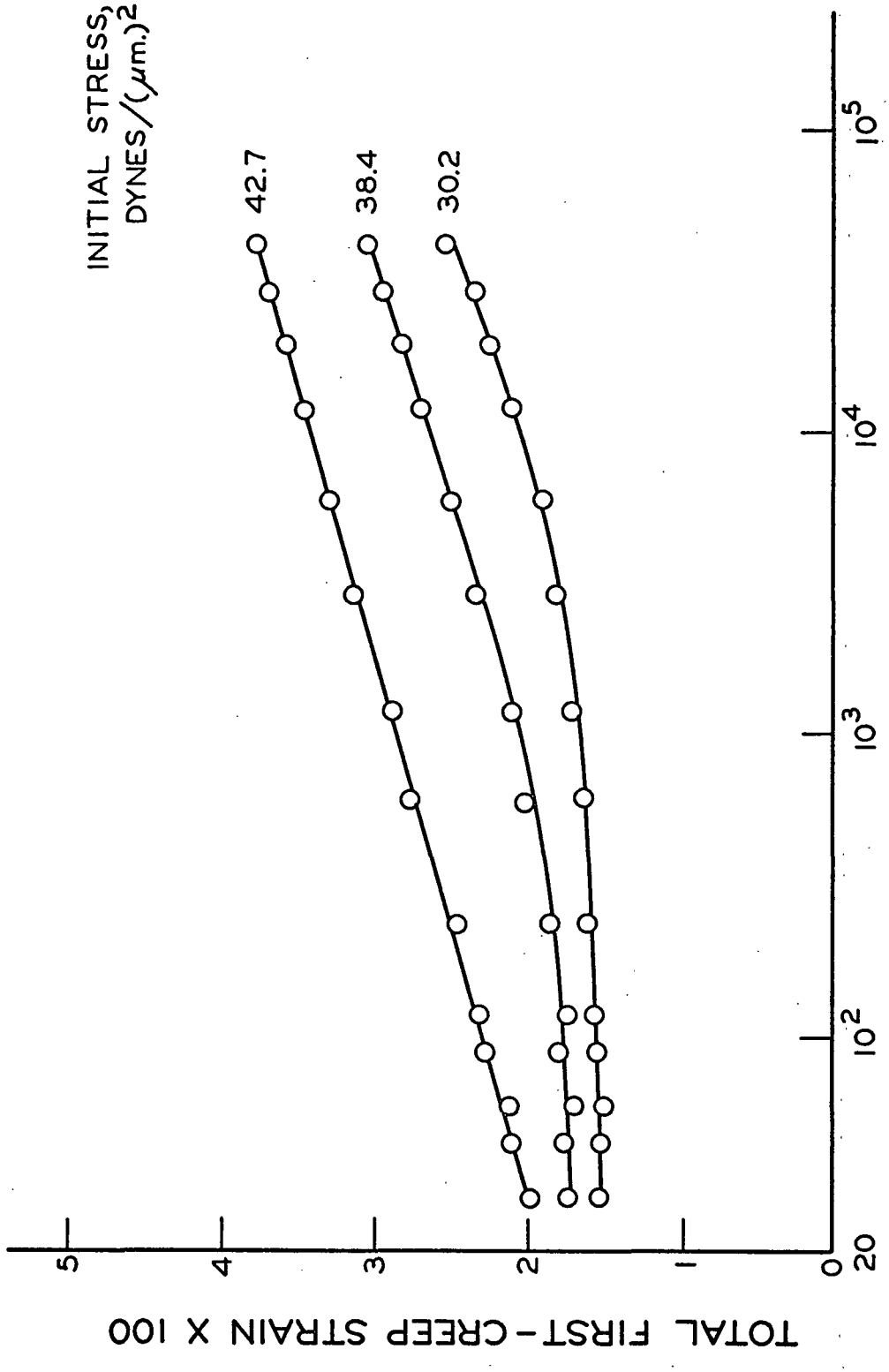

Figure 12. Typical Individual Fiber First-Creep Curves

amount of data, the problem involved is to select an appropriate method of combining the data to obtain a representative response for the fiber population tested. This problem may be approached by either of two methods.

The first method investigated for combining the data relied on the master creep curve concept. As discussed previously, this concept says that the effect of increasing the initial stress in creep tests is to speed up the various mechanisms of response. The observed response at any initial stress is merely some part of total possible response of the material. To evaluate the use of this concept for combining the raw data, a master creep curve was constructed. A total of 98 creep curves for 12 and 24-hour tests of fibers at a load of 20 grams was used. This involved plotting the quotient of the strain to the initial stress and then shifting the reduced curves along the time axis until they coincided in the regions of overlap. The resulting master creep curve is shown in Fig. 13. The time shifts required to produce coincidence are apparently linearly related to the initial stress as shown in Fig. 14. There is considerable scatter in the required time shift which is probably due to the inherent variation in the fiber population. The curve at an initial stress of 30.2 dynes/$(\mu m.)^2$ was selected as the base for the master creep curve since it represented the lowest reduced deformation, and only positive (toward longer times) time shifts were required. By allowing negative time shifts, any of the creep curves would be a possible basis for forming this generalized curve.

A second curve is also shown in Fig. 13. This curve represents the average deformation of all the creep curves and represents the second method tested for combining the raw data. The average deformation was determined at selected times for all tests at a given initial load. The shape of this average curve is the same as that of the master creep curve; the time shift required to bring

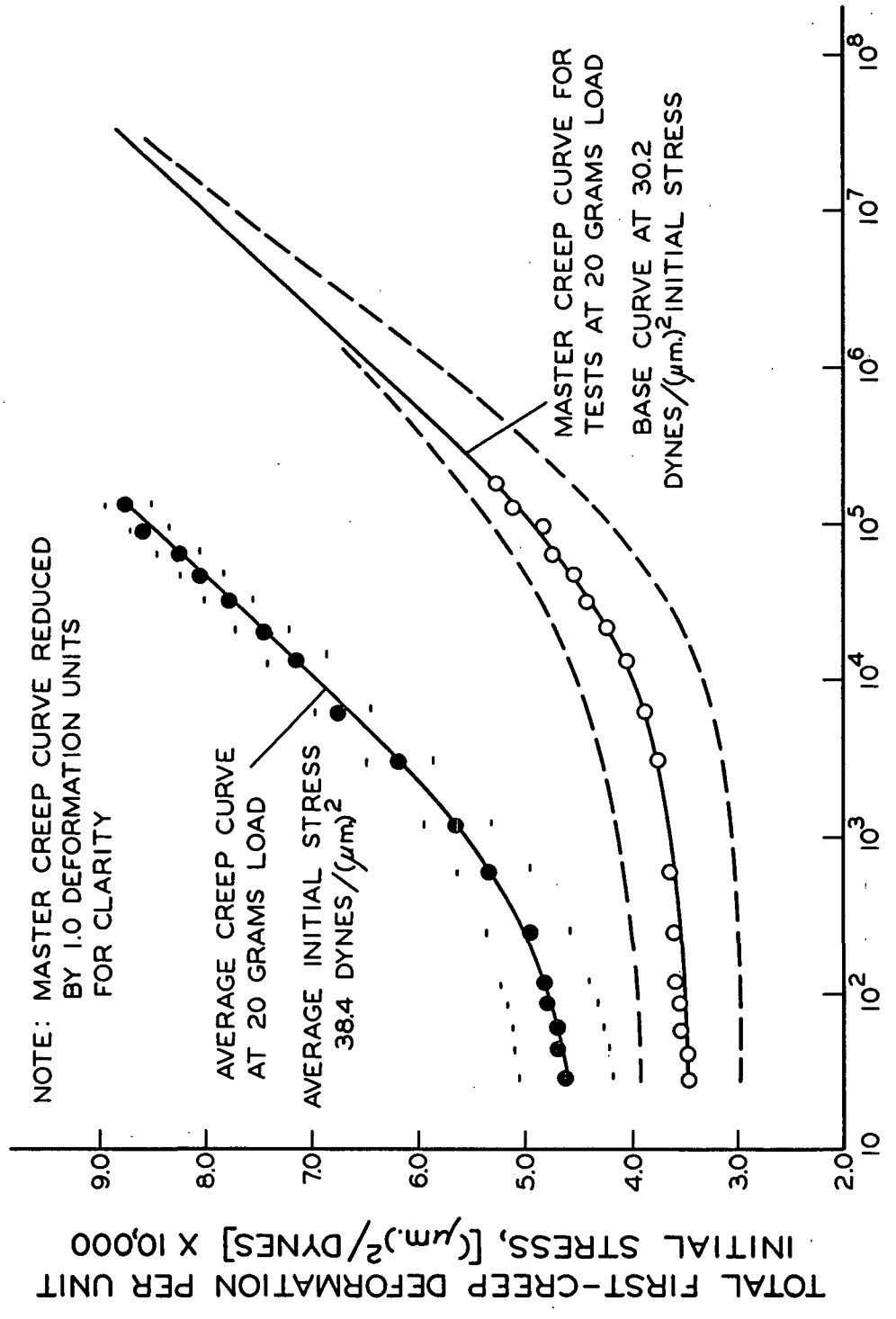

Figure 13. Test of Data Averaging Methods

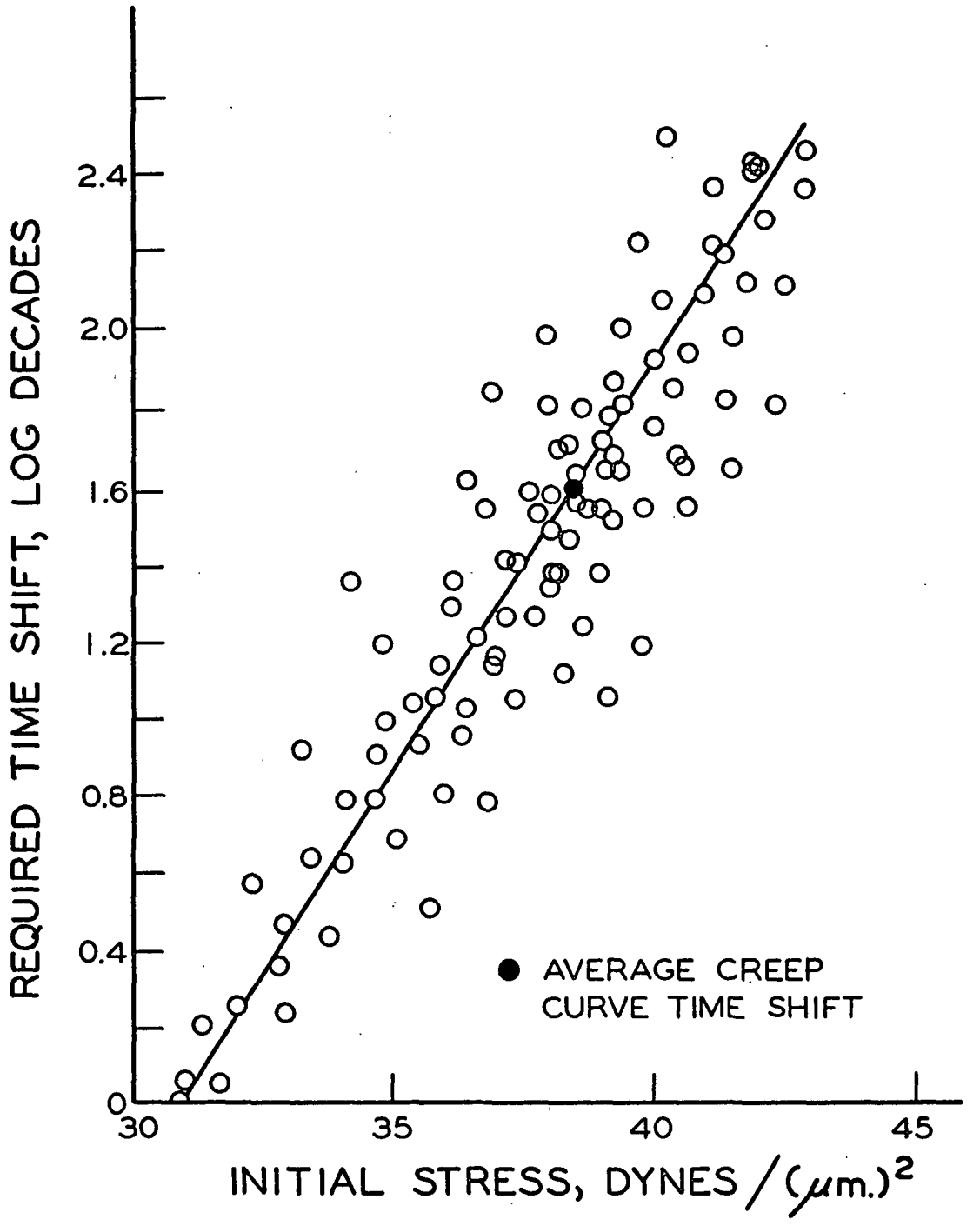

Figure 14. Time Shift Required to Form Individual Fiber Master Creep Curve at 20 Grams Load

the two curves into coincidence is 1.78 log decades. The average initial stress for the 98 fibers tested was 38.4 dynes/$(\mu m.)^2$, and when this time shift is plotted in Fig. 14 it falls on the line determined by time shifts necessary to form the master creep curve.

The master creep curve itself could have been based on the creep curve of some other fiber and then would have been coincident with the average curve or even on the other side of, or above, the average curve. There is no reason to suspect that the creep serving as the basis for forming the master creep curve is atypical, but the selection of any other base curve should serve equally well. The variation about these two curves is shown in Fig. 13. The dashed lines indicate the envelope of the data used in forming the two curves. The envelope for the average curve was drawn by calculating the standard deviation of each average deformation and drawing the dashed line at $\pm$ 3 S.D. from the average. The envelope for the master creep curve was drawn from the shifted curves and includes essentially all the data. It is immediately apparent that the data fit the average curve much better than they do the master creep curve.

The use of creep curves which more closely represent the median creep response at any initial load would result in a more uniform distribution of the data about the master creep curve formed from them. Since the individual creep data are better represented by the average curve, all future reference to fiber creep curves will be to the average curve unless otherwise specified.

FIRST-CREEP

Creep tests made on materials which have not been previously subjected to external loading is commonly termed first-creep. The work of this study was limited to first-creep testing. A first-creep curve at each applied load was plotted in Fig. 15 as the average deformation versus the logarithm of the time

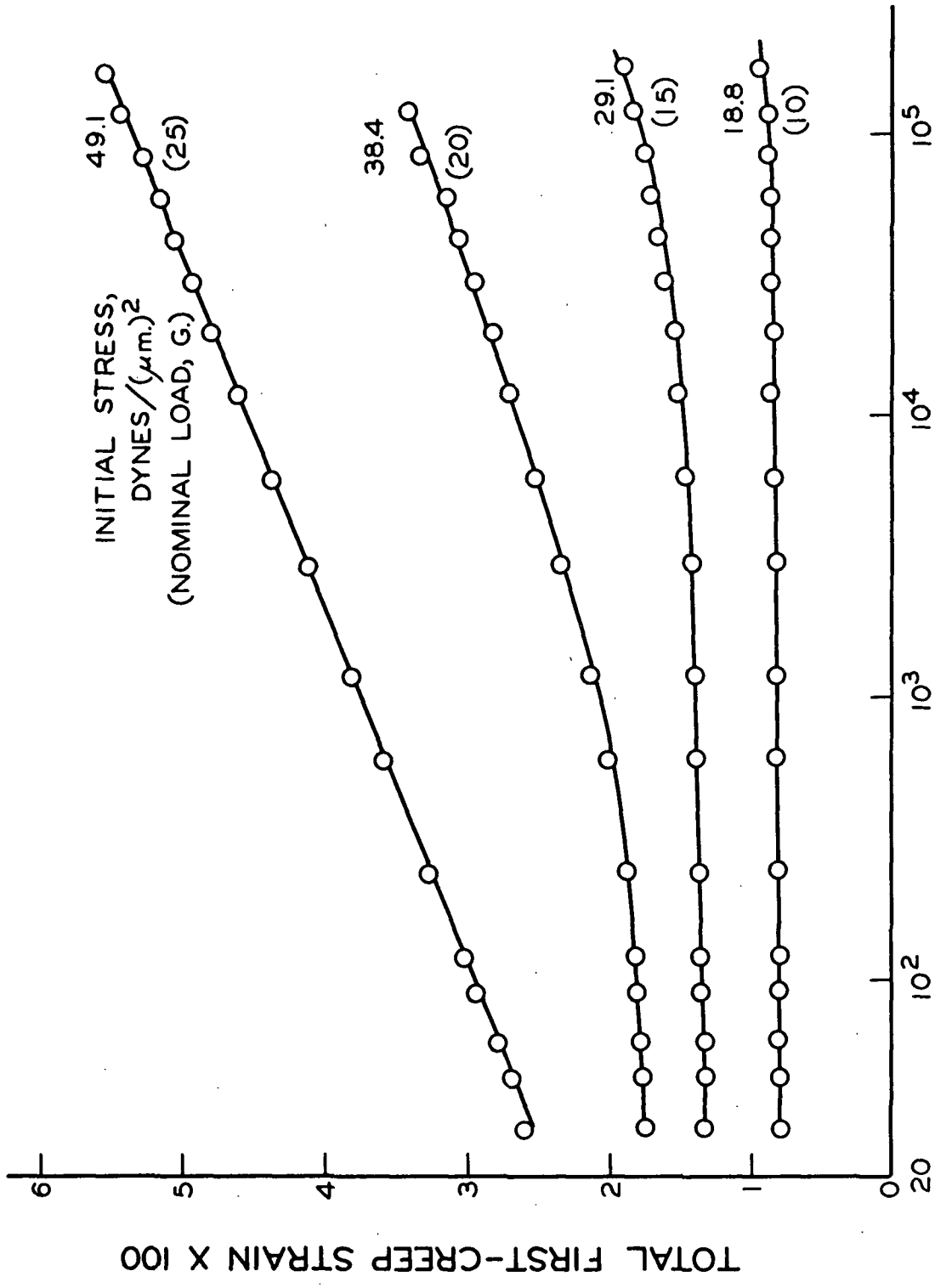

Figure 15. First-Creep Curves

in seconds. The average deformation was determined as discussed previously and is expressed as percentage of the initial span length. The average stress for the fibers tested is indicated on this plot. The duration of these tests was 12 hours (43,200 seconds), 24 hours (86,400 seconds), and limited data at 48 hours (172,800 seconds). The average data and the standard deviation of each average are given in Table IV in Appendix II.

Examination of the first-creep curves reveals that at least two types of delayed response are present. As the stress increases it appears that a limiting type of response is reached. For example, the entire creep curve at a load of 25 grams and the last two decades of log time at 20 grams is linear on the semi-logarithmic plot. This may be described by a logarithmic equation,

$$(\epsilon)\ 100 = K \log t + C$$

where t is the elapsed time in seconds, and K and C are constants. The constant C represents the total creep strain at one second and has no real significance since the logarithmic creep equation may not be valid at very low times. The constant K is the slope of the straight line. In all cases for fibers loaded at 25 grams this relationship was observed until termination of the test. About one-fourth of the fibers tested at this load failed before the end of the 24-hour test, and less than 10% of those still intact after 24 hours continued to the full 48 hours before rupture. A limiting creep behavior of this type has been observed for paper by Brezinski (34) and others (35-37). The behavior characterized by this equation will be referred to as logarithmic creep in the following discussion.

In order to compare further the limiting type of creep response to that of paper, the slopes of the logarithmic creep portions of the first-creep curves were plotted versus the initial stress in Fig. 16. In this plot the individual

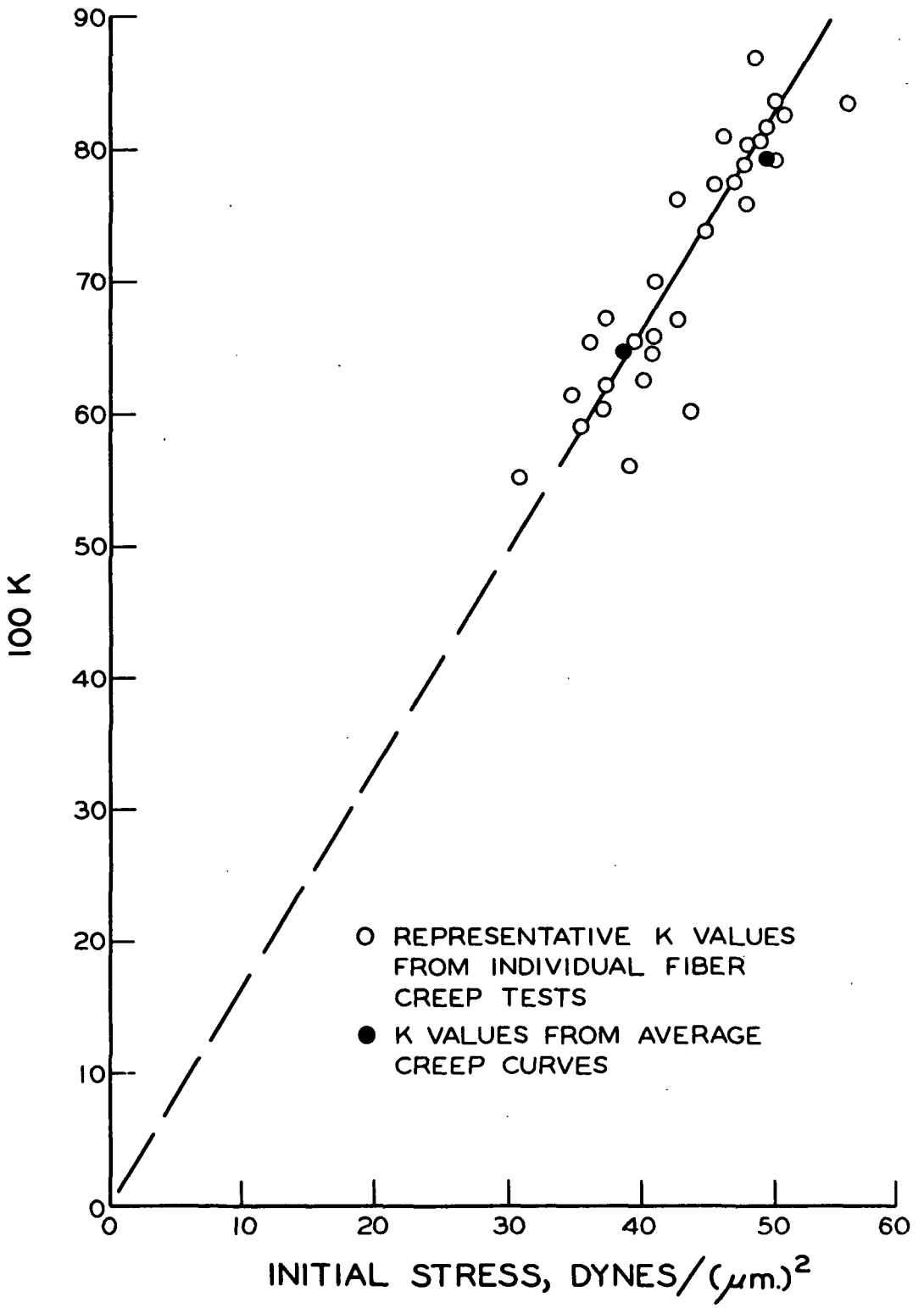

Figure 16. Relationship Between the Constant K of Logarithmic Creep and the Initial Stress

fiber creep curves were examined, and the slopes of the average creep curves are shown for comparison. There is apparently a linear relationship between the slope of logarithmic creep and the initial stress. The scatter about the line is likely due to inherent fiber differences. Brezinski found a similar relationship for the alpha pulp handsheets that he investigated. It would appear that intrafiber mechanisms were controlling at least the limiting creep behavior of these handsheets. Since the individual fibers studied in the present investigation are not the same as those which made up Brezinski's handsheets, a valid comparison is not possible. In view of this difference it would be most interesting to compare the creep behavior of both the individual fibers and the handsheets made from them. In this case evaluation of the intrafiber contribution to sheet creep could be made.

The creep curves at 15-gram loads and the first part of the curve at 20 grams appear to approach the limiting type of behavior as may be seen in Fig. 15. The first three log decades of the creep curve for 10 grams may also be described by a linear logarithmic equation. The slope of this line falls well below the line shown in Fig. 16. This curve could equally well be described by a second-order polynomial equation. Since an equation of this type, if higher orders were included, could be used to describe both the 10 and 15-gram curves along with the first two log decades of the 20-gram curve, it seems that little could be obtained by forcing a mathematical description of this nature.

It was stated above that at least two types of creep behavior were indicated by the creep curves. One of these types is described by the limiting behavior of logarithmic creep, and the other must be present to account for the behavior at lower initial stresses or shorter times. The term "initial creep" will be used to refer to the various types of behavior occurring before onset of logarithmic creep. An increase in initial stress appears to have two effects on fiber creep

behavior. First, there is an increase of the amount of delayed deformation for both the logarithmic response and the initial response preceding logarithmic behavior. Second, it appears that logarithmic creep response occurs at earlier times as the initial stress is increased.

MASTER CREEP CURVE

The master creep curve concept has been used to combine creep curves at various initial stresses to form a generalized curve which relates the three variables: time, initial stress, and deformation. The creep curves in Fig. 15 indicate that a speeding up of the various mechanisms of response is produced by increasing the initial stress. This speeding-up concept as discussed earlier in the historical review section was originally explored by Catsiff, Alfrey, and O'Shaughnessy (56) for nylon and later by Brezinski (34) and others (35-37) for paper.

A master creep curve could be constructed from the first-creep curves by simply reducing the deformations by the initial stress and shifting the reduced curves along the log-time axis until they coincide in the regions of overlap. The first-creep curves, reduced in deformation by a factor of initial stress, are shown in Fig. 17. Since the slopes of logarithmic creep are directly proportional to the initial stress, the logarithmic creep regions are parallel on this reduced plot. Each of the reduced curves appear to be separate portions of an overall curve. These reduced curves, when shifted along the time axis, form the master creep curve shown in Fig. 18.

The master creep curve has the time axis of the first-creep curve at a 10-gram load [19.3 dynes/$(\mu m.)^2$ average initial stress]. This curve was selected so that only positive time shifts were required to form the master curve. Excellent

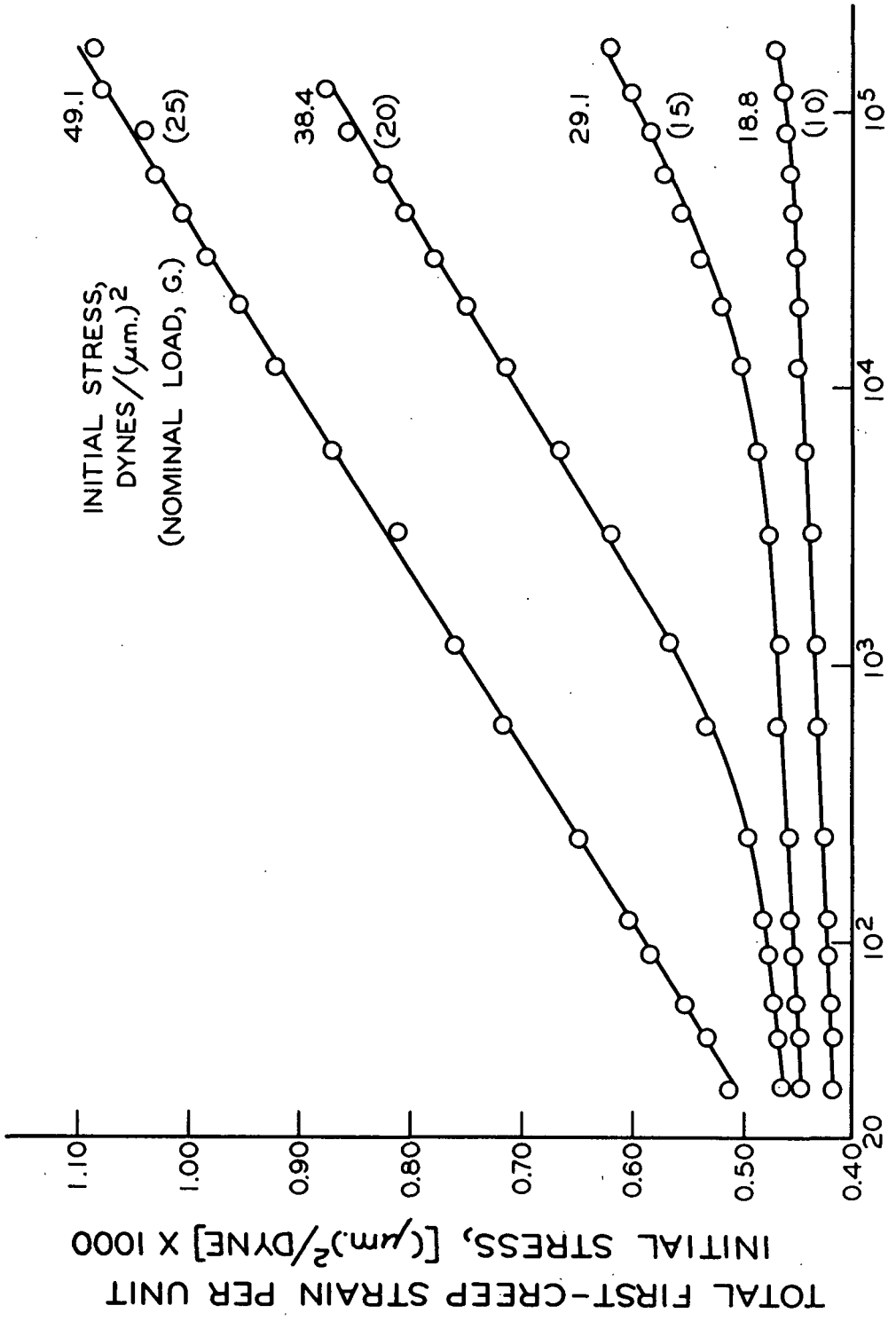

Figure 17. First-Creep Curves Reduced in Deformation by Factors of Initial Stress

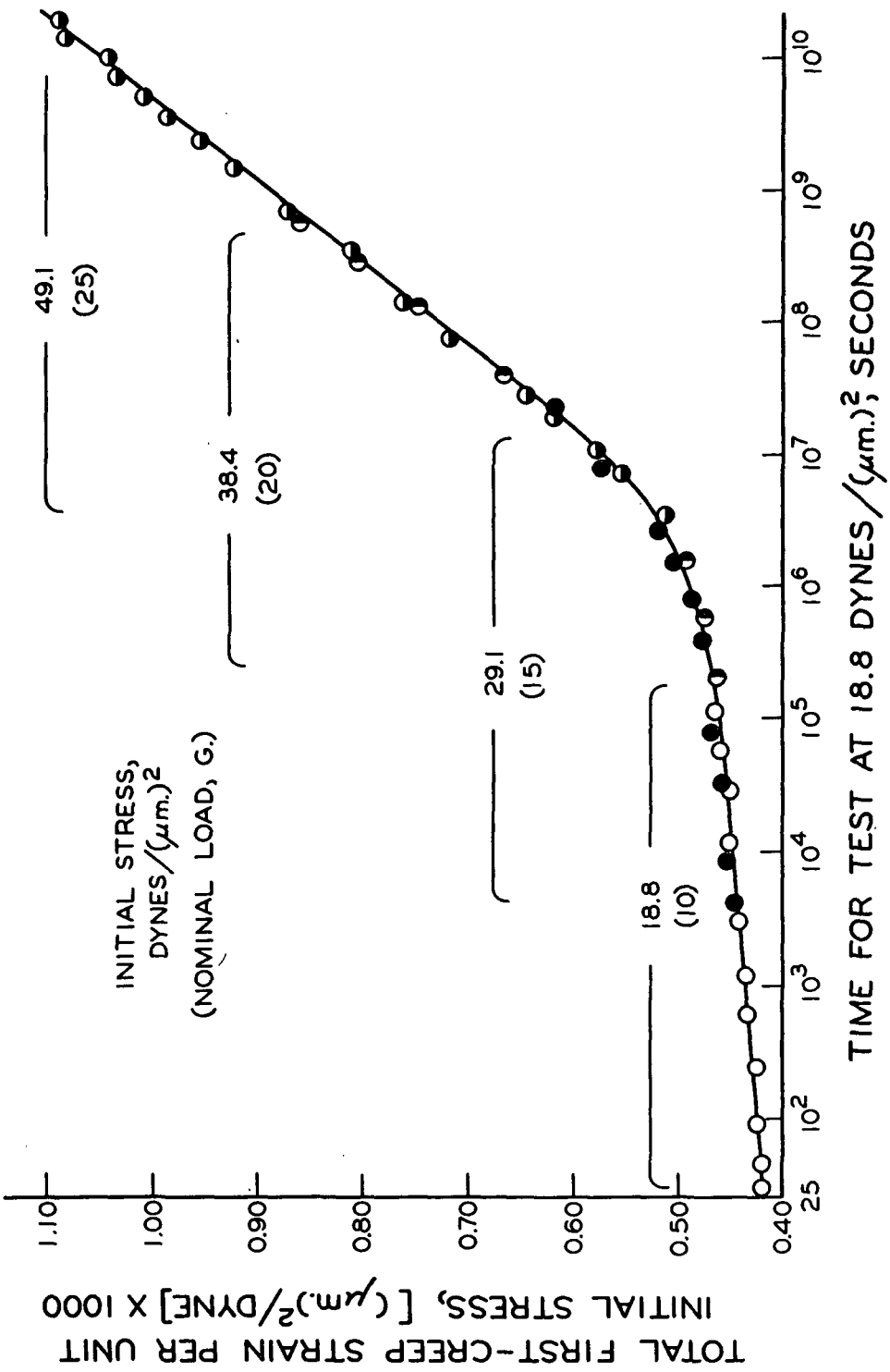

Figure 18. Master Creep Curve

agreement is obtained in the regions of overlap indicating that the stress effect on the time-dependent response of these fibers is a continuous process.

A master creep curve properly handled, provides a means of extrapolating an experimental creep curve at any initial stress to earlier or longer times. Both the immediate elastic deformation and the delayed deformation are included in the total deformation represented by the master creep curve, and each of these deformations is dependent on the initial stress applied to the fiber. By inference from the master creep curve, it may be assumed that both initial and logarithmic creep will occur at any initial stress.

Examination of the master creep curve reveals that for any initial stress the rate of creep steadily declines at an increasing rate as the time increases. For a homogeneous, noncrystalline polymer, the total creep response is characterized by a sigmoidal shape, and the rate of creep becomes almost zero at long times. The early portion of the master creep curve appears to follow such a sigmoidal path, but the inception of logarithmic creep stops this trend, and a finite though decreasing rate of creep exists up to fiber failure.

Figure 19 is a plot of the time shift in log decades versus the initial stress necessary to produce a master creep curve from the reduced creep curves. Brezinski (34) found that, for his handsheets, the shift in log-time required to form a master creep curve was linearly related to the initial stress, and he concluded that both the immediate elastic deformation and the delayed deformation were linearly related to the initial stress. Such linear relationships were not observed in this study and, for fibers, both the immediate elastic deformation and the delayed deformation may be dependent on the initial stress.

This difference in stress dependency may be due to the significant difference in the creep testing procedure of Brezinski and that used in this study.

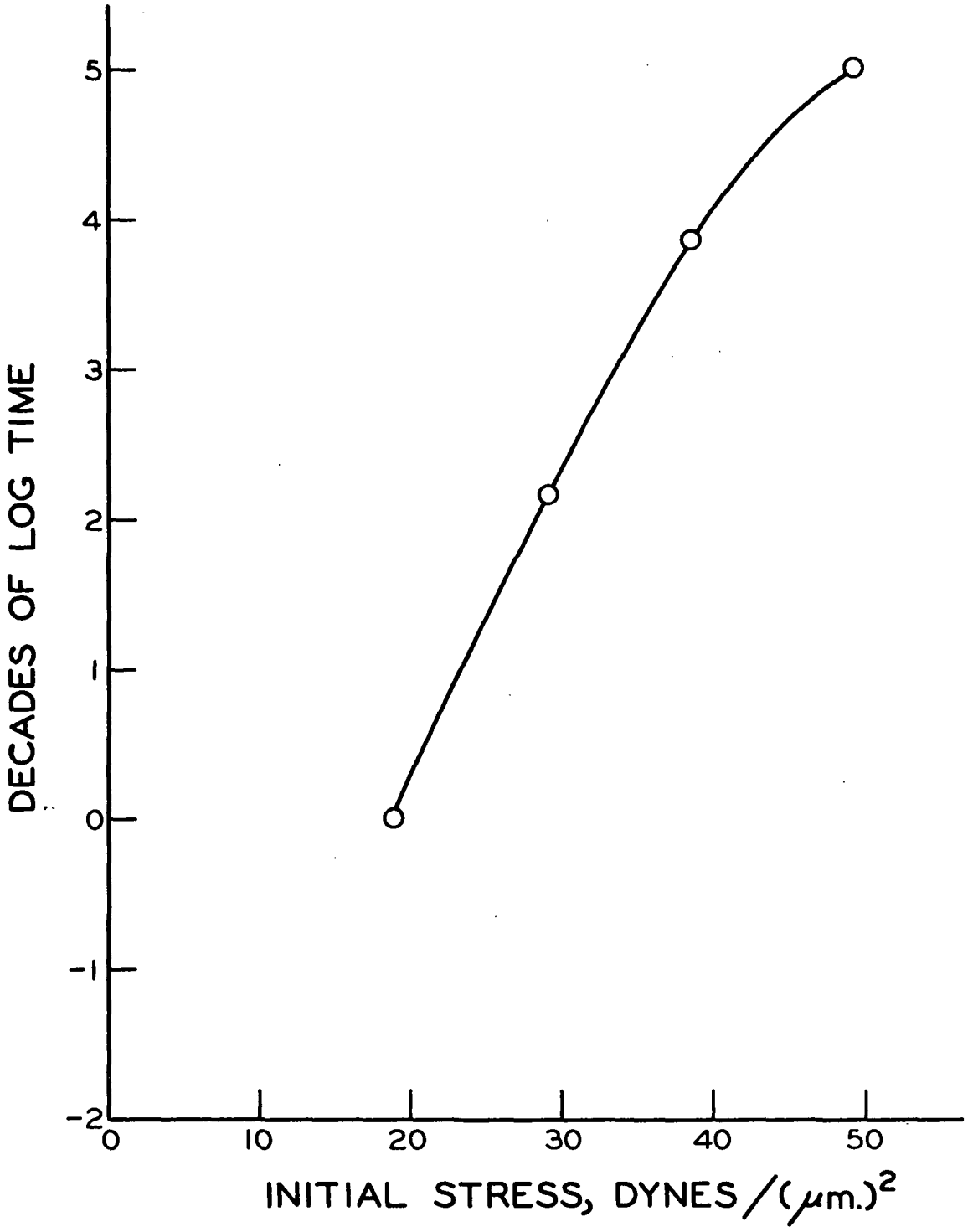

Figure 19. Time Shift Required to Form Master Creep Curve

Brezinski's procedure for handsheets resulted in a very rapid application of load (less than 0.5 second), but such rapid loading was not possible with individual fibers. In the present study the specimens were loaded at a rate of 1.0 gram per second. It is well known that individual pulp fibers experience a stress- or strain-induced stiffening during a constant rate of loading tensile test (9, 51). Such stiffening must have occurred in the fibers during the loading period. This stiffening or mechanical conditioning is a time-dependent phenomenon. The fibers would be expected to exhibit a progressive increase in their modulus of elasticity as the initial creep load was applied, and those fibers subjected to the higher loads would undergo the greatest change in modulus. The overall results of such stiffening would be to lower the immediate elastic deformation of the more highly stressed fibers. This would bring the creep curves closer together on the deformation axis and reduce the time-shift required to produce coincidence along the master creep curve. Thus, at least in part, mechanical conditioning during the loading period appears to be responsible for the non-linear relationship between the time shift and initial stress.

The effects of stress on the delayed deformation are not apparent from the data thus far presented except as there appear to be at least two types of time-dependent strain occurring. These types of stress behavior are related to structural adjustments within the fiber at both the molecular and microscopic levels. Such adjustments occur as the result of the applied stress and produce the observed time-dependent deformation of the fiber. The construction of a master creep curve and the agreement in the regions of overlap suggests that the structural changes in the creep tests are continuous, orderly functions of state. The time shift relationship to initial stress suggests that initial stress has some effect, independent of time, on the structural response.

It is clear that the first-creep curves alone are of limited value in interpreting the nature of the structural mechanisms of creep response in these fibers. For further information we shall look at the results of other tests conducted in this study.

FIRST-RECOVERY

The first-creep deformation which is recoverable within reasonable periods of time after removal of the creep load is termed the recoverable deformation of primary creep. A plot of the recoverable deformation versus the logarithm of recovery time is the recovery curve. First-recovery is that recovery immediately following first-creep. The average first-recovery curves, shown in Fig. 20, 21, and 22, followed first-creep tests of 12, 24, and 48-hour durations at four levels of initial stress. The averaged data for these curves are in Table V of Appendix II. Creep recovery was determined for the same time interval as first-creep and under the same conditions of temperature and humidity. The superposition principle states that the removal of a load may be considered as the application of a negative load. It is customary, however, to treat recovery deformation without the negative sign. The recovery deformations are considered as positive in relation to the position of the specimen at the end of the creep test even though the specimen length is actually being reduced. In calculating the recovery deformation, the original, before creep, span length was employed so that a consistent basis was used to express the strain. The recovery was determined relative to the length of the specimen at the end of the preceding creep test.

Examination of these recovery curves reveals that the shapes of all the curves appear to be sigmoidal, and similar mechanisms would be expected to govern the behavior of all tests. Attempts to form a master recovery curve by the technique used in forming the master creep curve failed for these data.

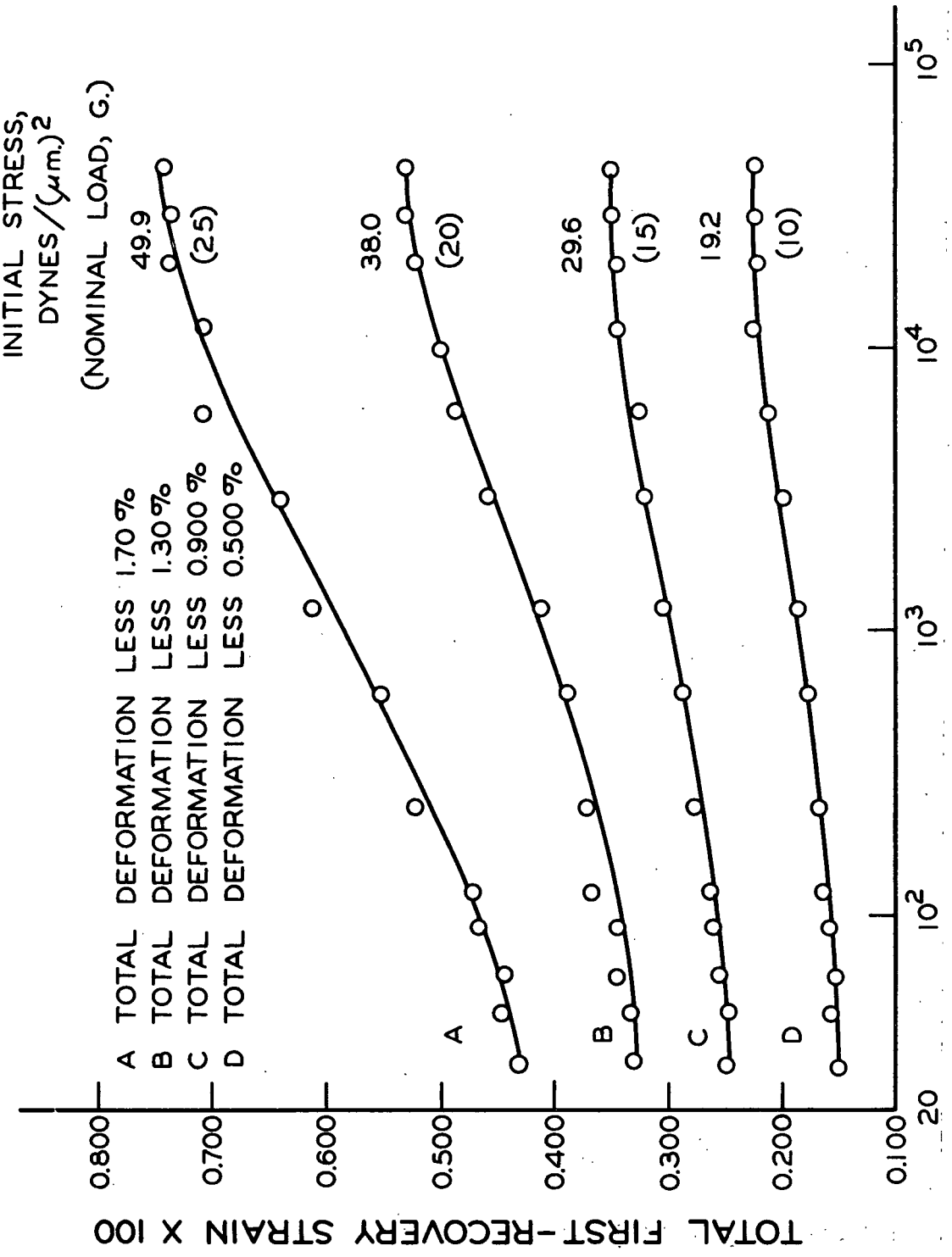

Figure 20. First-Recovery After 12 Hours of First-Creep

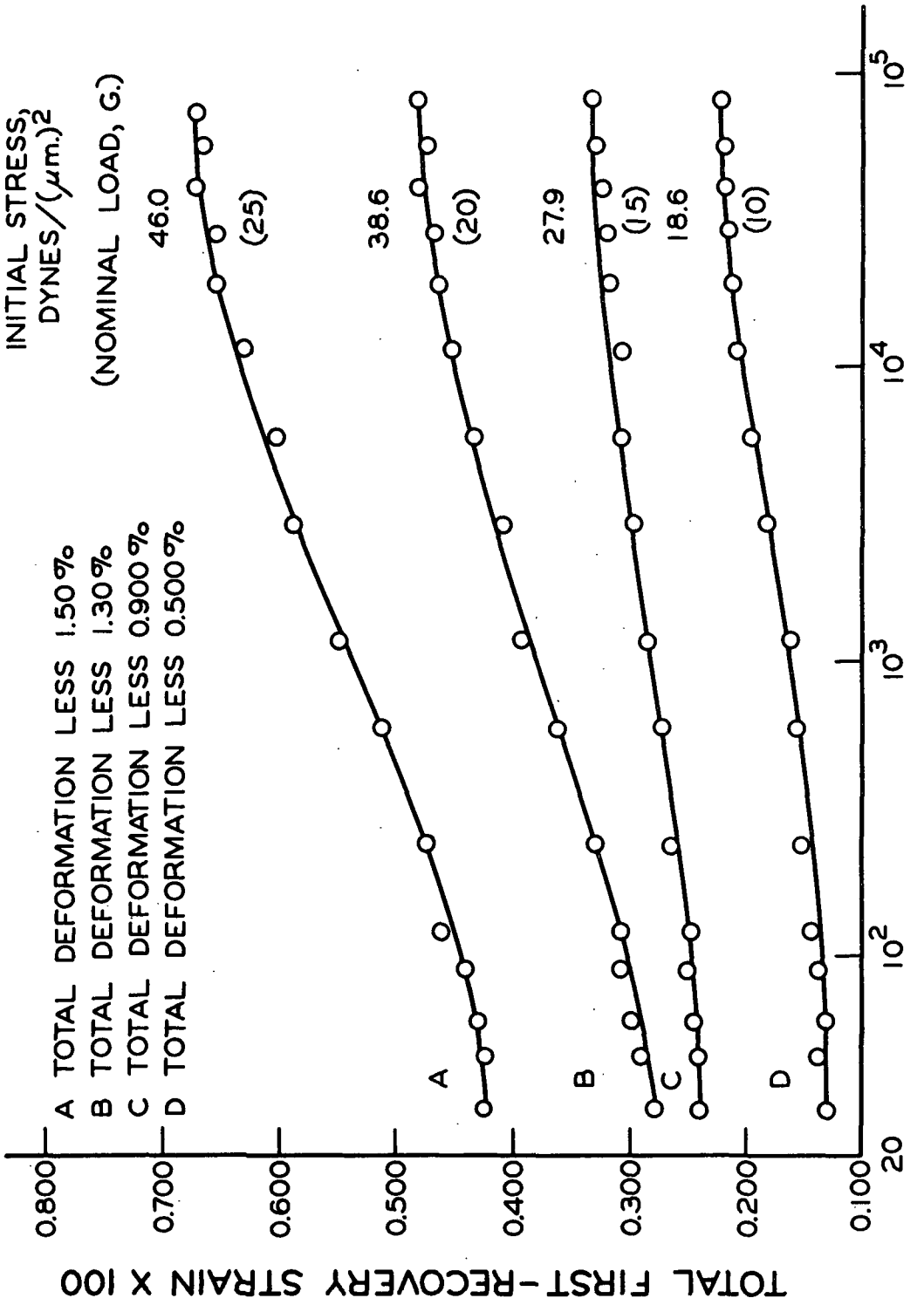

Figure 21. First-Recovery After 24 Hours of First-Creep

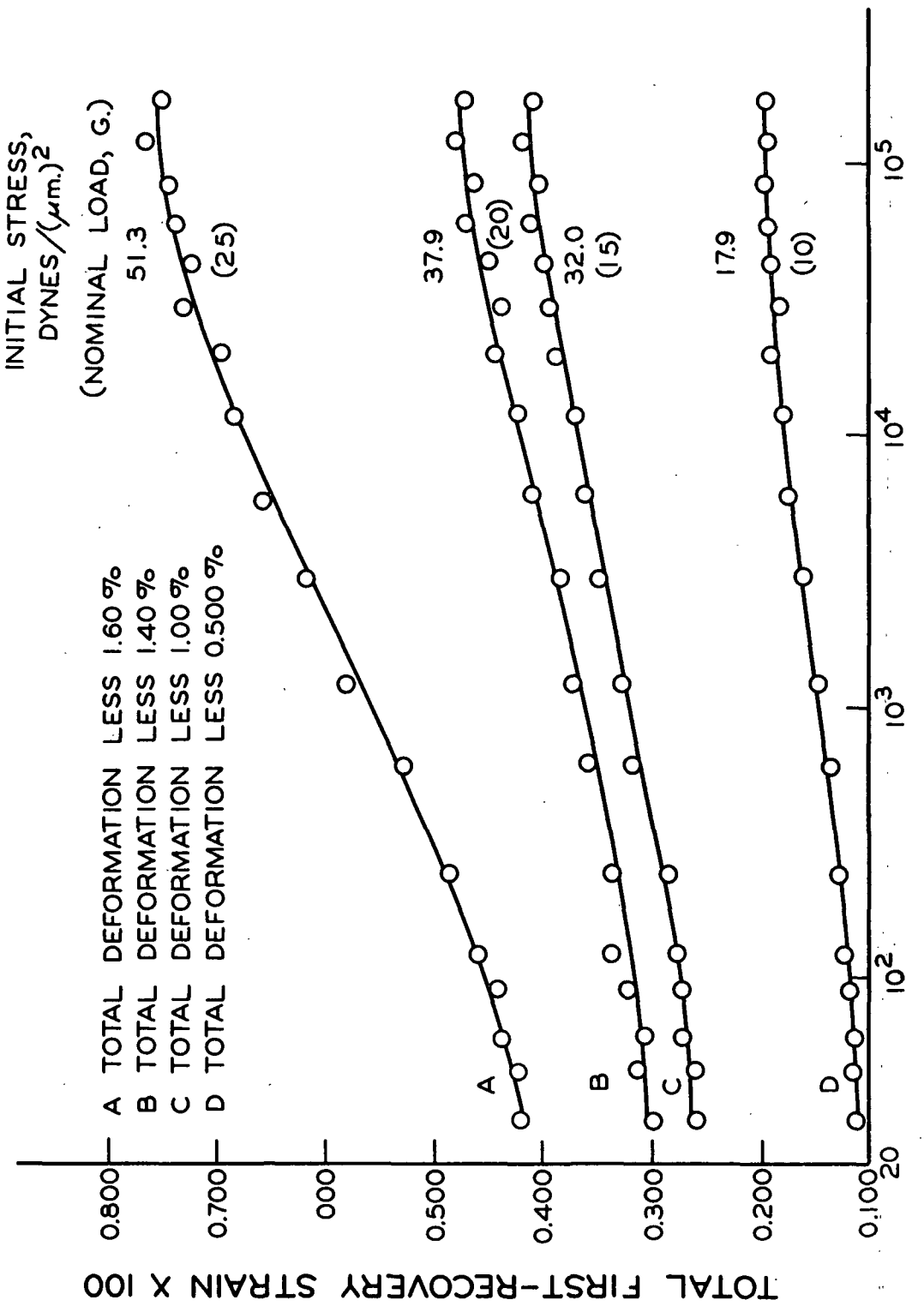

Figure 22. First-Recovery After 48 Hours of First-Creep

The agreement in regions of overlap was poor, and coincidence on the master curve could not be obtained. This failure may be attributed to the reduction in rate of first-recovery at long times.

In order to examine this behavior more closely, the percentage nonrecoverable deformation was plotted in Fig. 23 versus the initial creep stress for different times of first-creep. The nonrecoverable deformation is that portion of the total creep strain remaining in the specimen after creep recovery. Here it is clearly indicated that as both the time and initial stress of first-creep were increased, the nonrecoverable deformation was increased. Percentage nonrecoverable deformation was determined as the ratio of the nonrecoverable deformation to the total creep deformation times one hundred. From this plot it is apparent that the initial creep deformation is about 85% recoverable, but the deformation at high initial stress and long times is largely nonrecoverable (about 40% recoverable). As the time-under-load is increased at any initial stress, the amount of nonrecoverable deformation also increases. The standard deviation of the points representing tests of 48-hour duration is large due to the limited number of tests, and the dashed line shown in the figure represents the expected results of these tests had a statistically significant number been made.

If the total delayed deformation were produced by structural mechanisms related only to molecular configurational changes, it would be expected that complete recovery would be obtained if a sufficient recovery period were allowed. Complete recovery would also result from reversible stress-induced increases in crystallinity and crystallite orientation within the fibrils. It is more likely that only the rate of deformation is controlled by such configurational mechanisms, and the recoverability of the deformation is dependent on the breaking and reforming of secondary bonds in the amorphous material of the fiber. These new bonds would

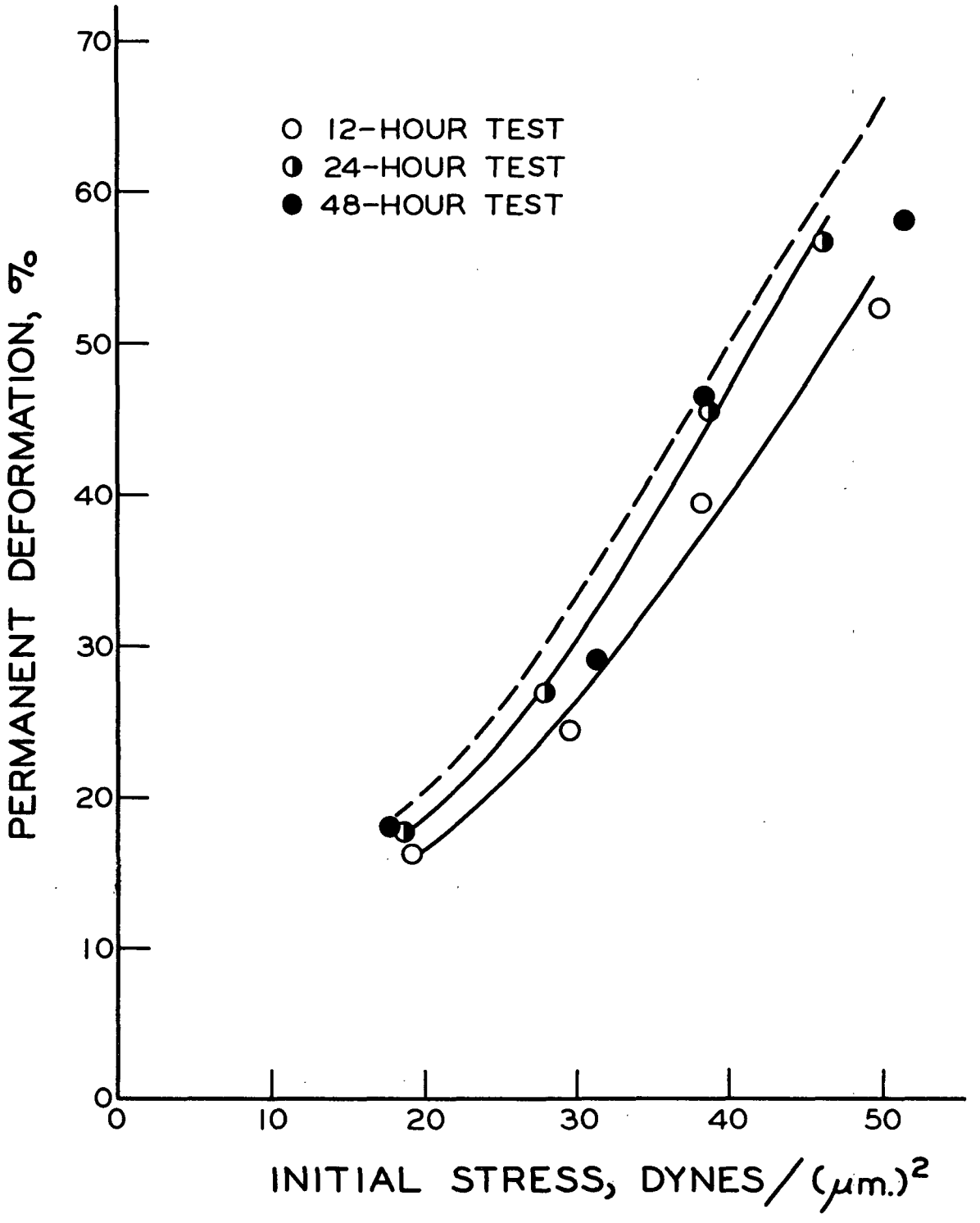

Figure 23. Permanent Fiber Deformation

tend to lock the molecular chain segments in the deformed position, and a permanent deformation of the fiber would result.

Configurational mechanisms in the amorphous regions of the fiber should govern the behavior of the fibrillar elements which support and transmit the applied load throughout the fiber. The fibrillar structure of the cellulosic material is thought to govern the observed mechanical properties of the fibers with a significant effect attributable to the amorphous hemicelluloses (51). If, as indicated earlier, the modulus of elasticity were to increase due to a sustained tensile stress, the immediate elastic recovery would be decreased when the load was removed, and the total recoverable deformation might be decreased. There are two probable mechanisms by which the elastic modulus may increase in response to creep conditions.

The first of these possible mechanisms is related to the effects of non-recoverable increases in crystallinity. The fringed micelle theory suggests that an increase in crystallinity would occur within the elementary fibrils at the expense of the amorphous cellulose matrix. This would produce a more completely crystalline load-supporting element. Such behavior should be exhibited by a relatively large increase in the elastic modulus of the fibrils. The fringed fibril theory suggests that an increase in crystallinity would increase the load-supporting cross-sectional area of the elements since the amorphous cellulose is assumed to surround an essentially crystalline fibrillar core. In this case there would not be a change in the nature of the fibrils. Such possible changes in crystallinity may be either reversible or only partially reversible. They are more likely to be only partially reversible due to the high secondary bond density of crystalline cellulose.

The second, and most probable, mechanism leading to a time-dependent increase in elastic modulus is simply that as creep progresses, a greater percentage of the

microfibrils share in supporting the external load. This would occur when the amorphous material (hemicelluloses and cellulose) separating the fibrils deforms and allows minute motion of these stiff, highly crystalline elements. The effect of such behavior would be to increase the uniformity of the stress distribution in the fiber. This change is not subject to experimental determination; thus basing the stress on the apparent area, it would appear that the modulus of elasticity has increased. Behavior of this type is widely recognized and is commonly discussed in terms of internal stress redistribution.

During the period of initial creep, configurational response would allow minute changes in the fibrillar structure in the regions of high internal stress concentration. As the fibrils adjust to support the load and relieve localized stress concentrations, the applied load will become less effective in producing further change. Once the regions of high stress concentration have been relieved by such adjustment, larger segments of the fibrils will become involved in any further redistribution of internal stress. As larger adjustments to the applied load occur, the probability of these adjustments becoming frozen-in will be increased.

The overall result of such redistribution of stress will be that at low times and low initial stress, the fiber deformation will be primarily in regions of high internal stress concentration; on removal of the applied load the stored energy of the fiber will also be concentrated. The new secondary bonds which serve to lock in the molecular configurational changes will be subjected to high stress, and much of the total deformation will be recovered. At longer times and higher initial stresses, the redistribution of stress will have progressed to the larger structural elements, and newly formed secondary bonds will be more numerous and more evenly distributed through the fiber and less susceptible to being disrupted once the external load is removed.

COMPARISON OF FIBER CREEP TO SHEET CREEP

The observed creep response of individual pulp fibers is very similar to that which has been determined for handsheets (34-36, 57). By applying the theory developed by Van den Akker (64) which relates the mechanical properties of a sheet to the component fiber properties and fiber orientation, an estimate was made of the response of a sheet composed of the fibers investigated in this study. Direct comparison of fiber to sheet creep response was not possible since there has been no study of the creep behavior of sheets made from this population.

Several important assumptions had to be made in order to apply the theory and calculate expected sheet response. It was first assumed that the handsheet structure was composed of randomly oriented fibers and that the sheet was well bonded. It was further assumed that the fiber segmental length between inter-fiber bonds was of the same order as the fiber diameter. The theory shows that the fibers oriented in the direction of the external stress will be under the largest tensile stress, and that those oriented at 90° to the applied stress will be subjected to the largest compressive load. For orientations between the two principal directions, fiber stress will vary continuously from maximum tension to maximum compression. In view of the stress conditions imposed on the fiber segments, it was necessary to assume that the creep response in compression was the same as that in tension except for the direction of deformation. This is perhaps the most important assumption, and it would be valid only for extremely small strains if it applies at all.

The modulus of elasticity used in calculation was regarded as a delayed modulus as suggested by Van den Akker (64). This concept is not valid for large creep deformation of the fibers where the strain and stress at a given time are not linearly related. The method for predicting sheet creep response

is outlined in Appendix III, and the various assumptions necessary for the calculations are discussed. A valid estimate of the quantitative effect of the assumptions could not be made, and the results serve only as a qualitative prediction of sheet behavior.

The results of these calculations are presented in Fig. 24 as a master creep curve for the hypothetical handsheet. The master creep curve for bleached sulfite pulp as determined by Sanborn (57) is also shown in this figure for comparison of the predicted to the observed creep behavior. These data were used for comparison since the pulp used for these handsheets was closer to the fibers investigated in the present study than were the alpha pulps used on other sheet creep studies.

It is obvious from the figure that the response predicted from individual fiber properties is similar to that observed in handsheet studies. Due to the various assumptions made to calculate sheet response, neither the reduced deformation or log-time axes of the two curves are necessarily on a common basis; and only the shape of the curves may be considered significant. In light of these assumptions, it may be suggested from this calculation that intrafiber mechanisms govern sheet behavior even at high stresses or long times. Of course, interfiber mechanisms would be expected to be of importance in the prerupture stress behavior of handsheets, in view of the evidence for interfiber bond rupture which has been presented by Page, et al. (65-67) and Sanborn (57). Only by direct comparison of the creep response of handsheets made from holocellulose fibers and a more rigorous mathematical treatment will it be possible to ascertain the relative significance of intrafiber and interfiber mechanisms governing the prerupture response of paper.

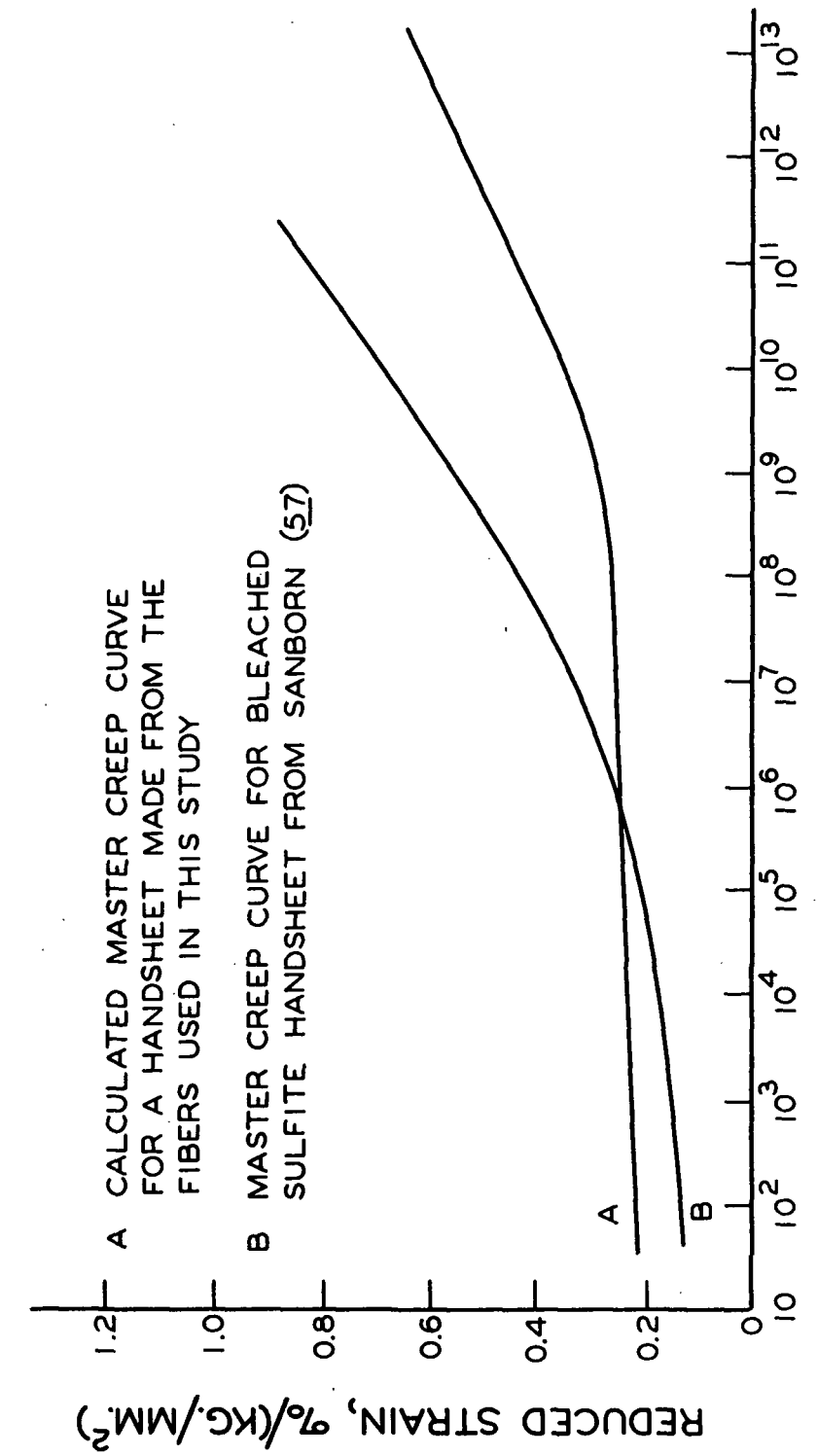

Figure 24. Master Creep Curve For Hypothetical Handsheet

CRYSTALLINITY AND CRYSTALLITE ORIENTATION

The results of x-ray diffraction study of both the crystallinity and crystallite or fibrillar orientation are shown in Table I. Laue diffraction patterns were obtained on a parallel bundle of 25 fibers. These fibers were subjected to creep loads of 10 and 20 grams per fiber for 14 hours followed by a comparable period of recovery. Diffraction patterns were made before application of the creep load, between 12 and 14 hours after application of the creep load, and between 12 and 14 hours after removal of the load.

TABLE I

CRYSTALLINITY AND CRYSTALLITE ORIENTATION

	Creep Load, g./fiber	Before Creep[a]	After Creep[a]	After Recovery[a]	Bundles Tested
Width at half height of 002 diffraction arc	10	4.31° (0.41°)	4.23° (0.39°)	4.12° (0.35°)	4
	20	4.06° (0.47°)	4.18° (0.43°)	4.27° (0.43°)	4
Crystallinity index	10	60.2 (6.0)	65.7 (5.8)	60.0 (6.0)	4
	20	63.7 (5.8)	61.3 (6.3)	64.2 (5.9)	4
Orientation as standard deviation of circumferential arc	10	8.78° (1.42°)	7.09° (1.40°)	7.94° (1.52°)	4
	20	8.62° (1.70°)	6.43° (1.36°)	7.73° (1.63°)	4

[a] Values in parentheses are the standard deviation of the average reported.

Analysis of the data shown in Table I indicated that there was no significant change in either of the measures of crystallinity for any of the test conditions (width at half height or crystallinity index). All reference to significance in this study was based on 95% confidence limits of the population mean as discussed

in Davies (68). If crystallization processes are occurring, they are not large enough to be determined by this technique, and it is doubtful that any other method would be sensitive to very small changes in the fiber crystallinity. There is a significant change in the measured orientation after creep. After recovery there is no significant difference in the orientation when compared with that after creep.

Interpretation of the data was difficult since it was complicated by the orientation of the fibers in the bundle. The fibers in the prepared bundles were not perfectly parallel, and the application of a load probably increased the fiber alignment which would result in an apparent increase in the measured intrafiber crystallite orientation. It was not possible to assess the magnitude of this effect, but it would reduce the significance of the measured orientation increase. For the determination after recovery the fiber alignment may be adversely affected by some of the fibers contracting more than others; this phenomenon may obscure a real permanent increase in fibril orientation. Only the data after creep should be almost free of such effects, and here orientation was slightly greater for the fibers loaded to 20 grams than for those loaded to 10 grams.

It may be concluded from these data that there was no significant change in the crystallinity of the fibers due to sustained stress at the levels investigated. Further, there was an increase in the crystallite orientation which indicates that there was movement of crystalline regions within the fibrils or, more likely, of the fibrils within the fibers.

MECHANICAL PROPERTIES OF FIBERS

It was originally hypothesized that the internal structure of fibers would undergo a time-dependent modification when subjected to an applied stress and that this structural behavior would be exhibited by changes in the mechanical

properties of the fibers. The work reported in this section was done to aid in interpreting the structural behavior of the fibers and to ascertain the significant effects of initial stress and time in creep tests on the mechanical properties of fibers.

The mechanical properties of the fibers are tabulated in Table II. This table contains the data for the influence of various loads and times-under-load after first-creep. Table III presents the mechanical properties of the fibers after first-recovery. The duration of recovery was the same as for the preceding creep test. The ultimate elongation was based on the original span before creep recovery tests.

Figure 25 is a plot of the modulus of elasticity versus initial stress for the three durations of first-creep. Generally, the modulus increases during creep and appears to reach a limiting value. This limiting value represents a 70% increase in modulus. It is interesting to note that this change is about the same as Spiegelberg (22) found for these fibers dried under tension.

At a given level of initial stress there was not a significant time-dependent change in the modulus of these fibers for creep times as long as 12 hours or more. Examination of the master creep curve indicates that test durations of 10 to 12 days would be required for the fibers loaded to 10 grams [$\cong$ 20 dynes/$(\mu m.)^2$ initial stress] to reach a modulus comparable to that observed after 24 hours at 15 grams [$\cong$ 30 dynes/$(\mu m.)^2$ initial stress]. Much longer times, approximately 700 days, would be needed for fibers initially loaded to 10 grams to reach the limiting modulus value.

In Fig. 25 the modulus of elasticity was also plotted versus the initial stress after first-recovery. These curves show that the change in modulus produced during first creep is partially recoverable. It should be noted that due to the method of

TABLE II

AVERAGE STRESS-STRAIN PROPERTIES BEFORE AND AFTER CREEP

		Non-stressed Fibers	10-Gram Creep Load			15-Gram Creep Load		
			12 hr.	24 hr.	48 hr.	12 hr.	24 hr.	48 hr.
Modulus of elasticity, dynes/(μm.)^2	Av.	2340	2760	2830	2810	3170	3450	3340
	S.D.,%	29.7	14.7	15.2	29.6	16.3	13.2	27.0
Breaking load, grams	Av.	48.8	56.8	57.2	59.3	64.7	60.3	59.2
	S.D.,%	33.2	24.3	26.3	32.8	25.2	23.1	34.9
Tensile strength, dynes (μm.)^2	Av.	99.7	105.3	107.1	104.0	107.2	112.1	120.4
	S.D.,%	25.5	17.8	16.2	28.9	15.7	16.6	37.6
Ultimate elongation, %	Av.	5.62	5.41	5.27	5.52	4.87	4.76	4.95
	S.D.,%	29.2	15.2	16.7	24.5	14.5	15.9	27.3
Work-to-rupture, dyne-μm./(μm.)^3	Av.	2.62	2.78	2.86	2.84	3.19	3.07	3.21
	S.D.,%	32.4	35.6	30.9	41.8	25.6	34.3	48.2
Cross-sectional area, (μm.)^2	Av.	490	539	524	561	547	539	492
	S.D.,%	15.7	14.8	10.9	23.7	13.6	11.2	20.1
Number of fibers tested		30	50	48	10	49	51	8

TABLE II (Continued)

AVERAGE STRESS-STRAIN PROPERTIES BEFORE AND AFTER CREEP

		20-Gram Creep Load			25-Gram Creep Load		
		12 hr.	24 hr.	48 hr.	12 hr.	24 hr.	48 hr.
Modulus of elasticity, dynes/(μm.)^2	Av.	4010	3980	4060	4100	4070	4040
	S.D.,%	10.3	11.2	28.6	13.2	12.7	26.5
Breaking load, grams	Av.	61.0	60.8	63.4	64.6	59.2	67.1
	S.D.,%	20.0	26.2	30.7	21.7	22.1	32.8
Tensile strength, dynes/(μm.)^2	Av.	118.3	119.8	109.3	122.7	119.1	129.5
	S.D.,%	15.4	13.7	34.1	16.1	14.9	39.4
Ultimate elongation, %	Av.	4.28	4.21	4.33	3.87	3.95	3.51
	S.D.,%	16.8	17.2	29.7	14.3	15.5	33.7
Work-to-rupture, dyne-μm./(μm.)^3	Av.	3.42	3.48	3.39	3.45	3.40	3.43
	S.D.,%	32.7	31.8	39.6	33.8	31.7	45.2
Cross-sectional area, (μm.)^2	Av.	515	508	580	527	497	518
	S.D.,%	10.6	12.3	25.8	11.7	10.9	24.7
Number of fibers tested		47	50	9	45	48	7

TABLE III

AVERAGE STRESS-STRAIN PROPERTIES AFTER RECOVERY

		10-Gram Load			15-Gram Load		
		12 hr.	24 hr.	48 hr.	12 hr.	24 hr.	48 hr.
Modulus of elasticity, dynes/(μm.)^2	Av.	2690	2800	2790	3480	3570	3810
	S.D., %	15.7	13.8	27.5	16.3	11.9	29.6
Breaking load, grams	Av.	53.3	49.5	56.5	53.1	56.4	50.4
	S.D., %	22.3	27.8	34.1	25.2	20.3	31.7
Tensile strength, dynes/(μm.)^2	Av.	101.8	100.5	96.5	104.6	104.5	107.5
	S.D., %	15.4	12.7	30.6	16.2	15.7	37.8
Ultimate elongation, %	Av.	5.58	5.49	5.71	5.20	5.13	4.70
	S.D., %	17.6	15.2	25.7	15.9	16.7	29.7
Work-to-rupture, dyne-μm./(μm.)^3	Av.	3.03	3.08	2.97	2.76	2.85	2.74
	S.D., %	33.2	31.9	46.7	32.9	32.4	38.7
Cross-sectional area, (μm.)^2	Av.	523	492	586	507	539	468
	S.D., %	13.7	12.8	28.6	10.7	12.7	23.5
Number of fibers tested		52	48	9	50	49	10

TABLE III (Continued)

AVERAGE STRESS-STRAIN PROPERTIES AFTER RECOVERY

		20-Gram Load			25-Gram Load		
		12 hr.	24 hr.	48 hr.	12 hr.	24 hr.	48 hr.
Modulus of elasticity, dynes/(μm.)^2	Av.	3950	4070	4040	4060	4030	4010
	S.D., %	16.7	15.6	27.8	13.7	12.7	34.8
Breaking load, grams	Av.	61.9	61.4	62.0	59.9	65.3	63.5
	S.D., %	26.2	23.9	35.0	24.5	22.8	39.6
Tensile strength, dynes/(μm.)^2	Av.	117.8	118.9	117.2	119.7	120.3	123.9
	S.D., %	15.1	14.5	32.8	16.3	14.1	40.7
Ultimate elongation, %	Av.	4.75	4.83	4.65	4.51	4.63	4.37
	S.D., %	17.2	16.3	27.3	14.8	15.7	33.7
Work-to-rupture, dyne-μm./(μm.)^3	Av.	2.64	2.76	2.82	2.73	2.83	2.42
	S.D., %	30.1	34.3	48.2	33.6	31.5	47.6
Cross-sectional area, (μm.)^2	Av.	526	517	528	501	544	487
	S.D., %	13.6	11.4	26.4	14.8	11.7	30.2
Number of fibers tested		46	51	10	49	48	6

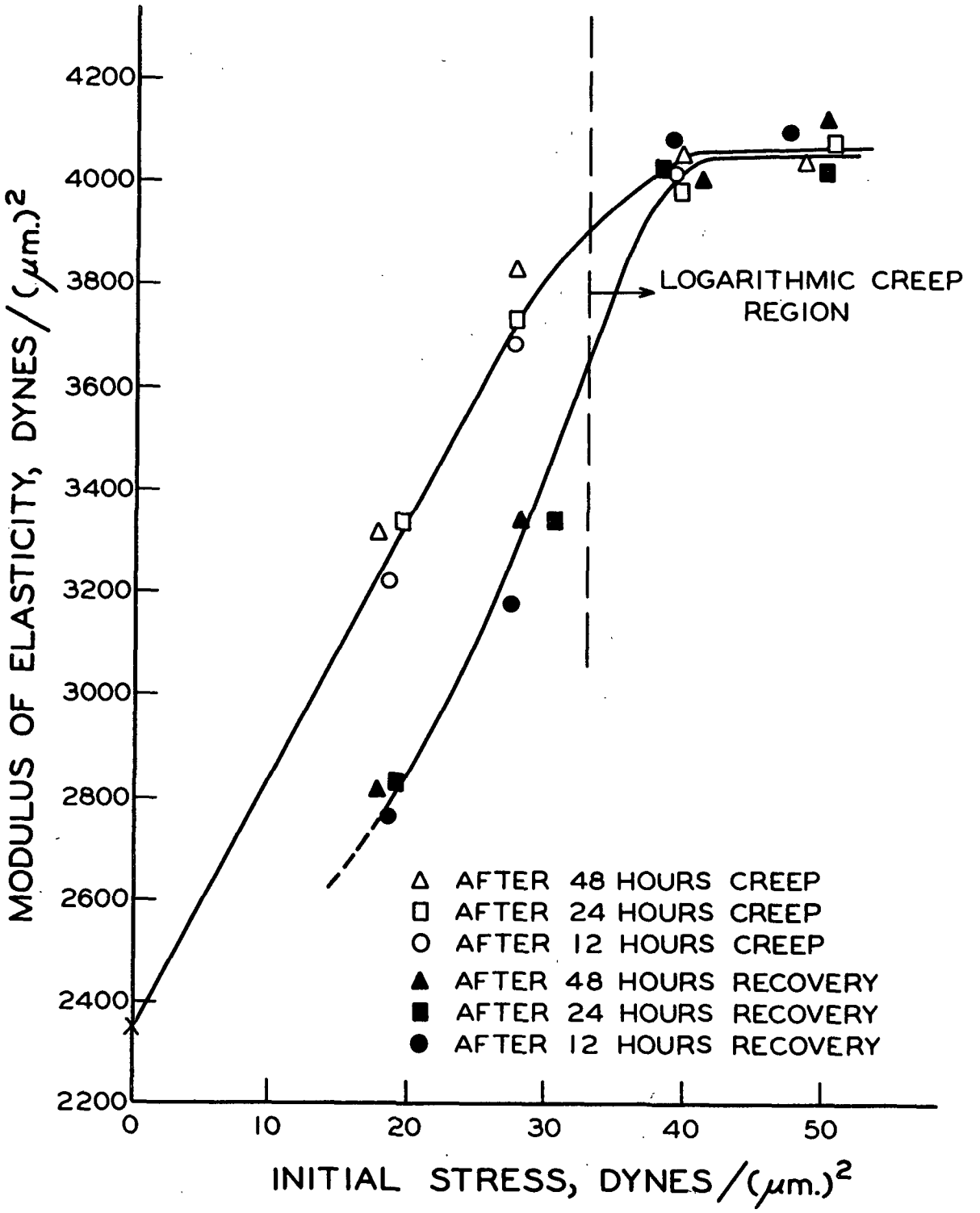

Figure 25. Modulus of Elasticity After Creep and After Recovery

testing these fibers after first-creep, they were free to recover for about 5 minutes before the load-elongation behavior was recorded. Thus, the values shown for first creep in Fig. 25 are lower by an unknown amount than the true value at the end of creep.

The amount of recovery of the elastic modulus is greater for short times and at a low initial stress. This indicates that in the initial creep response the structural changes leading to an increase of modulus are largely recoverable. It is also apparent that as creep progresses, the change in modulus is locked in to an increasing degree.

For the period of logarithmic creep response, the modulus is constant as logarithmic creep deformation increases. This indicates that structural changes leading to an increase in modulus have already occurred and that another mechanism is responsible for continued fiber deformation.

A comparison of the increase in modulus resulting from dry creep deformation and that resulting from drying under tension was made in Fig. 26. The values shown here for drying under tension were taken from the work of Spiegelberg (22) who investigated the same holocellulose fibers, and direct comparison should be valid. In this figure the modulus of elasticity is plotted versus the permanent fiber deformation. It is apparent that for large deformations the modulus values from both tests approach a common limiting value. Indeed, there is no significant difference in the values for permanent deformations above 1.0%. This comparison indicates that similar structural changes occur in these fibers whether stressed in a wet or dry condition.

It may be concluded from this comparison that, in the dry fibers, configurational response and secondary bonding phenomena are largely responsible for the rate of creep deformation, and only by such mechanisms may changes in the fibrillar structure

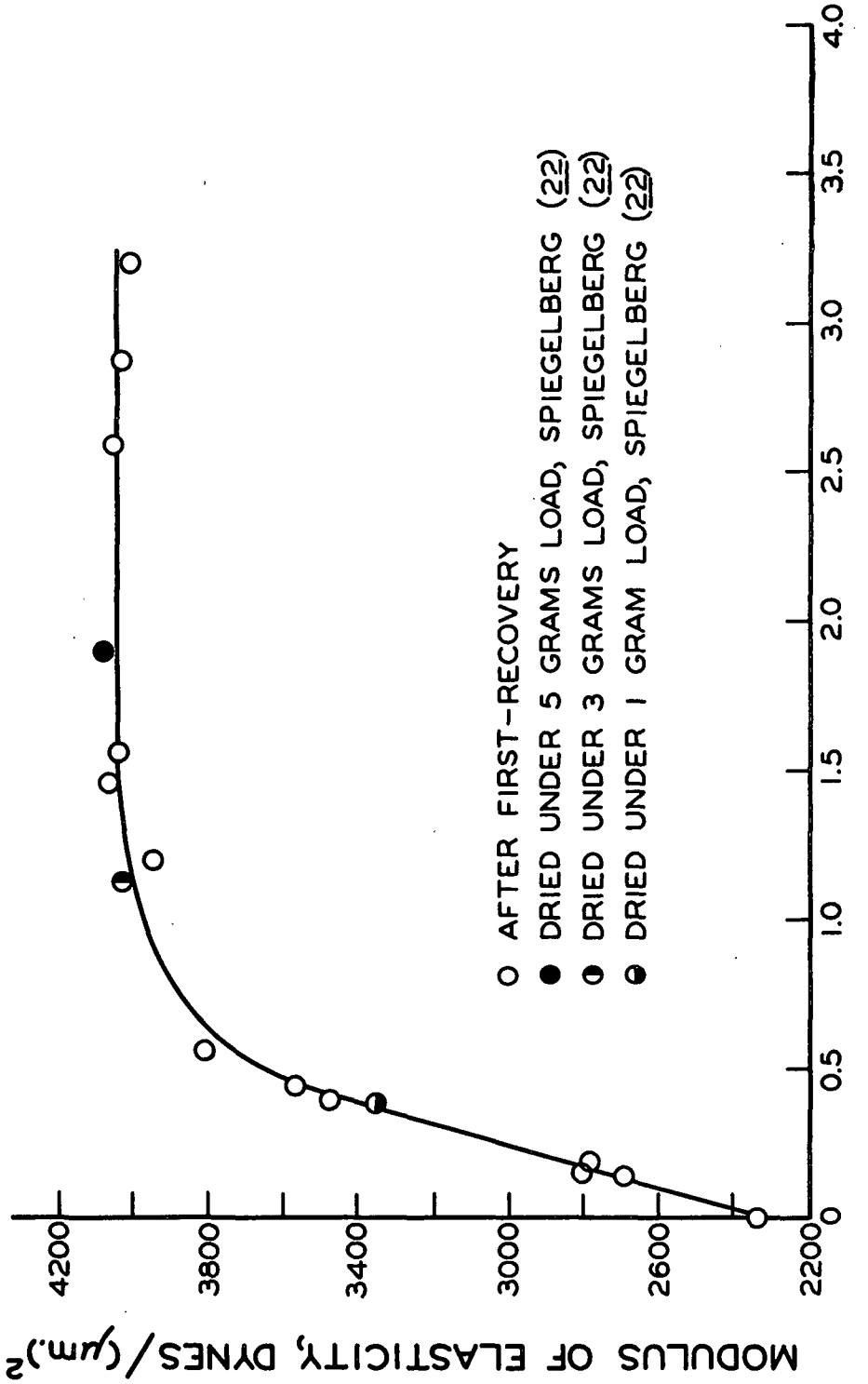

Figure 26. Relationship Between Elastic Modulus and Permanent Deformation

occur to affect fiber mechanical properties. This was indicated since, when wet, the structures formed by secondary bonds are largely destroyed, but the highly crystalline fibrils should not be greatly affected. Thus, the influence of the amorphous material on fiber deformation should be small. Once the fiber is dried in the extended position, secondary bonds will form to lock in some of the wet deformation. It may be assumed that changes in the mechanical properties of these fibers are determined by the changes in the fibrillar structure and that such changes are not dependent on the path followed to reach a given structural arrangement.

The effects of sustained stress on the tensile strength, ultimate elongation and work-to-rupture are indicated in Fig. 27. A significant increase in tensile strength occurs under these conditions, but increasing either the initial stress or the time of creep does not produce a further increase in this property. The tensile strength of a fiber depends on the discontinuities, such as pits and lamellae, and localized areas of stress concentration within the fiber. It would not be expected that creep response would alter this property further once the fiber structure has undergone initial adjustment to an applied stress. This indicates that initial creep response removes areas of stress concentration and that this removal is probably accomplished by the fibrillar elements adjusting so as to share more uniformly in supporting the applied load. Once this adjustment has occurred, further creep deformation occurs by mechanisms which do not significantly affect the larger discontinuities of the fiber structure. The data in Table III show that the tensile strength increase at low initial stress is almost totally lost during first-recovery, but once the creep response approaches logarithmic behavior this change is permanent.

The work-to-rupture increases as a result of creep deformation, and this property also reaches a limiting value at the start of logarithmic creep response.

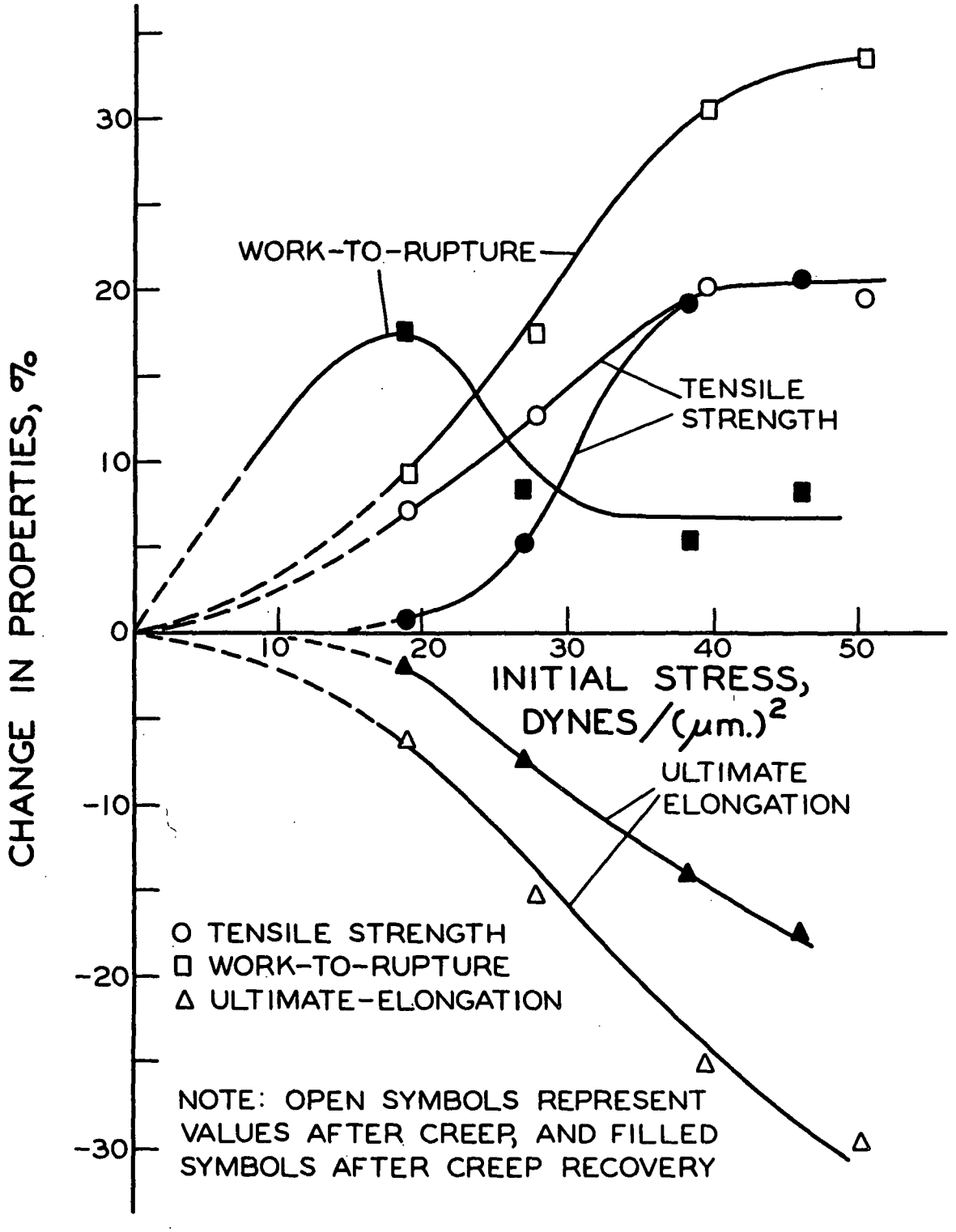

Figure 27. Change in Fiber Mechanical Properties Due to Creep and Creep Recovery

After recovery, the work-to-rupture appears to go through a maximum at low initial stress. This maximum may be a false impression. It is significant only at the 85% level, and the permanent creep deformation has stored energy in the system. There will be more energy stored during creep at high initial stresses where permanent deformation is the largest. The curves for work-to-rupture shown in Fig. 27 are for 24-hour tests, and the tests at 12 and 48 hours exhibit similar behavior.

Fiber ultimate elongation is dependent on the rupture of the specimen and should be governed by the weakest area of the fiber. It is interesting to note that the ultimate elongation, shown in Fig. 27, continues to decrease and does not level off at high initial stress as do the other mechanical properties of the fiber. In this figure, for the sake of clarity, only the 24-hour test results are shown, but the behavior is similar for the other test durations. It is apparent from this figure that after recovery, a significant increase in elongation occurs in comparison with the data taken after creep. This is the result of almost complete recovery of this property at low initial stress; and, indeed, for creep and recovery at 10 grams for 12 hours, complete recovery is obtained.

Not only the modulus of elasticity but also the tensile strength, ultimate elongation, and the work-to-rupture change during creep in a manner similar to that produced by drying under tension. Thus, it would appear that these properties are not dependent on the path followed to reach a given structural arrangement. The structural changes in dry fibers occur much more slowly than they do in wet fibers but in both cases the final structure must be very similar.

SUMMARY OF RESULTS AND CONCLUSIONS

The objectives of this thesis were to determine the action of sustained tensile stress on the structure of individual wood pulp fibers, and to determine the effect of the structural changes on the mechanical properties of the fibers. To fulfill these objectives, individual summerwood holocellulose fibers from one growth ring were obtained. Randomly selected fibers from this population were subjected to various conditions of axial tensile creep and creep recovery tests. Changes in the fibers' internal structure were inferred from their creep and recovery behavior, and x-ray diffractograms were obtained to provide a more direct evaluation of structural changes. The load-elongation properties of the fibers were determined both before and after creep and after creep recovery to evaluate the effect of sustained stress on the mechanical properties of the fibers. The data also provided additional information related to fiber structural modification. The results of these tests show that:

1. The first-creep response was composed of at least two types of behavior, and the limiting behavior could be described by a logarithmic creep equation.

2. The deformation behavior was a continuous process with no abrupt change from initial creep to logarithmic creep.

3. The initial creep behavior was largely recoverable (85%), but logarithmic creep resulted in largely permanent deformation (40% recoverable).

4. The structural changes in dry fibers caused by sustained tensile stress led to similar mechanical properties as those obtained when these fibers were dried under tension.

5. The crystallite or fibrillar orientation increased slightly, but there was no apparent change in cellulose crystallinity due to sustained stress. The orientation appeared to decrease slightly after first-recovery.

6. The modulus of elasticity increased with both initial stress and time under stress and approached a limiting value as logarithmic creep began. The limiting value represented a change of about 70% in this property. The amount of this change recovered following first-recovery decreased as the initial creep stress and the time under stress were increased.

7. The ultimate elongation decreased continuously as creep progressed, but after recovery from creep at low initial stress and early times, this property returned to the value of unstressed fibers.

8. The tensile strength of the fibers increased rapidly at low initial stresses and early times, and the increase was almost completely lost following first-recovery; but for creep conditions which produced large permanent deformations, only partial loss of the increased strength characteristic occurred.

9. The work-to-rupture increased as the result of creep deformation and reached a limiting value at the start of logarithmic creep.

These results, although they provide indirect evidence, strongly support the hypothesis that there are structural changes within the fiber resulting from tensile stress.

At least two types of structural changes occur during creep tests. First, as stress is applied to the fiber, localized areas of stress concentration are relieved by the molecules in the amorphous regions which undergo configurational changes to allow minute fibrillar movement which serves to redistribute the stress. This behavior is largely responsible for the changes in the mechanical properties of the fiber. Once this response extends to the point that secondary bonds are broken, the bonding groups reach new positions favorable to bond formation, and permanent changes start to occur in the fiber. These permanent changes will occur at very low fiber deformation due to the regions of high stress concentration

within the fiber. Configurational changes and bond breakage and formation are time-dependent phenomena related to the applied stress.

The second type of structural change, associated with logarithmic creep, occurs after localized areas of stress concentration have been relieved and probably involves the movement of relatively large segments of cellulosic fibrils. Since the mechanical properties of the fiber are no longer significantly affected by further fiber deformation in this region, it appears that adjustment of the load-bearing elements to produce redistribution of internal stress no longer occurs to an important extent, and these elements must now extend as a unit. The rate of extension is probably governed by the configurational and bonding changes previously discussed. Since this response involves large segments of the fiber, many secondary bonds must rupture and may reform in new positions, locking the deformed structure and producing nonrecoverable fiber deformation. At a given level of permanent deformation, the structural changes locked in the fibers by dry creep are of the same nature as those produced through drying under tension.

The only direct experimental evidence for structural changes comes from the x-ray diffraction data, and these show only that a small increase in crystallite orientation occurs. This evidence serves to substantiate the structural behavior inferred from the viscoelastic and mechanical behavior of the fibers.

The mechanical properties of the fiber are dependent on the internal structure of the fiber and change as the structure reacts to an applied stress. Of the properties studied, the modulus of elasticity is the property most sensitive to structural changes and is dependent on prerupture behavior of the fiber. The tensile strength, ultimate elongation, and work-to-rupture are also affected by the structural changes produced by sustained stress. Only the ultimate elongation is affected as the fiber deforms in the region of logarithmic creep. This shows

that the total elongation of the fiber is almost constant up to rupture and does not depend on the path followed to achieve the elongation.

It is apparent from the results of this study when considered in light of Van den Akker's theory of paper structure that the directional mechanical properties of machine-made paper may be attributable in part to sustained tension in the dried sheet. Such tension would produce creep in the fibers and increase their elastic modulus and tensile strength. Although not evaluated in this study, the behavior of those fibers compressively loaded in a sheet may significantly reduce these mechanical properties and add to the anisotropy of the sheet.

ACKNOWLEDGMENTS

This thesis was completed with the aid of contributions both large and small from many individuals. To all of these, too numerous to list, the author wishes to express a most sincere thanks.

Special appreciation is expressed to Dr. J. A. Van den Akker, the chairman of this thesis advisory committee, and Dr. K. Ward, Jr., member of the committee. The late Dr. G. R. Sears was also a member of the advisory committee, and his unfailing interest and encouragement were a continual inspiration.

In addition, Mr. H. Marx and Mr. M. Filz of The Institute of Paper Chemistry instrument shop offered invaluable advice and aid in the design and machining of the apparatus required for this work.

Finally, but definitely not last, the author expresses his sincere thanks to his wife, Gail, who offered both inspiration and encouragement leading to the completion of this study.

LITERATURE CITED

1. Morton, W. E., and Hearle, J. W. S. Physical properties of textile fibers. Manchester and London, Butterworth and Co., Ltd., and The Textile Institute, 1962. 609 p.

2. Ott, E., Spurlin, H. M., and Grafflin, M. W., Ed. Cellulose and cellulose derivatives. 2nd ed. New York, Interscience, 1954. 1601 p.

3. Meredith, R., Ed. The mechanical properties of textile fibers. New York, Interscience, 1956. 333 p.

4. Meyer, K. H., and Misch, L., Helv. Chem. Acta 20, no. 2:232-44(1937).

5. Mark, H. Interaction and arrangement of cellulose chains. In Ott's Cellulose and cellulose derivatives. 2nd. ed., Part I. p. 217-30. New York, Interscience, 1954.

6. Hearle, J. W. S., J. Polymer Sci. 28, no. 117:432-5(1958).

7. Hearle, J. W. S., J. Textile Inst. Proc. 53, no. 8:449-64(1962).

8. Jentzen, C. A. The effect of stress applied during drying on the mechanical properties of individual pulp fibers. Doctor's Dissertation. Appleton, Wis., The Institute of Paper Chemistry, 1964. 130 p.

9. Jentzen, C. A., Tappi 47, no. 7:412-18(1964).

10. Tønnesen, B. A., and Ellefsen, ø., Norsk Skogind. 14, no. 7:266-9(1960).

11. Manley, R. St. J. Summary, I. P. C. Pioneering Research Program. p. 88-101. Appleton, Wis., The Institute of Paper Chemistry, 1964.

12. Dolmetsch, H., Papier 17, no. 12:710-21(1963).

13. Brown, H. P., Panshin, A. J., and Forsaith, C. C. Textbook of wood technology. Vol. I. New York, McGraw-Hill, 1949, 652 p.

14. Wardrop, A. B., Svensk Papperstid. 66, no. 7:231-47(1963).

15. Bailey, I. W., Ind. Eng. Chem. 30, no. 1:40-7(1938).

16. Hock, C. W. Microscopic structure of native cellulose. In Ott's Cellulose and cellulose derivatives. 2nd ed. Part I. p. 347-78. New York, Interscience, 1954.

17. Rollins, M., and Trip, V., Forest Prod. J. 493-7(1961).

18. Frey-Wyssling, A. The general structure of fibers. In Bolam's Fundamentals of papermaking fibers. p. 1-6. Kenley, Surrey, England, Tech. Sect. of the Brit. Paper and Board Makers' Assoc., Inc., 1958.

19. Emerton, H. W., The outer secondary wall. I. Its structure. In Bolam's Fundamentals of papermaking fibers. p. 35-54. Kenley, Surrey, England, Tech. Sect. of the Brit. Paper and Board Makers' Assoc., Inc., 1958.

20. Bucher, H. Discontinuities in the microscopic structure of wood fibers. In Bolam's Fundamentals of papermaking fibers. p. 7-26. Kenley, Surrey, England, Tech. Sect. of the Brit. Paper and Board Makers' Assoc., Inc., 1958.

21. Jayme, G., and Hunger, G. Electron microscope 2- and 3-dimensional classification of fibre bonding. In Bolam's Formation and structure of paper. Vol. I. p. 135-70. London, Tech. Sect. of the Brit. Paper and Board Makers Assoc., Inc., 1962.

22. Spiegelberg, H. L. The effect of hemicelluloses on the mechanical properties of individual pulp fibers. Doctor's Dissertation. Appleton, Wis., The Institute of Paper Chemistry, 1966. 115 p.

23. Leopold, B., and McIntosh, D., Tappi 44, no. 3:235-40(1961).

24. Leopold, B., Tappi 44, no. 3:232-5(1961).

25. Meier, H., J. Polymer Sci. 51, no. 155:11-18(1961).

26. Meier, H., Pure Appl. Chem. 5:37-52(1962).

27. Preston, R. D., Polymer 3:511-28(1962).

28. Rånby, B. G. The fine structure of cellulose fibrils. In Bolam's Fundamentals of papermaking fibers. p. 55-82. Kenley, Surrey, England, Tech. Sect. of the Brit. Paper and Board Makers' Assoc., Inc., 1958.

29. Alfrey, Turner, Jr. Mechanical behavior of high polymers. New York, Interscience, 1948. 581 p.

30. Ferry, J. D. Viscoelastic properties of polymers. New York, John Wiley and Sons, Inc., 1961. 482 p.

31. Meyer, K. H., and Lotmar, W., Helv. Chem. Acta 19, no. 1:69-86(1936).

32. Leaderman, H. Elastic and creep properties of filamentous materials and other high polymers. Washington, D. C., The Textile Foundation, 1943. 278 p.

33. Rance, H. F., In Meredith's Mechanical properties of wood and paper. Part B. Amsterdam, North Holland Publishing Company, 1953. 298 p.

34. Brezinski, J. P. A study of the viscoelastic properties of paper by means of tensile creep tests. Doctor's Dissertation. Appleton, Wis., The Institute of Paper Chemistry, 1955. 242 p.; Tappi 39, no. 2:116-28(1958).

35. Parker, J. L. The effects of ethylamine decrystallization of cellulose fibers on the viscoelastic properties of paper. Doctor's Dissertation. Appleton, Wis., The Institute of Paper Chemistry. 1962. 146 p.; Tappi 45, no. 12:936-43(1962).

36. Schulz, J. H. The effect of strain applied during drying on the mechanical behavior of paper. Doctor's Dissertation. Appleton, Wis., The Institute of Paper Chemistry, 1961. 161 p.; Tappi 44, no. 10:736-44(1961).

37. Press, J. J., J. Appl. Phys. 14, no. 5:224-33(1943).

38. Mark, H., and Press, J. J., Rayon Textile Monthly 24:297-9, 339-41, 405 (1943).

39. Negishi, M., J. Soc. Textile Cellulose Ind. Japan 2:34-8(1946).

40. Negishi, M., J. Soc. Textile Cellulose Ind. Japan 3:21-4(1947).

41. Hartler, N., Kull, G., and Stockman, L., Svensk Papperstid. 66, no. 8:309-11 (1963).

42. Pierce, F. T., J. Textile Inst. Trans. 17:T355-68(1926).

43. Wakeham, H. Mechanical properties of cellulose and its derivatives. In Ott's Cellulose and cellulose derivatives. 2nd ed. Part III. p. 1247-1356. New York, Interscience, 1954.

44. Ziifle, H. M., Eggerton, F. V., and Segal, L., Textile Res. J. 29, no. 1:13-20 (1959).

45. Orr, R. S., Burgis, A. W., Andrews, F. R., and Grant, J. N., Textile Res. J. 29, no. 4:349-55(1959).

46. Ward, K., Textile Res. J. 20, no. 6:363-72(1950).

47. Sisson, W. A., Textile Res. J. 7, no. 11:425-31(1937).

48. Orr, R. S., De Luca, L. B., Burgis, A. W., and Grant, J. N., Textile Res. J. 29, no. 2:144-50(1959).

49. Krässig, H., and Kitchen, W., J. Polymer Sci. 51, no. 155:123-72(1961).

50. Wardrop, A. B., Australian J. Sci. Res. (B4) 4, no. 4:391-414(1951).

51. Spiegelberg, H. L., Tappi 49, no. 9:388-96(Sept., 1966).

52. Jayme, B. A., Tappi 42, no. 6:461-7(1959).

53. Jayme, B. A., Forest Prod. J. 10, no. 6:316-22(1960).

54. Boltzmann, L., Pogg. Ann. Physik 7:624(1876).

55. O'Shaughnessy, M. T., Textile Res. J. 18, no. 5:263-86(1948).

56. Catsiff, E., Alfrey, T., and O'Shaughnessy, M. T., Textile Res. J. 23, no. 11:808-20(1953).

57. Sanborn, I. B. A study of irreversible, stress-induced changes in the macrostructure of paper. Doctor's Dissertation. Appleton, Wis., The Institute of Paper Chemistry, 1961. 161 p.; Tappi 45, no. 6:465-74(1962).

58. Wise, L. E., Murphy, M., and D'Addieco, A. A., Paper Trade J. 122, no. 2: 35(1946).

59. Hardacker, K. W., Tappi 45, no. 3:237-46(1962).

60. Hardacker, K. W., and Van den Akker, J. A. To be published.

61. Lathrop, A. L., and Hardacker, K. W., Tappi 45, no. 2:169-72(1962).

62. Segal, L., Creely, J. J., Martin, A. E., and Conrad, C. M., Textile Res. J. 29, no. 10:786-94(1959).

63. Gjonnes, J., Norman, N., and Viervol, H., Acta Chem. Scand. 12, no. 3:489-94; no. 10:2028-33(1958).

64. Van den Akker, J. A. Some theoretical considerations on the mechanical properties of fibrous structures. In Bolam's The formation and structure of paper. Vol. I. p. 205-41. London, Tech. Assoc. of the Brit. Paper and Board Makers' Assoc., Inc., 1962.

65. Page, D. H., Paper Technol. 1, no. 4:407-11(1960).

66. Page, D. H., and Tydeman, P. A., Paper Technol. 1, no. 5:519-30(1960).

67. Page, D. H., Tydeman, P. A., and Hunt, M. The behavior of fibre-to-fibre bonds in sheets under dynamic conditions. In Bolam's The formation and structure of paper. Vol. I. p. 249-63. London, Tech. Assoc. of the Brit. Paper and Board Makers' Assoc., Inc., 1962.

68. Davies, O. L. Statistical method in research and production. New York, Hafner Publishing Company, 1958. 396 p.

APPENDIX I

FIBER MOUNTING

An investigation was made of the fiber mounting procedure. The purpose of this study was to determine the effects of the mounting glue on measured creep deformations. Epoxy resin, Epon 907*, was used to glue the fibers to steel pins, and it was necessary to evaluate the creep response of this material. The general technique used was the same used in determining fiber load-elongation properties on the FLER (59).

Nine-micron glass fibers were mounted using 10:8, 10:7, and 10:6 mixtures by weight of resin component A to B. Slight etching with 2% hydrofluoric acid was used to prepare the glass surface. The slightest contamination on the fiber surface prevented good adhesion. It was noted that if these fibers were dried on a teflon-coated glass plate sufficient surface contamination occurred to allow slippage in the glue. By drying the fibers on a carefully washed cotton cloth, this problem was eliminated.

Two methods were used to determine the flow characteristics of the epoxy. First, the mounted fibers were subjected to sustained stress in the FCRR, and the elongation-time behavior recorded. Second, photomicrographs were used to detect time-dependent changes in the glue line and bulk epoxy.

Creep runs made on the glass fibers at 1-mm. span indicated that after 48 hours curing time the 10:8 mixture extended approximately 3%, and the 10:7 mixture extended about 1% based on the span length. The tests were run for 24 hours under a 20-gram load. Figure 28 is a plot of two of the creep runs made

*Manufactured by Shell Chemical Company.

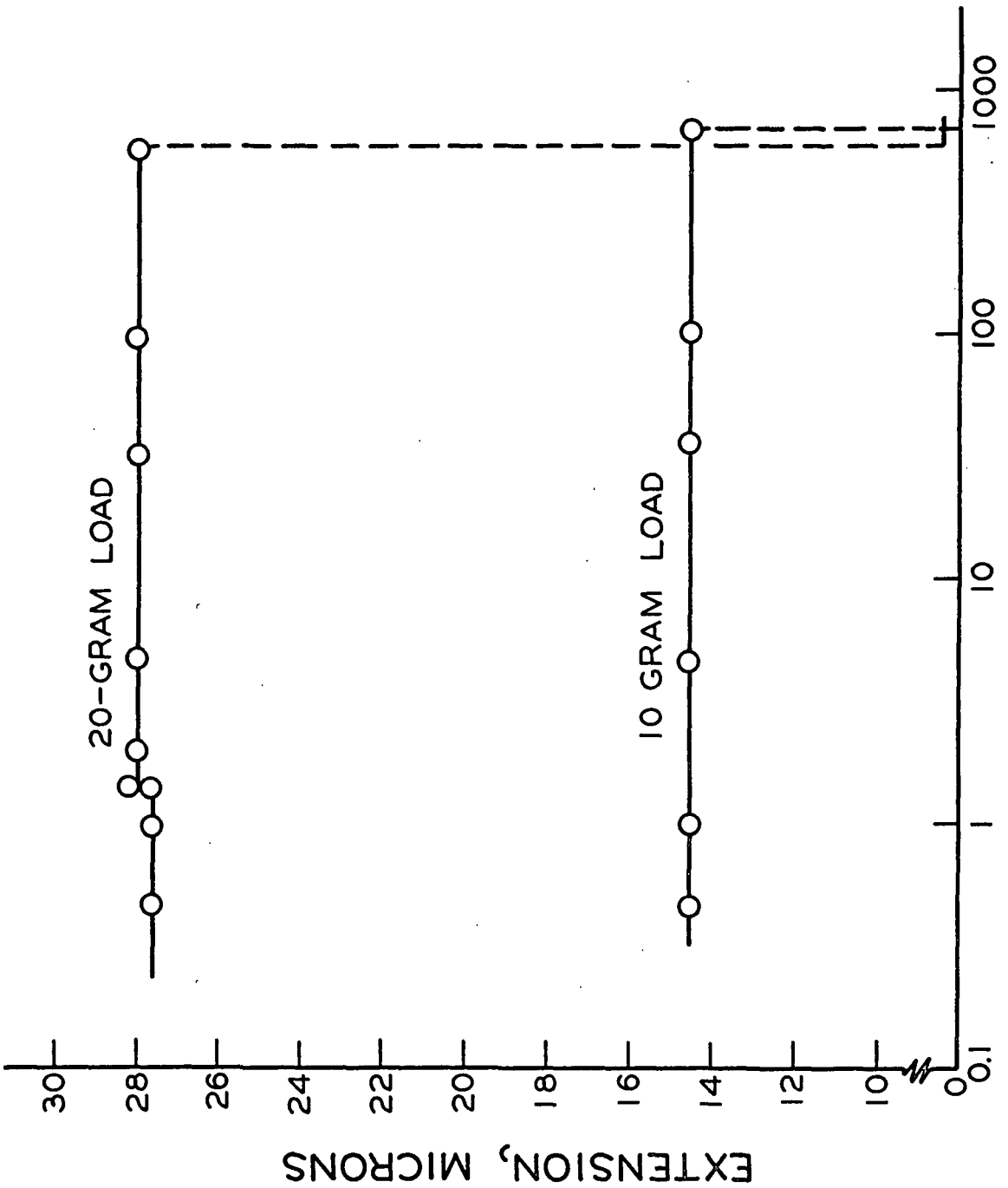

Figure 28. Creep of Glass Fibers

utilizing glass fibers mounted with the 10:6 mixture. The data for the lower curve were obtained at a 10-gram load. This load approximates the maximum stress on the epoxy-fiber interface which would occur for pulp fibers loaded to 25 grams. It is not valid to assume that the entire bond is evenly stressed, so data were also collected at a 20-gram load utilizing the glass fibers. At the high load level three types of behavior were noted: (1) the fibers pulled out before or just after load was reached; (2) a small elongation occurred shortly after loading, followed by no further elongation and, (3) there was no measurable change in elongation after loading. The latter case held for eight out of ten fibers at the ten-gram load level (two pulled out). These data indicated that there were no appreciable creep of the mounting material at test conditions and that any effect of this material would be limited to elastic deformations. As may be seen in the figure, the elongation returned to zero on unloading. The slip accounts for the slight residual elongation of the 20-gram run.

Photomicrographs were taken of the glue joint between fiber and epoxy in order to determine changes in the configuration of the glue line and bulk epoxy. The photographs were taken at 100X magnification, and there was no apparent deformation of the epoxy. The photographs were taken before loading to 15 grams, ten minutes after loading, and twelve hours after loading and showed no change in the outline of the glue joint. It appeared that the glue line extended very slightly between the first two photographs, but there was no apparent change between the last two pictures in the series.

These data served to confirm that there was no bulk flow in the 10:6 mixture of epoxy and that only small, probably elastic, deformation resulted from the stress applied to the epoxy. Therefore, there should be no error in the measured fiber elongation data due to creep in the epoxy. A very slight elongation will probably

be recorded due to epoxy elastic deformation, but this effect should be relatively constant for all creep tests and will not adversely affect the tests. The small effects of elastic deformation should cancel in creep recovery experiments.

APPENDIX II

AVERAGE DATA FROM CREEP AND RECOVERY TESTS

The creep data used to construct the curves presented in Fig. 15, 17, and 18 are contained in Table IV. Table V contains the recovery data used to construct the curves in Fig. 20, 21, and 22. Each point given in the tables represents the average behavior of a group of fibers. The number of fibers in each group is shown in the tables. The averaging procedure was discussed in the section of this thesis entitled "Treatment of Data."

TABLE IV

AVERAGE TIME-DEFORMATION DATA IN CREEP TESTS[a]

Nominal Load – 10 Grams

Time of test	12 hours		24 hours		48 hours	
Av. initial stress, dynes/(μm.)^2	18.5	19.2	19.1	18.6	17.7	17.9
Time, seconds						
30	0.798	0.803	0.801	0.790	0.760	0.742
45	0.800	0.804	0.805	0.794	0.762	0.743
60	0.808	0.810	0.804	0.799	0.769	0.799
90	0.813	0.812	0.810	0.807	0.773	0.752
120	0.803	0.807	0.808	0.806	0.770	0.753
240	0.813	0.809	0.813	0.810	0.782	0.760
600	0.824	0.819	0.818	0.821	0.794	0.775
1,200	0.830	0.828	0.830	0.825	0.797	0.778
3,000	0.839	0.842	0.838	0.837	0.806	0.787
6,000	0.844	0.845	0.842	0.841	0.813	0.795
12,000	0.860	0.863	0.859	0.856	0.818	0.801
20,000	0.853	0.857	0.857	0.860	0.824	0.804
30,000	0.857	0.858	0.864	0.862	0.830	0.811
43,000	0.862	0.866	0.861	0.864	0.835	0.815
60,000	--	--	0.868	0.869	0.840	0.822
85,000	--	--	0.875	0.871	0.843	0.824
120,000	--	--	--	--	0.856	0.831
170,000	--	--	--	--	0.865	0.846
Av. S. D., %	25.3	23.0	28.1	30.2	43.1	40.8
No. of fibers tested	50	52	48	48	10	9

[a] Deformation expressed as strain x 100.

TABLE IV (Continued)

AVERAGE TIME-DEFORMATION DATA IN CREEP TESTS[a]

Nominal Load – 15 Grams

Time of test	12 hours		24 hours		48 hours	
Av. initial stress, dynes/(μm.)^2	27.4	29.6	27.8	27.9	25.2	32.0
Time, seconds						
30	1.19	1.32	1.25	1.26	1.14	1.44
45	1.20	1.32	1.25	1.25	1.15	1.42
60	1.20	1.33	1.26	1.27	1.14	1.44
90	1.21	1.34	1.27	1.29	1.17	1.45
120	1.21	1.34	1.28	1.28	1.16	1.47
240	1.22	1.35	1.29	1.29	1.17	1.47
600	1.23	1.36	1.29	1.31	1.18	1.48
1,200	1.25	1.38	1.30	1.32	1.20	1.49
3,000	1.26	1.40	1.34	1.34	1.21	1.53
6,000	1.31	1.45	1.35	1.37	1.25	1.55
12,000	1.35	1.49	1.42	1.41	1.30	1.61
20,000	1.41	1.54	1.48	1.49	1.36	1.63
30,000	1.47	1.60	1.52	1.52	1.43	1.71
43,000	1.53	1.65	1.57	1.59	1.47	1.75
60,000	--	--	1.60	1.62	1.52	1.80
85,000	--	--	1.66	1.68	1.58	1.84
120,000	--	--	--	--	1.64	1.92
170,000	--	--	--	--	1.70	1.98
Av. S.D., %	24.7	29.8	26.5	23.1	39.2	38.4
No. of fibers tested	49	50	51	49	8	10

[a] Deformation expressed as strain x 100.

TABLE IV (Continued)

AVERAGE TIME-DEFORMATION DATA IN CREEP TESTS[a]

Nominal Load – 20 Grams

Time of test	12 hours		24 hours		48 hours	
Av. initial stress, dynes/(μm.)^2	38.9	38.0	39.4	38.6	34.5	37.9
Time, seconds						
30	1.81	1.77	1.83	1.79	1.60	1.75
45	1.82	1.79	1.85	1.81	1.61	1.77
60	1.84	1.81	1.87	1.82	1.63	1.78
90	1.86	1.82	1.88	1.84	1.65	1.80
120	1.88	1.84	1.90	1.85	1.67	1.82
240	1.93	1.88	1.95	1.92	1.70	1.87
600	2.06	2.04	2.10	2.06	1.86	2.01
1,200	2.20	2.15	2.21	2.18	2.00	2.14
3,000	2.40	2.36	2.42	2.39	2.10	2.34
6,000	2.58	2.55	2.60	2.56	2.38	2.52
12,000	2.76	2.72	2.74	2.75	2.54	2.70
20,000	2.88	2.85	2.89	2.87	2.69	2.83
30,000	2.99	2.96	3.00	2.99	2.80	2.94
43,000	3.10	3.05	3.12	3.08	2.91	3.04
60,000	--	--	3.18	3.16	2.98	3.12
85,000	--	--	3.27	3.25	3.06	3.21
120,000	--	--	--	--	3.17	3.31
170,000	--	--	--	--	3.26	3.40
Av. S.D., %	25.2	24.1	26.7	21.9	39.7	45.4
No. of fibers tested	47	46	50	51	9	10

[a] Deformation expressed as strain x 100.

TABLE IV (Continued)

AVERAGE TIME-DEFORMATION DATA IN CREEP TESTS[a]

Nominal Load – 25 Grams

Time of test	12 hours		24 hours		48 hours	
Av. initial stress, dynes/(μm.)^2	47.5	49.9	50.3	46.0	48.3	51.3
Time, seconds						
30	2.46	2.58	2.60	2.38	2.49	2.65
45	2.55	2.66	2.69	2.45	2.58	2.73
60	2.65	2.75	2.78	2.58	2.69	2.84
90	2.79	2.91	2.94	2.71	2.81	2.99
120	2.88	3.01	3.02	2.82	2.93	3.07
240	3.12	3.24	3.27	3.04	2.15	3.30
600	3.44	3.57	3.58	3.35	2.47	3.63
1,200	3.67	3.79	3.81	3.60	2.69	3.86
3,000	3.99	4.12	4.12	3.92	4.03	4.16
6,000	4.23	4.35	4.38	4.15	4.26	4.42
12,000	4.46	4.60	4.60	4.37	4.49	4.64
20,000	4.64	4.76	4.79	4.58	4.67	4.85
30,000	4.78	4.89	4.93	4.70	4.82	4.97
43,000	4.92	5.03	5.05	4.83	4.95	5.11
60,000	--	--	5.16	4.95	5.05	5.20
85,000	--	--	5.27	5.05	5.15	5.32
120,000	--	--	--	--	5.29	5.46
170,000	--	--	--	--	5.40	5.56
Av. S. D., %	23.2	28.7	27.3	25.1	42.8	54.3
No. of fibers tested	45	49	48	48	7	6

[a] Deformation expressed as strain x 100.

TABLE V

AVERAGE TIME-DEFORMATION DATA IN FIRST-RECOVERY TESTS[a]

	Nominal Creep Load 10 Grams			Nominal Creep Load 15 Grams		
Time of test	12 hr.	24 hr.	48 hr.	12 hr.	24 hr.	48 hr.
Av. initial stress, dynes/(μm.)^2	19.2	18.6	17.9	29.6	27.9	32.0
Time, seconds						
30	0.653	0.633	0.612	1.15	1.14	1.26
45	0.655	0.635	0.614	1.15	1.14	1.26
60	0.656	0.637	0.615	1.16	1.15	1.27
90	0.658	0.640	0.618	1.16	1.15	1.28
120	0.663	0.644	0.624	1.16	1.15	1.28
240	0.668	0.652	0.629	1.18	1.16	1.29
600	0.676	0.658	0.637	1.19	1.18	1.32
1,200	0.686	0.669	0.647	1.20	1.18	1.32
3,000	0.700	0.683	0.661	1.22	1.20	1.35
6,000	0.710	0.698	0.670	1.23	1.21	1.36
12,000	0.718	0.707	0.677	1.24	1.21	1.37
20,000	0.722	0.712	0.681	1.24	1.22	1.39
30,000	0.724	0.716	0.686	1.25	1.22	1.39
43,000	0.723	0.717	0.689	1.25	1.23	1.40
60,000	--	0.718	0.691	--	1.23	1.40
85,000	--	0.719	0.692	--	1.23	1.40
120,000	--	--	0.693	--	--	1.41
170,000	--	--	0.693	--	--	1.41
Av. S. D., %	27.6	24.3	47.2	29.6	27.4	45.3
No. of fibers tested	52	48	9	50	49	10

[a] Deformation expressed as strain x 100.

TABLE V (Continued)

AVERAGE TIME-DEFORMATION DATA IN FIRST-RECOVERY TESTS[a]

	Nominal Creep Load 20 Grams			Nominal Creep Load 25 Grams		
Time of test	12 hr.	24 hr.	48 hr.	12 hr.	24 hr.	48 hr.
Av. initial stress, dynes/(μm.)^2	38.0	38.6	37.9	49.9	46.0	51.3
Time, seconds						
30	1.63	1.58	1.70	2.13	1.92	2.02
45	1.64	1.59	1.71	2.14	1.92	2.02
60	1.64	1.60	1.70	2.14	1.93	2.04
90	1.65	1.61	1.72	2.17	1.94	2.04
120	1.67	1.61	1.74	2.17	1.96	2.06
240	1.68	1.64	1.74	2.22	1.97	2.09
600	1.71	1.66	1.76	2.25	2.01	2.13
1,200	1.74	1.69	1.77	2.31	2.05	2.18
3,000	1.76	1.72	1.78	2.34	2.09	2.21
6,000	1.79	1.74	1.81	2.39	2.10	2.25
12,000	1.80	1.75	1.82	2.41	2.13	2.28
20,000	1.82	1.76	1.84	2.44	2.15	2.29
30,000	1.83	1.77	1.84	2.44	2.16	2.33
43,000	1.83	1.78	1.85	2.44	2.17	2.32
60,000	--	1.77	1.87	--	2.16	2.34
85,000	--	1.78	1.86	--	2.17	2.34
120,000	--	--	1.88	--	--	2.36
170,000	--	--	1.87	--	--	2.35
Av. S. D., %	22.7	25.4	46.7	29.3	26.1	42.9
No. of fibers tested	46	51	10	49	48	6

[a] Deformation expressed as strain x 100.

APPENDIX III

CALCULATION OF HYPOTHETICAL HANDSHEET MASTER CREEP CURVE

The calculation of a master creep curve for a hypothetical handsheet made from the fibers used in this study was based on the theory of Van den Akker (64) for the mechanical properties of fibrous structures. The sheet is assumed to be isotropic and composed of uniform ribbonlike fibers, all having a width of 45 μm. and a thickness of 12 μm. The sheet is further assumed to have a basis weight of 100 g./m.^{2} and the sheet density is 0.75 g./cm.^{3}. It is also assumed that Poisson's ratio for the sheet, ν, is 0.300. The test specimen from this sheet is assumed to be 61.4-mm. wide, and the initial stress on the sheet is 1.58 kg./mm.^{2} in accordance with the work of Sanborn (57).

In order to calculate the initial stress on fibers oriented at various angles, θ, it is first necessary to estimate the sheet elastic deformation. From the present study the fiber Young's modulus $\underline{E}_0$, before mechanical action on the sheet, is 2340 dynes/(μm.)^2. It is assumed that the fiber modulus of rigidity is 1/3 $\underline{E}_0$ or 780 dynes/(μm.)^2. From the theory of Van den Akker the sheet Young's modulus, $\mathcal{E}$, is

$$\mathcal{E} = \left\{W/\mathcal{J} \langle A \rangle_{Av} \rho \langle s \rangle_{Av}\right\} \left\{ [(1+\nu)/2] \int_0^{\pi} \int_0^{\infty} \int_0^{\infty} \int_0^{\infty} (s/h) \sin^2\theta \cos^2\theta P_\theta P_A P_I P_s \, ds \, dI \, dA \, d\theta \right.$$

$$+ \int_0^{\pi} \int_0^{\infty} \int_0^{\infty} AEs \sin^4\theta P_\theta P_A P_s \, ds \, dA \, d\theta$$

$$\left. - \nu \int_0^{\pi} \int_0^{\infty} \int_0^{\infty} AEs \sin^2\theta \cos^2\theta \, P_\theta P_A P_s \, ds \, dA \, d\theta \right\}.$$

where $\underline{W}$ = mass of fibers per unit area of sheet

$\mathcal{T}$ = sheet thickness

$\langle \underline{A} \rangle_{\underline{Av}}$ = average fiber cross-sectional area

ρ = fiber wall density

$\langle \underline{s} \rangle_{\underline{Av}}$ = average fiber segmental length

ν = Poisson's ratio for sheet

$\underline{s}$ = fiber segmental length

$\underline{A}$ = fiber cross-sectional area

$\underline{E}$ = Young's modulus of the fibers

$\underline{P}_\theta$, $\underline{P}_A$, $\underline{P}_I$, $\underline{P}_s$ are the distribution functions for fiber orientation, cross-sectional area, moment of inertia, and segmental length, respectively.

The term $\underline{h}$ is defined as

$$h = (s^2/12EI) + (1/AG)$$

where $\underline{I}$ is the moment of inertia of the fiber cross section referred to the neutral axis in the $\underline{z}$ direction and $\underline{s}$ is assumed to equal 50 μm.

Substituting the appropriate values assuming that $\underline{A}$, $\underline{I}$, and $\underline{s}$ are constant and integrating one finds that $\mathcal{E}$ = 472.8 dynes/(μm.)^2. From this value and the initial stress, the initial elastic strain is estimated to be 0.00328.

Now it is possible to determine the initial stress on fiber segments oriented at various angles. From the theory it may be shown that the tension in a segment is

$$T_o = eAE(\sin^2\theta - \gamma \cos^2\theta)$$

where $\underline{T}_o$ is the initial tensile force in a fiber segment oriented at an angle θ. The angle θ is referred to a perpendicular to the direction of applied stress. The tensile stress, $\underline{T}_o/\underline{A}$, at various angles is shown in Table VI.

TABLE VI

TENSILE STRESS IN FIBERS AT VARIOUS ORIENTATIONS

θ, degrees	Tensile Stress, dynes/$(\mu m.)^2$
5	-2.23
15	-1.66
25	-0.61
35	0.84
45	2.42
55	4.05
65	5.47
75	6.57
85	7.09

Utilizing the initial stress in the fibers shown in Table VI a master creep curve based on the various initial stresses was determined for the fibers in the sheet. This involved extrapolation of the master creep curve for individual fibers shown in Fig. 18 to lower initial stresses and shorter times. The fiber elastic deformation was used to determine a starting point for these curves at $\underline{t}$ = 30 seconds. The time shifts employed came from a linear extrapolation of the curve in Fig. 19 which is a plot of time shift versus initial stress for the fibers used in this study. The resulting master creep curves may be regarded as a plot of $1/\underline{E}$ versus log time from which $\underline{E}$ may be determined at selected times after application of a creep load.

From Van den Akker's theory it may be shown that the sheet extension, $\underline{e_x}$, is

$$e_x = \mathcal{T}\langle A\rangle_{Av}\rho\langle s\rangle_{Av}/\mathcal{W}\left\{[(1+\gamma)/2]\int_0^{\pi}\int_0^{\infty}\int_0^{\infty}\int_0^{\infty}(s/h)\sin^2\theta\cos^2\theta P_\theta P_A P_I P s\,ds\,dI\,dA\,d\theta\right.$$

$$\left. + \int_0^{\pi}\int_0^{\infty}\int_0^{\infty} AEs\,\sin^4\theta P_\theta P_A P_s\,ds\,dA\,d\theta - \upsilon\int_0^{\pi}\int_0^{\infty}\int_0^{\infty} AEs\,\sin^2\theta\cos^2\theta P_\theta P_A P_s\,ds\,dA\,d\theta\right\}.$$

Rearranging and simplifying the above expression and substituting the assumed values for the various quantities, one has

$$e_x = 4.87/E[\int_0^{\pi} \sin^4\theta d\theta - 0.268 \int_0^{\pi} \sin^2\theta\cos^2\theta d\theta].$$

The total sheet strain was estimated by integrating the above equation over 10-degree intervals and assuming that $\underline{E}$ is constant over the interval and equal to the value at the interval mid-point. The appropriate values of $\underline{E}$ were obtained as discussed previously and the integration performed.

The resulting strain and the reduced strain (plotted in Fig. 24) for various times after application of a creep load to the hypothetical sheet are given in Table VII.

TABLE VII

CREEP RESPONSE OF HYPOTHETICAL HANDSHEET

Time, seconds	Strain, %	Reduced strain, %/(kg./mm.^{2})
30	0.339	0.215
10^2	0.345	0.218
10^3	0.358	0.226
10^4	0.368	0.233
10^5	0.379	0.240
10^6	0.392	0.248
10^7	0.404	0.255
10^8	0.420	0.266
10^9	0.463	0.293
10^{10}	0.564	0.357
10^{11}	0.706	0.447
10^{12}	0.849	0.537
10^{13}	0.989	0.626
10^{14}	1.14	0.719
10^{15}	1.28	0.811